UNIVERSIDADE ESTADUAL PAULISTA – UNESP
Instituto de Biociências, Letras e Ciências Exatas - Campus de São José do Rio Preto

Veridianna Camilo Pattini

Evaluation of curcumin derivatives: antifungal activity and possible applications

São José do Rio Preto - Brasil
Groningen - Países Baixos
2025

Veridianna Camilo Pattini

Evaluation of curcumin derivatives: antifungal activity and possible applications

Tese apresentado em regime de co-tutela, à Universidade Estadual Paulista (UNESP), Instituto de Biociências, Letras e Ciências Exatas, São José do Rio Preto e Faculty of Medical Sciences, University Medical Center Groningen (UMCG), University of Groningen (RUG), Groningen para obtenção da Dupla Titulação de Doutora em Microbiologia.

Área de concentração: Microbiologia

Orientador: Prof. Dr. Luis Octavio Regasini (UNESP)
Orientadora: Profª. Drª. Henny C. van der Mei (UMCG/RUG)
Co-orientadora: Profª. Drª. Margarete Teresa Gottardo de Almeida (UNESP/FAMERP)

São José do Rio Preto - Brasil
Groningen - Países Baixos
2025

P321e

Pattini, Veridianna Camilo

Evaluation of curcumin derivatives : antifungal activity and possible applications / Veridianna Camilo Pattini. -- , 2025
138 p. : il., tabs.

Tese (doutorado) – Universidade Estadual Paulista (UNESP), Instituto de Biociências Letras e Ciências Exatas, São José do Rio Preto e Faculty of Medical Sciences, University Medical Center Groningen (UMCG), University of Groningen (RUG), Groningen,

Orientador: Luis Octavio Regasini
Orientadora: Henny C. van der Mei
Coorientadora: Margarete Teresa Gottardo de Almeida

1. Biofilme. 2. Candida albicans. 3. Micoses. 4. Antifúngico. 5. Coatings. I. Título.

Sistema de geração automática de fichas catalográficas da Unesp. Dados fornecidos pelo autor(a).

IMPACTO POTENCIAL DESTA PESQUISA

Esta pesquisa contribui significativamente para o avanço científico e tecnológico na área de antifúngicos, ao desenvolver curcuminoides mais estáveis e potentes que a curcumina. Os compostos propostos demonstraram elevada atividade antifúngica e antibiofilme, com potencial para diversas aplicações médicas.

Do ponto de vista inovador e econômico, os curcuminoides com síntese simplificada podem ser explorados como produtos de menor custo e maior viabilidade industrial. Socialmente, os resultados atendem a uma demanda urgente por novas estratégias contra infecções fúngicas, contribuindo para a saúde pública e o controle de infecções hospitalares.

A pesquisa reforça a internacionalização, tendo sido desenvolvida em parceria com instituições brasileiras e holandesas, e apresenta inserção local e nacional em temas estratégicos de inovação em saúde. Além disso, promove o desenvolvimento sustentável ao reduzir o impacto ambiental dos tratamentos convencionais. Por fim, fortalece o conhecimento interdisciplinar nas áreas de Química Medicinal, Microbiologia e Biomateriais.

POTENTIAL IMPACT OF THIS RESEARCH

This research significantly contributes to the scientific and technological advancement in the field of antifungals by developing curcuminoids that are more stable and potent than curcumin. The proposed compounds demonstrated high antifungal and antibiofilm activity, with potential for various medical applications.

From an innovation and economic perspective, curcuminoids with simplified synthesis can be explored as lower-cost products with greater industrial feasibility. Socially, the results address an urgent demand for new strategies against fungal infections, contributing to public health and hospital infection control.

The research strengthens internationalization, having been developed in partnership with Brazilian and Dutch institutions, and shows local and national engagement in strategic health innovation topics. Furthermore, it promotes sustainable development by reducing the environmental impact of conventional treatments. Finally, it reinforces interdisciplinary knowledge in the fields of Medicinal Chemistry, Microbiology, and Biomaterials.

AGRADECIMENTOS

The word I would use to define myself is privileged. Not in a material sense, but in a way that money cannot buy—being surrounded by great people throughout my journey. My PhD experience was no exception.
In this section, I want to acknowledge some important people who supported me during this process, though I know that no words can truly express how grateful I am.

First of all, I would like to express my gratitude to my supervisors**, Prof. Henny Van der Mei**, **Prof. Luis Octavio Regasini**, and **Prof. Margarete Gottardo de Almeida**, for giving me this opportunity, trusting me throughout this process, and making this project possible.

Dear **Henny**, thank you for accepting me as your PhD student and giving me the opportunity to be part of your group during the challenging pandemic period. I deeply admire you as a woman and as a leader—your supervisory approach, attention to detail, time management, and patience are truly inspiring. I have learned so much from you. Thank you for always being available when I needed guidance. I am grateful for your support over these years.

Luis, gostaria de dizer que serei eternamente grata por ser a peça-chave do meu interesse pela pesquisa em antimicrobianos e por fazer parte do meu crescimento científico desde o início. Tudo começou em 2017, quando eu tinha apenas uma ideia de que gostaria de iniciar meu mestrado na área de microbiologia médica, mas ainda estava meio perdida. Então, você me apresentou a química medicinal, e eu me encantei! Admiro muito sua trajetória e sou imensamente grata por você acreditar e confiar em mim durante todos esses anos.

Professora Margarete, muito obrigada por me aceitar de braços abertos em seu grupo de pesquisa. Desde o primeiro dia, me senti acolhida no laboratório, onde conheci não apenas colegas de trabalho, mas amigos queridos. Gostaria que a senhora soubesse que a admiro muito e serei eternamente grata. Obrigada, professora, pelo seu suporte durante esses anos, por estar sempre disponível para responder todas as minhas questões e sempre pronta para me auxiliar no que for possível.

I would like to thank the members of the assessment committee—**Prof. Maria J. Soares Mendes Giannini**, **Prof. Maria L. Scroferneker**, **Prof. Yijin Ren**, and **Prof. Prashant K. Sharma**—for the time you all dedicated to evaluating and approving my thesis.
I would also like to express my gratitude for all the support from BBT, with special thanks to the technicians.

Jelly and **Gesinda**, thank you for welcoming me when I first started in the lab, for teaching me all the rules and procedures, helping me with the flow chamber experiments, and always being so kind and patient. I truly appreciate all your support over these years.

Marja, thank you for always being there to support me in the lab whenever I needed, and for all the laughs and enjoyable moments.

Willem, thank you for "saving me" countless times, even when you wanted to assign someone else to do it (hahaha). Honestly, I truly appreciate all your help, your ideas, and your support during troubleshooting. You are great!

Joop, thank you for all your help with AFM and XPS. Beyond your expertise, which I admire, you have a kind soul. I appreciate that you were always there to help out whenever needed, with great patience.

Ed, Hoe gaat het met jou? Thank you for the small talks in Dutch and for helping me with IT problems, especially with the password updates that I kept forgetting (hahaha). I appreciate your kindness, positive energy, and dedication to helping people.

Willy, thank you for your help in ordering materials related to the gene expression experiments, for assisting with RNA extraction, and later, together with **Emma**, for helping with qPCR. Thank you both!

Paulien, thanks a lot for "saving me" that afternoon with the qPCR data analysis. I truly appreciate it!

Thank you to the amazing office mates from Office 1305: **Irem**, **Arturo**, **Gao** (amigaaa), **Rouijia**, **Fenghua**, **Sebastian**, and **Elkin**. I appreciate our daily chats and the support you provided during this time. You are all wonderful, and I wish you all the best!

Aos meus amigos brasileiros do departamento—**Clara**, **Victor**, **Lais**, **Liliana** (Non è brasiliana, ma l'abbiamo adottata! Ahaha Giusto che tu sia in questa lista) e **Jordy** (também não é brasileiro, mas foi adotado hahaha)—muito obrigada por estarem presentes em vários momentos desta minha jornada, pelos inúmeros cafés acompanhados de boas conversas, auxilio na parte experimental, na trocas de experiencias e risadas! Sou grata por ter conhecido cada um de vocês!

Às minhas amigas lusitanas, **Maria** e **Micaela**: Amigaaaas, vocês foram um dos grandes presentes que recebi no departamento! Eu adorei cada experiência que pudemos compartilhar juntas—nossas viagens, nossos jantares, cafés, trocas de experiências, risadas e conselhos.

And also, a big thank you to all the other great people from BBT that I had the opportunity to meet: **Lu Yuan**, **Devlina**, **Jhon**, **Elles**, **Clio**, **Renata** (...) I appreciate our talks during coffee breaks and all the shared moments we had outside the department. It was a pleasure to have met you all!

Sou também muito grata pela minha trajetória nos laboratórios: **Laboratório de Antibióticos e Quimioterápicos** (UNESP) e **Laboratório de Microbiologia** (FAMERP). Meu agradecimento especial vai às pessoas queridas que encontrei nessa jornada: **Jullyanna**, **Letícia Ribeiro**, **Luceli**, **Emília**, **Natália**, **Mariela**, **Thiago**, **Maicon**, **Taiza**, **Letícia Mozaner**, **Letícia Bianco** e **Bianca**. Sou grata por todos os momentos que compartilhamos, nossas risadas, nossos almoços, e sinto saudades!

Às minhas queridas paraninfas **Paula Martins** e **Beatriz Fumelli**.

Paula, sua amizade é um grande presente para mim. Nos conectamos desde a primeira vez que nos conhecemos e, depois, nossa conexão se fortaleceu cada vez mais. Sou tão grata por sua vida, pela sua amizade, pela presença, e é claro que você seria a minha paraninfa! Te admiro muito como mulher, como profissional, como amiga, e você é uma inspiração para mim.

Bia, minha amiga, minha office mate e, agora, minha paraninfa! Em pouco tempo, me senti conectada com você. Sou muito grata pela sua parceria, pela conexão, pela energia boa compartilhada e por todos os nossos momentos. Que venham mais aventuras!
Isaura, minha paraninfa não oficial em modelo remoto (hahah). Isa, sou muito grata pela sua vida, pela nossa amizade, por todo o apoio e por todos os momentos que passamos juntas, que fortaleceram ainda mais nossos laços. Tenho uma imensa admiração por você, e tenho orgulho de tê-la como amiga. Sentirei sua falta durante esse período no Brasil e aguardo ansiosamente pelo seu retorno!

During the pandemic and the shifts we had to make in the department, I didn't know anyone in The Netherlands for a while. As I always say how lucky I am to find great people to bond with, I was fortunate enough to meet these great souls who made my days, evenings, sunny and rainy days, great festivals, summers, and still continue doing so: **Francesca**, **Tineke**, **Bianca**, **Marta**, **Claudia**, and **Florencia**. I could fill this space with words, but I know I will never fully express how grateful I am for having found you girls.

Aos meus amigos brasileiros, que trazem o quentinho de casa para a gente. Sou grata pela oportunidade de ter conhecido a maioria de vocês durante a Copa do Mundo. O presente foi ainda melhor do que o Brasil ser hexa (se bem que seria melhor se tivesse sido, hahaha). Alguns conheci por conta de eventos do grupo e outros na UMCG. Quero dizer que sou grata a cada jantar, cada evento, cada comida com gosto de abraço, almoços no restaurante da UMCG, as horas do cafezinho, a cada troca de experiências com várias risadas, as trocas mais profundas que temos no clube do livro, e por toda ajuda no caos da minha mudança (quem viveu, sabe hahahah). **Sidney**, **Pedro**, **Jéssica**, **Felipe**, **Alexandra**, **Vinicius**, **Matheus**, **Victória**, **Mariana Albuquerque**, **Mariana Baravelli**, **Julia**, **Lais**, **Carmen**, **Lucas de Freitas** e **Beatriz Nasser**.

Às minhas amigas de longa data, que estão sempre presentes, em todas as diferentes fases da vida e independentemente da distância geográfica: **Jéssica Pinotti**, **Giovana Paschoalotto**, **Flávia Lourenço**, **Natalia Assunção** e **Bianca Machado**.

À minha família, especialmente à minha mãe **Joana**, ao meu pai **Walter** (*in memoriam*), ao meu irmão **Riccieri** e à minha sobrinha **Pietra**. Vocês são minha base, minha essência. A presença de vocês tem sido fundamental para minha jornada, e sou profundamente grata por tudo.

Mãe, serei eternamente grata por ter uma mulher como você como minha mãe e por ter tido um homem como o meu Pai como pai. Sou grata pela criação de vocês, pelas oportunidades que me proporcionaram e pelo amor incondicional. Sem vocês, nada disso seria possível. Muito obrigada, Mãe, por tudo fez e continua fazendo por mim!

Ri, muito obrigada por todo apoio de sempre, por ter sido a peça-chave de tantas oportunidades que tive em minha vida. Sempre serei eternamente grata por todas as portas que você me ajudou a abrir e por tudo o que continua fazendo por mim. Você faz parte e foi fundamental na minha conquista.

Pi, sou imensamente grata por todo o apoio diário que você me ofereceu ao longo dos anos. Você é muito mais do que uma sobrinha, é uma grande amiga, da qual tenho muito orgulho de ter em minha vida. Agradeço por todas as conversas, os conselhos, o apoio constante e por sempre estar ao meu lado, torcendo por mim.

O presente trabalho foi realizado com apoio da Coordenação de Aperfeiçoamento de Pessoal de Nível Superior – Brasil (CAPES) – Código de Financiamento 001.

This work was supported by the Abel Tasman Talent Program (ATTP) of the Graduate School of Medical Sciences (GSMS) of the University of Groningen.

RESUMO

Os biofilmes microbianos são os principais causadores de infecções relacionadas ao uso de dispositivos médicos. *Candida albicans* destaca-se dentre as espécies fúngicas mais frequentes em infecções nosocomiais, sendo o principal agente causador das infecções da corrente sanguínea associadas a dispositivos vasculares. Afim de prevenir estas infecções, estudos estão sendo realizados para o desenvolvimento de superfícies anti-incrustantes. O uso de agentes antimicrobianos tem demonstrado resultados promissores, porém sua utilização como revestimento em superfícies pode contribuir para o surgimento de cepas resistentes. Como uma alternativa ao uso de antimicrobianos, a curcumina destaca-se como um material de revestimento eficaz. No entanto, sua estabilidade em condições fisiológicas limita sua aplicação médica. Modificações na estrutura química da curcumina têm se mostrado eficiente para superar essas limitações e melhorar sua atividade biológica. Neste trabalho encontra-se um compilado de estudos acerca de modificações químicas utilizando a curcumina como modelo estrutural no desenvolvimento de compostos antifúngicos e possíveis revestimentos em superfícies de dispositivos médicos. O trabalho foi dividido em 5 seções: A **Seção 1** fornece uma visão geral básica das infecções fúngicas e destaca a motivação desta pesquisa. Na **Seção 2** foi investigado o potencial antifúgico de uma série de análogos de curcumina. Foi observado que a substituição de metoxilas nas posições 3 dos anéis A e B da curcumina resultam em atividade antifúngica de amplo espectro, contra diversas espécies de fungos filamentosos e de *Candida*. A **Seção 3** apresenta a substituição do fragmento β-dicetona na curcumina por uma monocarbonila contra espécies de *Candida,* demonstrando atividades antifúngicas potentes. Afim de explorar aplicabilidades dos curcuminoides, na **Seção 4** foi desenvolvido um revestimento de superfície multifuncional com potencial antifúngico e anti-biofilme. Na **Seção 5**, os principais achados de cada estudo foram sintetizados, e sugestões para pesquisas futuras foram apresentadas. Com base nos resultados, fornecemos insights sobre as relações entre estrutura química e atividade biológica dos curcuminoides, abrindo caminhos para o desenvolvimento de novos análogos bioativos destinados ao tratamento de infecções fúngicas e à prevenção da formação de biofilmes por meio de revestimentos antiaderentes.

Palavras–chave: anti-biofilme; anti *Candida*; curcumina; antifúngico; modificações de superfícies.

ABSTRACT

Biofilms are crucial in medical-related infections, especially those associated with medical devices. *Candida albicans* emerge as the most prevalent causative agent of bloodstream infections associated with vascular devices in hospital settings. In order to overdue this problem, studies are exploring surface modifications to create antifouling materials for medical devices and implants. Although antimicrobial agents have demonstrated promising outcomes, their persistent application on surfaces can contribute to the emergence of resistant strains. Curcumin has exhibited potential as an effective coating material. However, its stability under physiological conditions limits its medical application. Modifications in the curcumin structure overcome this limitation and improve its bioactivities. This work is a compilation of studies about chemical structural modifications using curcumin as a model for developing antifungal compounds and possible surface coatings for medical devices. It was divided into 5 chapters: **Chapter 1** provides a basic overview of fungal infections and highlights the motivation for this research. In **Chapter 2**, the antifungal potential of a series of curcumin analogs was investigated. The substitution of methoxyl at position 3 of the rings A and B of curcumin structure results in broad-spectrum antifungal activity against several filamentous fungi and *Candida* species. In **Chapter 3**, the replacement of the β-diketone fragment in the curcumin by a monocarbonyl moiety against *C. albicans* was investigated and showed potent antifungal activities. In order to explore monocarbonyl curcuminoid applications, **Chapter 4** presents the development of a multifunctional surface coating with antifouling and antifungal potential. In **Chapter 5**, the findings of each study have been emphasized and suggestions have been made for future research and perspectives. Based on the combined results from all chapters, we provide insights into the chemical structure and activity relationships of curcuminoids, paving the way for developing new bioactive analogues for treating fungal infections and preventing biofilm formation through antifouling coatings.

Keywords: anti-biofilm; anti *Candida*; curcumin; antifungal; surface modifications

SUMÁRIO

1. INTRODUCTION

Fungal infections

In recent decades, fungal infections have grown considerably, with a mortality rate equivalent to tuberculosis and 3-fold more than malaria. According to the estimate made by Bongomin et al. (2017), about 1.6 million deaths are related to chronic or acute fungal infections annually (Bongomin *et al.*, 2017). The World Health Organization reports that approximately 400,000 and 1.5 million people die each year from malaria (World Health Organization, 2019a) and tuberculosis (World Health Organization, 2019b) .

Candida species are considered common commensal fungi of the natural microbiota, colonizing mucous membranes and the digestive tract. When these species play a commensal role, they offer immunological protection against systemic infection. However, when physiological changes occur, such as temperature, pH, hormonal changes, or changes in the patient's immune system, they can become opportunistic pathogens. In this scenario, *Candida albicans* stand out as the most frequent opportunistic fungus among nosocomial infections(Adeniyi, Adekoya e Ogunware, 2020). The pathogenicity of this species and the non-*albicans* species is mediated by numerous factors, especially adhesion and biofilm formation (Staniszewska, 2020).

Biofilms are complex communities of microorganisms adhering to a biotic or abiotic substrate, surrounded by an extracellular matrix of polysaccharides, proteins, nucleic acids, and enzymes excreted by the microorganisms (Cooper, 2010). The formation process of biofilms is controlled by quorum sensing, an intercellular communication system that regulates gene expression of virulence factors based on population density. The organization in a microbial community offers several advantages over the planktonic form, such as an increased ability to disseminate and resist unfavourable conditions including pH changes, temperature fluctuations, and toxic substances making biofilm-forming microorganisms difficult to treat (Grech e Balzan,

2019). Antimicrobials, for example, do not efficiently penetrate the interior of the biofilm and are often inactivated by enzymes excreted in the extracellular matrix, which results in the impairment of the effectiveness of antibiotics and antimycotics. Additionally, the relatively high density and close proximity in a biofilm favors the transfer of resistance genes and contributes to the greater resistance of biofilm-forming microorganisms to antimicrobials, resulting in relapses in conventional treatments(Chenoweth, Gould e Saint, 2014; Cooper, 2010).

Currently, the treatment for fungal infections is mainly restricted to azoles, polyenes, and echinocandins (Bellmann e Smuszkiewicz, 2017). However, factors such as the increasing number of resistant strains, the narrow spectrum due to intrinsic resistance, toxicity, and low bioavailability affect the effectiveness of antifungals (Chenoweth, Gould e Saint, 2014; Cooper, 2010). The effectiveness of antifungals can be even more affected when the infection is associated with medical devices. Studies have linked the presence of medical devices, such as vascular catheters, to the development of *Candida* bloodstream infections (candidemia) (Magill *et al.*, 2014). When a catheterized patient has an associated infection, the recommendation is to remove the device, as mortality rates are higher if vascular catheters stay in the patient. However, removing vascular access can pose challenges for critically-ill patients, and despite removal, mortality rates remain high (Andes *et al.*, 2012).

Given the problem caused by *Candida* spp. biofilm formation, it is crucial to develop substances with the ability to penetrate and degrade fungal biofilms. In cases of long-term device use it is necessary to develop efficient strategies to inhibit *C. albicans* adhesion and growth on the surface of the medical device, preventing the fungal infection.

Curcumin and curcuminoids as treatment and prevention of fungal infections

Natural products are sources of prototypes for the discovery and development of new drugs and bioactive substances (Bernardini *et al.*, 2018; Thomford *et al.*, 2018). A survey of the sources

of drugs approved in the period from 1981 to 2014 indicated that more than 65% of antimicrobials originated from natural products and their derivatives, as well as from synthetic substances based on natural ones (pharmacophores of natural products), confirming the importance of research in Natural Product Chemistry for the development of new antimicrobial agents (Newman e Cragg, 2016).

The therapeutic potential of curcumin has been widely known and used since ancient times. Research compiles on its pharmacological potential and natural and synthetic analogues (curcuminoids), including anti-inflammatory, antioxidant, antitumor, anti-HIV and antimicrobial activity as anti-protozoal, nematicidal, antibacterial, and antifungal (ARAÚJO, 2018). For *Candida* species, the natural curcumin exhibited an anti-adhesion effect on oral epithelial cells of HIV-positive patients(Martins *et al.*, 2008), hyphal growth inhibitory activity of *C. albicans*(Sharma *et al.*, 2010), as well as reduced metabolic activity and biomass of *C. albicans*, *Candida glabrata,* and *Candida tropicalis* biofilms when associated with light excitation (Dovigo *et al.*, 2011).

However, problems associated with curcumin stability under physiological conditions prevent its clinical use. Our research group demonstrated that the replacement of the β-diketone fragment in the curcumin by a monocarbonyl moiety made the curcumin much more stable and improved its bioactivities (Figure 1)(Morão *et al.*, 2019; Silva *et al.*, 2018).

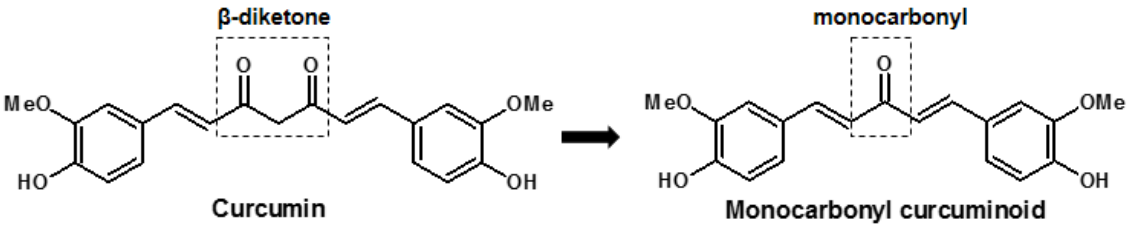

Figure 1. The β-diketone fragment in the curcumin was replaced by the monocarbonyl moiety to increase the stability of curcumin (Morão *et al.*, 2019; Silva *et al.*, 2018).

The antifungal effect of the synthetic monocarbonyl curcumin analogs, such as the curcuminoids, have been little explored, and only a few papers describe the antifungal activity of monocarbonyl curcumin analogs like susceptibility tests against planktonic cells (Ding *et al.*, 2017; Nagargoje *et al.*, 2020).

Curcumin coating for biomedical applications

In recent years, the development of surfaces coated with antimicrobial agents has been recognized as an important strategy for surface disinfection and for mitigating the risk of microbial cross-feeding(Abreu *et al.*, 2013; Campoccia, Montanaro e Arciola, 2013). The reports in the literature about natural curcumin have shown promising potential as an antimicrobial product to coat materials in various sectors. However, it is associated with other compounds, encapsulated or immobilized due to its structural stability limitation. In the food industry, curcumin was used to photo-crosslink papain to the food packaging material(Manohar *et al.*, 2015). In the healthcare sector, it was loaded in multilayered nanofibrous mats which were used for wound healing(Gaydhane, Kanuganti e Sharma, 2020), and in another study, they used curcumin loaded gold nanoparticles that were coated on surgical sutures(Sunitha S *et al.*, 2017). Additionally, a coating mixture of curcumin, chlorhexidine, and silver has demonstrated prevention and inhibition of bacterial colonization, along with lubricious properties (Modak *et al.*, 2019).

To enhance the stability and applicability of curcumin as a coating, a chemical modification was undertaken using monocarbonyl curcuminoids (see Figure 1). To date, there are no investigations in the literature on the coating of medical devices with monocarbonyl curcuminoids, which creates opportunities for novel approaches in combating fungal infections, particularly those caused by biofilm-forming *Candida species*. Understanding the mechanisms of action of monocarbonyl curcuminoids as an antifungal agent and exploring their potential as

a coating on materials can lead to innovative approaches in combating *Candida* biofilm-associated infections.

Aim of this thesis

This thesis aims to investigate the antifungal potential of curcuminoids, elucidating the influence of chemical modifications on their antifungal activity and explore their innovative strategies as a surface coating to prevent *Candida* biofilm formation.

References

ABREU, A. C. *et al.* Current and emergent strategies for disinfection of hospital environments. **Journal of Antimicrobial Chemotherapy**, v. 68, n. 12, p. 2718–2732, 2013.

ACHTERMAN, R. R.; WHITE, T. C. Dermatophyte virulence factors: identifying and analyzing genes that may contribute to chronic or acute skin infections. **International Journal of Microbiology**, v. 2012, p. 358305, 2012.

ADENIYI, T. E.; ADEKOYA, A. A.; OGUNWARE, A. E. Antimicrobial Resistance among Fungal Species Obtained from Patients with Genito-urinary Tract Infections. v. 3, n. 1, p. 5–14, 2020.

AFEWERKI, S. *et al.* Advances in antimicrobial and osteoinductive biomaterials. *Em*: **Racing for the Surface**. Cham: Springer International Publishing, 2020. p. 3–34.

AKABERI, M.; SAHEBKAR, A.; EMAMI, S. A. Turmeric and Curcumin: From traditional to modern medicine. *Em*: **Studies on Biomarkers and New Targets in Aging Research in Iran** . [s.l: s.n.]. v. 1291p. 15–39.

ALALWAN, H. *et al.* The anti-adhesive effect of curcumin on *Candida albicans* biofilms on denture materials. **Frontiers in Microbiology**, v. 8, p. 669, 2017.

ALBUQUERQUE MARANHÃO, F. C. DE *et al.* Mycoses in northeastern Brazil: epidemiology and prevalence of fungal species in 8 years of retrospective analysis in Alagoas. **Brazilian Journal of Microbiology**, v. 50, n. 4, p. 969–978, 2019.

ALI MALAYERI, F.; REZAEI, A.; RAIESI, O. Antifungal agents: Polyene, azole, antimetabolite, other and future agents. **Journal of Basic Research in Medical Sciences**, v. 5, n. 2, p. 48–55, 2018.

ANDES, D. R. *et al.* Impact of Treatment Strategy on Outcomes in Patients with Candidemia and Other Forms of Invasive Candidiasis: A Patient-Level Quantitative Review of Randomized Trials. **Clinical Infectious Diseases**, v. 54, n. 8, p. 1110–1122, 2012.

APISARIYAKUL, A.; VANITTANAKOM, N.; BUDDHASUKH, D. Antifungal activity of turmeric oil extracted from Curcuma longa (Zingiberaceae). **Journal of Ethnopharmacology**, v. 49, n. 3, p. 163–169, 1995.

ARAÚJO, L. F. **PLANTAS MEDICINAIS NO CONTROLE DE FUNGOS PATOGÊNICOS HUMANOS PATOS**. [s.l.] Instituto de Biotecnologia da Universidade Federal de Uberlândia, 2018.

BAERT, F. *et al.* Updating the taxonomy of dermatophytes of the BCCM/IHEM collection according to the new standard: a phylogenetic approach. **Mycopathologia**, v. 185, p. 161–168, 2020.

BELLMANN, R.; SMUSZKIEWICZ, P. Pharmacokinetics of antifungal drugs: practical implications for optimized treatment of patients. **Infection**, v. 45, n. 6, p. 737–779, 2017.

BERNARDINI, S. *et al.* Natural products for human health: an historical overview of the drug discovery approaches. **Natural Product Research**, v. 32, n. 16, p. 1926–1950, 2018.

BOKHARI, H. *et al. Galleria mellonella* is low cost and suitable surrogate host for studying virulence of human pathogenic *Vibrio cholerae*. **Gene**, v. 628, p. 1–7, set. 2017.

BONGOMIN, F. *et al.* Global and Multi-National Prevalence of Fungal Diseases — Estimate Precision. **Journal of Fungi**, v. 3, p. 57, 2017.

BRASCH, J.; BECK-JENDROSCHEK, V.; MAHN, V. Photochemical inhibition of *Trichophyton rubrum* by different compoundings of curcumin. **Mycoses**, v. 61, n. 6, p. 393–399, 2018.

BRUELLHOFF, K. *et al.* Surface Coating Strategies to Prevent Biofilm Formation on Implant Surfaces. **The International Journal of Artificial Organs**, v. 33, n. 9, p. 646–653, 2010.

BUSSCHER, H. J.; MEI, H. C. VAN DER. Microbial adhesion in flow displacement systems. **Clinical Microbiology Reviews**, v. 19, n. 1, p. 127–141, 2006.

CAMPOCCIA, D.; MONTANARO, L.; ARCIOLA, C. R. A review of the biomaterials technologies for infection-resistant surfaces. **Biomaterials**, v. 34, n. 34, p. 8533–8554, 2013.

CHEN, E. *et al.* Fungal-host interaction: Curcumin modulates proteolytic enzyme activity of *Candida albicans* and inflammatory host response *In Vitro*. **International Journal of Dentistry**, v. 2018, p. 2393146, 2018.

CHEN, H. *et al.* The regulation of hyphae growth in *Candida albicans*. **Virulence**, v. 11, n. 1, p. 337–348, 2020.

CHEN, M.; YU, Q.; SUN, H. Novel strategies for the prevention and treatment of biofilm related infections. **International Journal of Molecular Sciences**, v. 14, n. 9, p. 18488–18501, 2013.

CHENOWETH, C. E.; GOULD, C. V.; SAINT, S. Diagnosis, Management, and Prevention of Catheter-Associated Urinary Tract Infections. **Infectious Disease Clinics of North America**, v. 28, n. 1, p. 105–119, 2014.

CIESIELSKI, F. *et al.* Recognition of membrane sterols by polyene antifungals amphotericin B and natamycin, A (13)C MAS NMR study. **Frontiers in Cell and Developmental Biology**, v. 4, p. 57–68, 2016.

CLSI. Reference method for broth dilution antifungal susceptibility testing of yeasts; approved standard—Third Edition. **CLSI document M27-A3**, v. 28, 2008a.

CLSI. Reference Method for Broth Dilution Antifungal Susceptibility Testing of Filamentous Fungi; Approved Standard—Second Edition. **CLSI document M38-A2**, v. 28, 2008b.

COOPER, I. R. Microbial biofilms : case reviews of bacterial and fungal pathogens persisting on biomaterials and environmental substrata. **Current Research, Technology and Education Topics in Applied Microbiology and Microbial Biotechnology**, p. 807–817, 2010.

DING, T. *et al.* Curcumin liposomes interfere with quorum sensing system of *Aeromonas sobria* and in silico analysis. **Scientific Reports**, v. 7, n. 1, p. 1–16, 2017.

DONG, H. *et al.* Synergistic antifungal effects of curcumin derivatives as fungal biofilm inhibitors with fluconazole. **Chemical Biology & Drug Design**, v. 97, n. 5, p. 1079–1088, 2021.

DOVIGO, L. N. *et al.* Susceptibility of clinical isolates of *Candida* to photodynamic effects of curcumin. **Lasers in Surgery and Medicine**, v. 43, n. 9, p. 927–934, 2011.

ERMIS, M.; ANTMEN, E.; HASIRCI, V. Micro and Nanofabrication methods to control cell-substrate interactions and cell behavior: A review from the tissue engineering perspective. **Bioactive Materials**, v. 3, n. 3, p. 355–369, set. 2018.

FROST, D. J. *et al.* A whole-cell *Candida albicans* assay for the detection of inhibitors towards fungal cell wall synthesis and assembly. **The Journal of Antibiotics**, v. 48, n. 4, p. 306–310, 1995.

GAYDHANE, M. K.; KANUGANTI, J. S.; SHARMA, C. S. Honey and curcumin loaded multilayered polyvinylalcohol/cellulose acetate electrospun nanofibrous mat for wound healing. **Journal of Materials Research**, v. 35, n. 6, p. 600–609, 2020.

GOFFENA, J.; TOENJES, K. A.; BUTLER, D. K. Inhibition of yeast-to-filamentous growth transitions in *Candida albicans* by a small molecule inducer of mammalian apoptosis. **Yeast**, v. 35, n. 3, p. 291–298, 2018.

GRECH, A.; BALZAN, M. Quorum sensing. **Medical Portals Ltd.**, v. 18, n. 2, p. 11–13, 2019.

HAJIFATHALI, S. *et al.* Investigation of the antifungal effects of curcumin against nystatin-resistant *Candida albicans*. **Dental Research Journal**, v. 20, p. 50, 2023.

HAO, B. *et al.* Caspofungin Kills *Candida albicans* by Causing both Cellular Apoptosis and Necrosis. **Antimicrobial Agents and Chemotherapy**, v. 57, n. 1, p. 326–332, 2013.

HARDING, C. R. *et al.* Use of *Galleria mellonella* as a Model Organism to Study *Legionella pneumophila* Infection. **Journal of Visualized Experiments**, n. 81, 2013.

HOLLAND, L. M. *et al.* Comparative phenotypic analysis of the major fungal pathogens *Candida parapsilosis* and *Candida albicans*. **PLoS Pathogens**, v. 10, n. 9, p. e1004365, 2014.

IGNASIAK, K.; MAXWELL, A. *Galleria mellonella* (greater wax moth) larvae as a model for antibiotic susceptibility testing and acute toxicity trials. **BMC Research Notes**, v. 10, n. 1, p. 428, 2017.

IRACANE, E. *et al.* Identification of an Exceptionally Long Intron in the *HAC1* Gene of *Candida parapsilosis*. **mSphere**, v. 3, n. 6, p. e00532-18, 2018.

JEMEL, S. *et al. Galleria mellonella* for the evaluation of antifungal efficacy against medically important fungi, a Narrative Review. **Microorganisms**, v. 8, n. 3, p. 390, 2020.

KIM, B.-T. *et al.* Synthesis of Dihydroxylated Chalcone Derivatives with Diverse Substitution Patterns and Their Radical Scavenging Ability toward DPPH Free Radicals. **Bulletin of the Korean Chemical Society**, v. 29, n. 6, p. 1125–1130, 2008.

KIM, HYOUNG JA *et al.* Synthesis of 4-(2-Amino)ethoxy-3′,4′-dihydroxychalcones and Their Antioxidant and Cytotoxic Effects on Human Tumor Cells. **Bulletin of the Korean Chemical Society**, v. 36, n. 5, p. 1335–1339, 2015.

KUMAR, A. *et al.* Curcumin targets cell wall integrity via calcineurin-mediated signaling in *Candida albicans*. **Antimicrobial Agents and Chemotherapy**, v. 58, n. 1, p. 167–175, 2014.

KUMAR, ANAND *et al.* Fungicidal versus fungistatic therapy of invasive *Candida* infection in non-neutropenic adults: a meta-analysis. **Mycology**, v. 9, n. 2, p. 116–128, 2018.

LEE, JIN-HYUNG *et al.* Antibiofilm and antivirulence activities of 6-gingerol and 6-shogaol against *Candida albicans* due to hyphal inhibition. v. 8, n. August, p. 1–10, 2018.

LEE, W.; LEE, D. G. An antifungal mechanism of curcumin lies in membrane-targeted action within *Candida albicans*. **IUBMB Life**, v. 66, n. 11, p. 780–785, 2014.

LEMES, T. H. *et al.* In vitro antifungal activity of *Candida* culture extracts against *Trichophyton rubrum* and *Trichophyton mentagrophytes*. **Brazilian Journal of Case Reports**, v. 1, n. 4, p. 135–152, 2021.

LEMES, T. H. *Candida parapsilosis* culture extracts: in vitro, antagonistic action against *Candida albicans*, *Candida auris* and *Candida parapsilosis*. **Brazilian Journal of Case Reports**, v. 3, n. 1, p. 24–29, 2022.

LIBER-KNEĆ, A.; ŁAGAN, S. Surface testing of dental biomaterials—determination of contact angle and surface free energy. **Materials**, v. 14, n. 11, p. 2716, 2021.

MAGILL, S. S. *et al.* Multistate point-prevalence survey of health care–associated infections. **New England Journal of Medicine**, v. 370, n. 13, p. 1198–1208, 2014.

MANOHAR, C. M. *et al.* Design of a papain immobilized antimicrobial food package with curcumin as a crosslinker. **PLoS ONE**, v. 10, n. 4, p. 1–17, 2015.

MARQUES, B. C. *et al.* Methoxychalcones: effect of methoxyl group on the antifungal, antibacterial and antiproliferative activities. **Medicinal Chemistry**, v. 16, n. 7, p. 881–891, 2019.

MARTINS, C. V. B. *et al.* Curcumin as a promising antifungal of clinical interest. **Journal of Antimicrobial Chemotherapy**, v. 63, n. 2, p. 337–339, 2008.

MELLO, V. G. *et al.* Virulence factors and antifungal susceptibility in *Candida* species isolated from dermatomycosis patients. **Mycopathologia**, v. 186, n. 1, p. 71–80, 2021.

MODAK, S. M. *et al.* **Coatings and methods for infection-resistant medical devices**. United States Patent Application US 2019/0133126 A1, 2019.

MORÃO, L. G. *et al.* A simplified curcumin targets the membrane of *Bacillus subtilis*. **MicrobiologyOpen**, v. 8, n. 4, p. e00683, 2019.

NAGARGOJE, A. A. *et al.* Quinoline based monocarbonyl curcumin analogs as potential antifungal and antioxidant agents: synthesis, bioevaluation and molecular docking study. **Chemistry and Biodiversity**, v. 17, n. 2, p. e1900624, 2020.

NELSON, K. M. *et al.* The essential medicinal chemistry of curcumin. **Journal of Medicinal Chemistry**, v. 60, n. 5, p. 1620–1637, 2017.

NEWMAN, D. J.; CRAGG, G. M. Natural Products as Sources of New Drugs from 1981 to 2014. **Journal of Natural Products**, v. 79, n. 3, p. 629–661, 2016.

NOBILE, C. J. *et al.* Function of *Candida albicans* Adhesin Hwp1 in Biofilm Formation. **Eukaryotic Cell**, v. 5, n. 10, p. 1604–1610, 2006.

NOUREDDIN, S. A.; EL-SHISHTAWY, R. M.; AL-FOOTY, K. O. Curcumin analogues and their hybrid molecules as multifunctional drugs. **European Journal of Medicinal Chemistry**, v. 182, p. 111631, 2019.

PEREIRA, J. A. *et al.* Antibiofilm and cytotoxic effect of 3,3′-dihydroxycurcumin (DHC) as photosensitizer agent in antimicrobial photodynamic therapy for endodontic purposes. **Photodiagnosis and Photodynamic Therapy**, v. 36, p. 102534, 2021.

PFALLER, M. A.; DIEKEMA, D. J. Epidemiology of invasive candidiasis: a persistent public health problem. **Clinical Microbiology Reviews**, v. 20, n. 1, p. 133–163, 2007.

POLAQUINI, C. R. *et al.* Antibacterial activity of 3,3′-dihydroxycurcumin (DHC) is associated with membrane perturbation. **Bioorganic Chemistry**, v. 90, p. 103031, 2019.

PRYSZCZ, L. P. *et al.* Unexpected genomic variability in clinical and environmental strains of the pathogenic yeast *Candida parapsilosis*. **Genome Biology and Evolution**, v. 5, n. 12, p. 2382–2392, 2013.

RAMAGE, G. *et al.* The filamentation pathway controlled by the Efg1 regulator protein is required for normal biofilm formation and development in *Candida albicans*. **FEMS Microbiology Letters**, v. 214, n. 1, p. 95–100, 2002.

SANCHES, C. V. G. *et al.* Diacetylcurcumin: a new photosensitizer for antimicrobial photodynamic therapy in *Streptococcus mutans* biofilms. **Biofouling**, v. 35, n. 3, p. 340–349, 2019.

SARDI, J. C. O. *et al. Candida* species: current epidemiology, pathogenicity, biofilm formation, natural antifungal products and new therapeutic options. **Journal of Medical Microbiology**, v. 62, n. 1, p. 10–24, 2013.

SARDI, J. DE C. O. *et al.* Unexplored endemic fruit species from Brazil: antibiofilm properties, insights into mode of action, and systemic toxicity of four *Eugenia* spp. **Microbial Pathogenesis**, v. 105, p. 280–287, 2017.

SARDI, J. DE C. O. *et al.* Antibacterial activity of diacetylcurcumin against *Staphylococcus aureus* results in decreased biofilm and cellular adhesion. **Journal of Medical Microbiology**, v. 66, n. 6, p. 816–824, 2017.

SHAHZAD, M. *et al.* Utilising polyphenols for the clinical management of *Candida albicans* biofilms. **International journal of antimicrobial agents**, v. 44, n. 3, p. 269–273, 2014.

SHARMA, M. *et al.* Antifungal curcumin induces reactive oxygen species and triggers an early apoptosis but prevents hyphae development by targeting the global repressor TUP1 in *Candida albicans*. **Bioscience Reports**, v. 30, n. 6, p. 391–404, 2010.

SHETTY, D. *et al.* Eliminating the heart from the curcumin molecule: monocarbonyl curcumin mimics (MACs). **Molecules**, v. 20, n. 1, p. 249–292, 2014.

SILVA, A. C. B. DA *et al.* Development of a novel anti-biofilm peptide derived from profilin of *Spodoptera frugiperda*. **Biofouling**, v. 36, n. 5, p. 516–527, 2020.

SILVA, G. *et al.* Curcumin Analog CH-5 Suppresses the proliferation, migration, and invasion of the human gastric cancer cell line HGC-27. **Molecules**, v. 23, n. 2, p. 279, 2018.

SINGH, A. K.; GAUR, V.; MAURYA, A. K. The role of biofilm in originating, mediating, and proliferating infectious diseases. *Em*: **Biofilms in Human Diseases: Treatment and Control**. Cham: Springer International Publishing, 2019. p. 43–57.

SPITZER, M.; ROBBINS, N.; WRIGHT, G. D. Combinatorial strategies for combating invasive fungal infections. **Virulence**, v. 8, n. 2, p. 169–185, 2017.

SRIVASTAVA, A.; CHANDRA, N.; KUMAR, S. The role of biofilms in medical devices and implants. *Em*: **Biofilms in Human Diseases: Treatment and Control**. Cham: Springer International Publishing, 2019. p. 151–165.

SRIVASTAVA, V.; SINGLA, R. K.; DUBEY, A. K. Emerging virulence, drug resistance and future anti-fungal drugs for *Candida* pathogens. **Current Topics in Medicinal Chemistry**, v. 18, n. 9, p. 759–778, 2018.

STANISZEWSKA, M. Virulence factors in *Candida* species. **Current Protein & Peptide Science**, v. 21, n. 3, p. 313–323, 2020.

SUNITHA S *et al.* Fabrication of surgical sutures coated with curcumin loaded gold nanoparticles. **Pharmaceutica Analytica Acta**, v. 08, n. 01, 2017.

THOMFORD, N. *et al.* Natural products for drug discovery in the 21st century: innovations for novel drug discovery. **International Journal of Molecular Sciences**, v. 19, n. 6, p. 1578, 2018.

TOLEDO, L. DE *et al.* Essential oil of *Cymbopogon nardus* (L.) rendle: a strategy to combat fungal infections caused by *Candida* species. **International Journal of Molecular Sciences**, v. 17, n. 8, p. 1252, 2016.

TORREZAN, G. S. *et al.* Use of glycerol, waste glycerol from biodiesel production and other protic solvents in bioactive α,β-unsaturated ketones synthesis. **Sustainable Chemistry and Pharmacy**, v. 16, p. 100250, 2020.

VIRK, R. S. *et al.* Curcumin-containing orthopedic implant coatings deposited on poly-ether-ether-ketone/bioactive glass/hexagonal boron nitride layers by electrophoretic deposition. **Coatings**, v. 9, n. 9, p. 572, 2019.

WORLD HEALTH ORGANIZATION. **World Malaria Report 2019**. Genebra: World Health Organization, 2019a. 232 p. ISBN 978-92-4-156572-1.

WORLD HEALTH ORGANIZATION 2019. **Global tuberculosis report 2019**. Genebra: World Health Organization, 2019b. 284 p. ISBN 978-92-4-156571-4.

Letters in Applied Microbiology

2. Antifungal activity of 3,3'-dimethoxycurcumin (DMC) against dermatophytes and *Candida* species

Veridianna Camilo Pattini, Carlos Roberto Polaquini, Thiago Henrique Lemes, Natália Seron Brizzotti-Mazuchi, Janaína de Cássia Orlandi Sardi, Mário Henrique Paziani, Marcia Regina von Zeska Kress, Margarete Teresa Gottardo de Almeida and Luis Octávio Regasini (2024) *Lett Appl Microbiol* **77** (3):ovae019.

Reproduced with permission from Oxford Academic

Abstract

Dermatomycosis is an infection with global impacts caused especially by dermatophytes and *Candida* species. Current antifungal therapies involve drugs that face fungal resistance barriers. This clinical context emphasizes the need to discover new antifungal agents. Herein, the antifungal potential of ten curcumin analogs was evaluated against four *Candida* and four dermatophyte species. The most active compound, 3,3'-dimethoxycurcumin (DMC), exhibited Minimum Inhibitory Concentration (MIC) values ranging from 1.9–62.5 μg mL^{-1} and 15.6–62.5 μg mL^{-1} against dermatophytes and *Candida* species, respectively. According to the checkerboard method, the association between DMC and terbinafine demonstrated a synergistic effect against *Trichophyton mentagrophytes* and *Epidermophyton floccosum*. Ergosterol binding assay indicated DMC forms a complex with ergosterol of *Candida albicans*, *C. krusei* and *C. tropicalis*. However, results from the sorbitol protection assay indicated that DMC had no effect on the cell walls of the tested *Candida* species. The *in vivo* toxicity, using *Galleria mellonella* larvae, indicated no toxic effect of DMC. Altogether, curcumin analog DMC was a promising antifungal agent with a promising ability to act against *Candida* and dermatophyte species.

Introduction

Dermatomycosis is the most frequent fungal infection, affecting people worldwide, mainly in tropical areas, where hot and humid conditions are predisposing factors to such infections (Albuquerque Maranhão, de *et al.*, 2019). Dermatophytes have been described as the primary etiologic agents of dermatomycosis, divided into seven genera: *Arthropoderma*, *Microsporum*, *Lophophyton*, *Nannizzia, Epidermophyton*, *Paraphyton,* and *Trichophyton* (Baert *et al.*, 2020). These fungi are keratinophilic and keratinolytic filamentous species, which use keratin as the principal source of amino acids. Genomic sequencing has identified several virulence factors contributing to their ability to infect keratinized tissues, including various protease-encoding genes essential for keratin degradation and consequent tissue damage (Achterman e White, 2012).

Candida species, while often commensal in the human microbiota, play a significant role in the development of dermatomycosis (Mello *et al.*, 2021). One of the most important virulence factors of *Candida* species is its conversion from planktonic yeast-form to a filamentous-form (hyphae or pseudohyphae), which demonstrates invasive abilities(Chen *et al.*, 2020). *Candida albicans* is the most relevant species associated with dermatomycosis. However, non-*albicans* species have emerged as epidemiologically relevant agents, including *Candida tropicalis* and *Candida parapsilosis* complex (Albuquerque Maranhão, de *et al.*, 2019). The rising incidence of *Candida* infections, especially among immunocompromised individuals, has led to increased morbidity and mortality. This situation is further exacerbated by the emergence of strains less responsive to treatment, a consequence of the widespread use of antifungal (Srivastava, Singla e Dubey, 2018).

In this context, *Curcuma longa,* popularly named turmeric, emerges as a potential source of therapeutic compounds. Its rhizomes contain three major compounds, curcumin, demethoxycurcumin, and *bis*-desmethoxycurcumin, which are responsible for their medicinal

activities. Curcumin, in particular, garnered attention due to its ability to interact with multiple biological targets, demonstrating effectiveness against several infections caused by bacteria, fungi, protozoa, and helminths (Akaberi, Sahebkar e Emami, 2021). Studies have shown that curcumin and its analogues exhibit activity against various *Candida* species, including drug-resistant strains (Hajifathali *et al.*, 2023), non-dermatophytes filamentous fungi (Nagargoje *et al.*, 2020), and dermatophytes (Brasch, Beck-Jendroschek e Mahn, 2018). Its antifungal activity involves disrupting cell wall integrity and plasma membrane, modulating proteolytic enzyme activity, and altering the membrane-associated properties of ATPase activity (Chen *et al.*, 2018; Kumar *et al.*, 2014; Lee e Lee, 2014). However, despite its promising antifungal potential, the clinical application of curcumin is limited by its poor solubility and bioavailability(Nelson *et al.*, 2017). This challenge has led to the synthesis and exploration of curcumin analogs, which aim to retain the biological efficacy of curcumin while overcoming its pharmacokinetic limitations (Noureddin, El-Shishtawy e Al-Footy, 2019).

Herein, we explored the antifungal activity of curcumin and its analogs. The most active compound, 3,3'-dimethoxycurcumin (DMC), was selected for detailed bioassays, including its effects when combined with the antimycotic drugs. Also, we investigated the DMC mode of action using ergosterol binding and sorbitol protection assays. In addition, the toxicity of DMC was evaluated against *Galleria mellonella* larvae.

Material and methods

Curcumin and its analogs

Curcumin (CAS number: 458-37-7) and all reagents were purchased from Merck® (Kenilworth, USA). Synthesis, purification, and identification of curcumin analogs were carried out according to our previous works (Pereira *et al.*, 2021; Polaquini *et al.*, 2019; Sanches *et al.*,

2019; Sardi *et al.*, 2017b). The ^{1}H and ^{13}C NMR spectra of curcumin analogs **1**–**10** and their detailed analyses were presented in Supplementary Material (Table S1 and Figures S1–S20).

Microorganisms and culturing conditions

Reference strains and clinical isolates of dermatophytes and *Candida* spp. were tested. The reference strains were purchased from the American Type Culture Collection (ATCC) and CBS-KNAW Fungal Biodiversity Center (CBS) and included: *C. albicans* ATCC 90028, *C. albicans* MIA2876, *Candida krusei* ATCC 40147, *C. krusei* ATCC 6258, *C. parapsilosis* ATCC 22019, *C. tropicalis* ATCC 13803, *C. tropicalis* ATCC 750 and *Trichophyton rubrum* CBS 118892. Clinical isolates of *C. albicans*, *C. krusei, C. parapsilosis*, *C. tropicalis*, *Epidermophyton floccosum*, *Microsporum canis*, *T. mentagrophytes* and *T. rubrum* were obtained from the collection of the Laboratory of Mycology, Department of Dermatological, Infectious, and Parasitic Diseases, São José do Rio Preto Medical School (FAMERP), São José do Rio Preto, Brazil (Lemes *et al.*, 2021, 2022). All clinical isolates used in this study and their origin were presented in Supplementary Material (Table S2). Yeasts were subcultured on Sabouraud Dextrose Agar (SDA) (Difco Laboratories, Detroit, MI, USA) for 24 h at 30 °C and dermatophytes on Potato Dextrose Agar (Difco Laboratories, Detroit, MI, USA) for 7 days at 36 °C.

Antifungal susceptibility assays

Antifungal susceptibility assays were determined by the broth microdilution method in 96-well microtiter plates, following the protocol of Clinical and Laboratory Standards Institute(CLSI, 2008a; b) guidelines M27-A3 (Reference Method for Broth Dilution Antifungal Susceptibility Testing of Yeasts) and M38-A2 (Reference Method for Broth Dilution Antifungal Susceptibility Testing of Conidium-Forming Filamentous Fungi), with minor modifications. The culture media and the reference antifungal drugs were purchased from Sigma-Aldrich®

(St. Louis, MO, USA). Briefly, compounds at 250 μg mL^{-1} in 10% DMSO in RPMI-1640 medium were two-fold diluted in RPMI-1640 medium buffered with MOPS (4-morpholinepropanesulfonic acid) and 2% glucose, then put into 96-well microtiter plates. Each aliquot of 100 μL microdilutions was inoculated with 100 μL of standardized fungal suspensions adjusted to the 0.5 McFarland scale, equivalent to 90% transmittance for *Candida* species and 70% for dermatophytes, using a Biospectro SP22 spectrophotometer at 530 nm. Dermatophyte suspension was further diluted at 1:50. The final testing concentrations were 0.5×10^6 cells mL^{-1} for *Candida* and 5×10^4 cells mL^{-1} for dermatophytes.

Growth and sterility controls were included for each assay, and all tests were performed in triplicate in two independent experiments. DMSO (2.5%) was used as a negative control to ensure that its concentration did not interfere with fungal growth. The reference antifungal drugs were selected based on their clinical applications: fluconazole was used against *C. albicans, C. tropicalis, C. krusei,* and *C. parapsilosis* and terbinafine was used as a reference antifungal drug against dermatophytes. The plates were incubated at 30 °C for 24 h for *Candida* strains and at 36 °C for five days for dermatophyte strains. MIC_{50} values were determined by optical density recorded by the plate reader ELISA at 530 nm and defined as the lowest concentration of compounds that inhibited fungal growth by 50%.

After the MIC_{50} values determination, aliquots (100 μL) from each well, which did not demonstrate visible turbidity, were subcultured on SDA plates and incubated at 30 °C for 24 h (*Candida* spp.) and 36 °C for five days (dermatophytes). The minimum fungicidal concentration (MFC) was the lowest concentration not showing fungal colonies on the agar plates (Lemes *et al.*, 2021).

Checkerboard assay

Interactions between DMC and antifungal drugs (fluconazole and terbinafine) were investigated by the checkerboard assay(Spitzer, Robbins e Wright, 2017). Briefly, antifungal drugs and

DMC were serially diluted two-fold along the X and Y axes of a 96-well plate, respectively. The final concentrations ranged from 16–0.03 μg mL^{-1} for terbinafine, 32–0.1 μg mL^{-1} for fluconazole and from 31.2–0.01 μg mL^{-1} for DMC. Plates were inoculated with DMC-susceptible strains and incubated in the same conditions described for the antifungal susceptibility assay. Fungal growth was assessed visually, and the fractional inhibitory concentration index (FICI) for each combination was calculated as follows: FICI = (MIC of the drug when combined with DMC / MIC of the drug alone) + (MIC of DMC when combined with the drug/ MIC of DMC alone). Combinations were classified according to the FICI values suggested (Spitzer et al. 2017): FICI ≤ 0.5 (synergism), FICI =0.5–4 (indifference), and FICI > 4 (antagonism). Three independent experiments were performed for each isolate.

Inhibitory activity of yeast-hyphae transition assay

Candida hyphae inhibition assay was carried out as previously described(Toledo, De *et al.*, 2016), with minor modifications in the incubation period. In order to ensure comparability and reproducibility with existing literature *C. albicans* ATCC 90028, a clinically relevant hyphae-forming strain, was chosen. Growth of *C. albicans* ATCC 90028 from a 24 h culture was transferred to a microplate with RPMI-1640 medium supplemented with 10% fetal bovine serum (FBS) to obtain a final concentration of 2.5×10^3 yeast mL^{-1}. DMC was added to the growth medium at a concentration of 15.5 μg mL^{-1} and incubated for 4 h at 37 °C. Fluconazole (0.25 μg mL^{-1}) was used as a positive control. RPMI-1640 medium supplemented with FBS and DMSO (2.5%) was used as a negative control to ensure that its concentration did not interfere with yeast-hyphae transition. The morphological state of *C. albicans* was analyzed by microscopy using a 40× objective lens on an optical light microscope (Bioval). The assay was performed in three independent experiments, and cells from 4 quadrants of a Neubauer chamber were counted for each experiment. Statistical significance differences in percentages of single cells, budding cells and developing hyphae cells were calculated using one-way ANOVA and

Turkey test with P value of <0.05 indicating statistical significance. Graphs and statistical analyses were performed using GraphPad Prism version 8.0.2 (GraphPad Software, San Diego, CA, USA).

Ergosterol binding assay

The MIC values of DMC were determined by the broth microdilution method(CLSI, 2008a) in the presence and absence of ergosterol (400 mg mL^{-1}) as previously described(Sardi *et al.*, 2017a). An aliquot of 100 µL RPMI-1640 medium was added to 96-well plates and DMC was serially diluted at a ratio of two. In order to obtain concentrations ranging between 2 000 and 0.48 µg mL^{-1}. Amphotericin B (Sigma Chemical Co., St. Louis, MO, USA) was used as a positive control because it is complexing ergosterol in fungal membranes. Yeast growth and media sterility were also checked. The fungal inoculum was prepared and adjusted to a final concentration of 2.5×10^3 CFU mL^{-1} in the wells. The plates were incubated at 35 ºC and read after 24 h. The dilution with the lowest concentration of DMC that exhibited no turbidity was determined to be the MIC.

Sorbitol protection assay

The MIC values of DMC were determined by the broth microdilution method(CLSI, 2008a) in the presence and absence of sorbitol (0.8 M) as previously described(Sardi *et al.*, 2017a). Aliquots of fungal inoculum (2.5×10^3 CFU mL^{-1}) prepared with RPMI-1640 previously supplemented with sorbitol (0.8 M) were added to the wells. Yeast growth and media sterility were also included. Caspofungin (Sigma Chemical Co., St. Louis, MO, USA) was used as a positive control. The plates were incubated at 35 ºC and read after 48 h. The dilution with the lowest concentration of DMC that exhibited no turbidity was determined to be the MIC.

Toxicity test against Galleria mellonella larvae

In vivo toxicity was performed on *G. mellonella* larvae. Groups of 5 individuals (250 to 300 mg larvae) in the sixth-instar developmental stage were used for each condition (naïve, inoculated with DMC, positive, and negative control), comprising 20 individuals. For each larva, 5 µL of DMC volume was injected into the last right proleg with a Hamilton syringe model 7000.5KH of 10 µL at a concentration of 125 µg mL^{-1}. The controls were untouched larvae (naïve), larvae inoculated with DMSO 10% (positive control), and DMSO 100% (negative control). After the inoculation, the larvae were maintained at 37 °C for 5 days and mortality was recorded daily (Ignasiak e Maxwell, 2017).

Results and discussion

Antifungal susceptibility assays

In this study, we synthesized a series of curcumin analogs (Table 1). The structure of curcumin analogs was confirmed by their melting point and ^{1}H and ^{13}C Nuclear Magnetic Resonance (NMR) spectral data analyses. All melting points and NMR spectra were the same as presented before (Polaquini *et al.*, 2019) and the structures, melting points, yields, and NMR spectra are presented in Supplementary Material.

Table 1 Structures of curcumin and its analogs

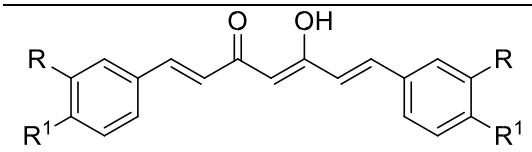

Compound	**R**	**R^1**
Curcumin	OH	OCH_3
1 (DMC)	OCH_3	H
2	H	OCH_3
3	$O(C=O)CH_3$	H
4	H	CH_3
5	H	CF_3
6	OH	H
7	H	OH
8	H	F
9	H	H
10	Cl	Cl

Curcuminoids **1**, **2**, **4**-**10** were achieved by one-step synthesis, resulting in yields of 63–93%. Curcuminoid **3** was synthesized by acetylation of curcuminoid **6** using acetic anhydride and pyridine, resulting in a yield of 87%. Out of ten curcumin analogs, six compounds presented fungal growth inhibition against dermatophytes and *Candida* species (Table 2).

Table 2 Minimum inhibitory concentration values (MIC) of curcumin and its analogs against *Candida* and dermatophyte species.

MIC_{50} intervals in µg mL^{-1}

Species (n)	CUR	DMC	2	3	4	5	6	7	8	9	10	FCZ	TER
Ca ATCC 90028	>62.5	31.2	>62.5	>62.5	>62.5	>62.5	>62.5	>62.5	>62.5	>62.5	>62.5	1–2	–
Ca (3)	>62.5	31.2	>62.5	>62.5	>62.5	>62.5	>62.5	>62.5	>62.5	>62.5	>62.5	0.25-1	–
Ca *	31.2	31.2	>62.5	31.2	>62.5	31.2	31.2	31.2	>62.5	>62.5	31.2	>512	–
Ck ATCC 40147*	>62.5	15.6	>62.5	>62.5	>62.5	>62.5	>62.5	>62.5	>62.5	>62.5	>62.5	16–32	–
Ck (3)*	>62.5	31.2	>62.5	>62.5	>62.5	>62.5	>62.5	>62.5	>62.5	>62.5	>62.5	16–32	–
Cp ATCC 22019	31.2	>62.5	31.3	>62.5	>62.5	>62.5	31.2	>62.5	>62.5	>62.5	>62.5	1	–
Cp (3)	>62.5	>62.5	>62.5	>62.5	>62.5	>62.5	31.2	>62.5	>62.5	>62.5	31.2	0,5–1	–
Ct ATCC 13803	>62.5	31.2	>62.5	>62.5	>62.5	31.2	>62.5	>62.5	>62.5	31.2	>62.5	0,25–2	–
Ct (3)	>62.5	31.2–62.5	>62.5	>62.5	31.2	>62.5	>62.5	>62.5	>62.5	>62.5	>62.5	0.5–4	–
Ct*	>62.5	62.5	>62.5	>62.5	>62.5	>62.5	>62.5	>62.5	>62.5	>62.5	>62.5	>512	–
Ef (2)	>62.5	2.9–62.5	>62.5	31.2	>62.5	>62.5	>62.5	>62.5	31.2	31.2	31.2	2	0.06
Mc (2)	>62.5	>62.5	>62.5	>62.5	>62.5	31.2	31.2	>62.5	>62.5	>62.5	>62.5	0.5–2	0.01–0.03
Tm(2)	>62.5	31.2–62.5	>62.5	>62.5	>62.5	>62.5	31.2	>62.5	>62.5	>62.5	>62.5	2–8	0.03–0.12
Tr CBS 118892	>62.5	3.9	>62.5	>62.5	>62.5	>62.5	31.2	>62.5	>62.5	>62.5	>62.5	0.5–4	0.01–0.06
Tr (2)	>62.5	1.9–62.5	>62.5	>62.5	>62.5	>62.5	31.2	>62.5	>62.5	>62.5	>62.5	0.5–1	0.01–0.03

Ca = *C. albicans*; Ck = *C. krusei;* Cp = *C. parapsilosis*; Ct = *C. tropicalis*; Ef= *E. floccosum*; Mc= *M. canis*; Tm= *T. mentagrophytes*; Tr= *T. rubrum*; n = number of clinical isolates; * Azole-resistant strains; CUR = curcumin; DMC = 3,3'-dimethoxycurcumin; FCZ = fluconazole; TER = terbinafine; – = not tested.

In literature, the studies of bioactive curcumin analogs have focused on the reactive α, β-unsaturated carbonyl bridge and there are few data about the effect of aromatic ring substituents on biological activities. Herein, we evaluated the groups methoxyl, acetoyl, methyl, trifluoromethyl, hydroxyl, fluorine, and chlorine. 3,3'Dimethoxycurcumin **(**DMC**)** exhibited the broadest spectrum and highest potency among the tested compounds, reducing the growth of *Candida* and dermatophyte species, including standard strains and clinical isolates, with MIC values ranging from 1.9 to 62.5 μg mL^{-1}. In addition, azole-resistant strains of *C. albicans*, *C. krusei* (inherently resistant species), and *C. tropicalis* were susceptible to DMC (MIC 15.6 μg mL^{-1} to 62.5 μg mL^{-1}). The substitution by methoxyl groups was investigated in curcumin analogs, suggesting that the methoxyl group played a key role on anti-inflammatory and antioxidant activities (Jankun et al. 2016). The antifungal effect of the methoxyl group against *Candida* species was explored in chalcones and the number and position of the methoxyl group was crucial for the anti-*Candida* activity (Marques *et al.*, 2019).

Curcumin exhibited low antifungal activity against the strains in the concentrations assessed. Previous investigations of anti-*Candida* activity of curcumin used concentrations higher than those used in this study. Some authors reported MIC values ranging from 100 μg mL^{-1} to 2000 μg mL^{-1} against planktonic cells of *C. albicans* (Alalwan *et al.*, 2017; Shahzad *et al.*, 2014) and 500 μg mL^{-1} to 1000 μg mL^{-1} against planktonic cells of *C. tropicalis*[31].

The strains of *C. parapsilosis* were not susceptible to DMC in the concentration range tested. The lack of activity against *C. parapsilosis* can be related to differential genome and phenotype when compared to other CTG clade species, including *C. tropicalis* and *C. albicans* (Holland *et al.*, 2014; Iracane *et al.*, 2018; Pryszcz *et al.*, 2013). Several genes present in *C. parapsilosis* are absent in the genome of *C. albicans* like *CPAG_00563*, *CPAG_00817*, *CPAG_01781*, *CPAG_03408*, *CPAG_03503*, *CPAG_04790*, *CPAG 05383* (Nosek et al. 2009). The intron sizes between *C. parapsilosis* and other CTG clade species also presents significant

differences. *C. albicans*, *C. dubliniensis*, and *C. tropicalis* demonstrate shorter introns (19 to 22 nucleotides) than *C. parapsilosis* introns (up to 840 nucleotides). This intron size variation may have implications for gene regulation and alternative mechanisms for regulating the unfolded protein response in different *Candida* species(Iracane *et al.*, 2018). Another significant difference can be observed in the phenotypic screen, including the role of CPH2 in the hypoxic response of *C. parapsilosis*, but not in *C. albicans*. In *C. albicans*, CPH2 is a regulator of hyphal growth with no known hypoxic role (Holland *et al.*, 2014)**.**

Clinically important dermatophyte species such as *E. floccosum*, *T. mentagrophytes* and *T. rubrum* were susceptible to DMC (MIC 1.9 µg mL^{-1} to 62.5 µg mL^{-1}). Few studies described the effect of curcumin against dermatophytes, one study reported no inhibition against the clinical isolates of *E. floccosum*, *T. mentagrophytes* and *T. rubrum* dermatophytes (MIC > 10000 µg mL^{-1})(Apisariyakul, Vanittanakom e Buddhasukh, 1995). Curcumin associated with photodynamic therapy (420 nm LED) displayed *in vitro* antidermatophytic effect against clinical isolates of *T. rubrum* (Brasch, Beck-Jendroschek e Mahn, 2018), with MIC values ranging from 2500 to 5000 µg mL^{-1}.

DMC exhibited fungistatic action against all sensitive *Candida* and dermatophyte species, with MFC values exceeding 62.5 µg mL^{-1}. Azoles exhibit fungistatic action and are the largest group of antifungal drugs in current pharmacotherapy. Some studies highlighted that although fungicidal therapies, such as polyenes (e.g., amphotericin B), demonstrate higher initial cure rates and reduced microbial persistence compared to fungistatic therapies, they also demonstrated a risk of renal toxicity. This nephrotoxicity has been linked to increased mortality, longer hospital stays, and higher healthcare costs(Kumar *et al.*, 2018). Therefore, for certain systemic mycoses, the use of amphotericin B has been replaced by triazoles due to its toxicity(Ali Malayeri, Rezaei e Raiesi, 2018). DMC demonstrated MIC values that were either lower or similar to fluconazole for clinically important fungal species.

Its effectiveness against fluconazole-resistant strains indicated DMC could be a viable alternative or complementary treatment. While MIC values of DMC were higher than those of amphotericin B, the clinical use of this polyene is often limited due to its severe side effects. In summary, the low MIC values displayed by DMC and its effectiveness against azole-resistant strains encouraged us to select it for detailed antifungal and toxicity investigations.

Checkerboard assay

The synergetic effects of DMC with antifungal drugs (fluconazole and terbinafine) were evaluated by checkerboard assay and expressed as FICI values (Table 3). The DMC-fluconazole combination against *Candida* species and the DMC-terbinafine against *T. rubrum* demonstrated FICI values of 0.7 and 1.5, respectively, indicating an indifferent combination. However, a synergistic association was established between DMC and terbinafine (FICI = 0.3) against *T. mentagrophytes* and *E. floccosum*. The combination of antifungal agents to combat dermatomycosis has numerous advantages over conventional monotherapy. In particular, the combinations of drugs can delay or prevent the development of resistance by fast action of dermatophyte population, which has slower growth than yeasts. Other traditional advantages of association between antifungal compounds include the action in new antifungal molecular targets as well as the reduction of toxicity (Spitzer, Robbins e Wright, 2017). In this context, the synergistic combination between DMC and terbinafine can have promising therapeutic relevance.

Table 3. Antifungal effect of the combination between 3,3'-dimethoxycurcumin (DMC) and terbinafine (TER) or fluconazole (FCZ) against *Candida* and dermatophyte species.

Strains	Combination	MIC (µg mL^{-1})				FICI	Type of
		Alone		Combined			
		combination					
		DMC	d	**DMC**	d	$FICI_{dmc} + FIC_d$	
Ca ATCC 90028	**DMC** + FCZ	31.2	1	0.5	1	1	Indifferent
Ca1	**DMC** + FCZ	31.2	0.5	31.2	0.2	1.5	Indifferent
Ca2	**DMC** + FCZ	31.2	0.2	15.6	0.2	1.5	Indifferent
Ca3	**DMC** + FCZ	31.2	0.2	7.8	0.1	0.7	Indifferent
Ck ATCC 40147	**DMC** + FCZ	31.2	32	3.9	16	0.6	Indifferent
Ck1	**DMC** + FCZ	31.2	32	7.8	16	0.7	Indifferent
Ck2	**DMC** + FCZ	31.2	16	3.9	16	1.1	Indifferent
Ck3	**DMC** + FCZ	31.2	32	31.2	16	1.5	Indifferent
Ct ATCC 13803	**DMC** + FCZ	31.2	2	7.8	1	0.7	Indifferent
Ef2	**DMC** + TER	2.9	0.06	0.06	0.01	0.3	Synergistic
Tm2	**DMC** + TER	31.2	0.12	0.5	0.03	0.3	Synergistic
Tr CBS 118892	**DMC** + TER	3.9	0.2	1	0.12	0.7	Indifferent
Tr1	**DMC** + TER	1.9	0.03	1.9	0.03	1	Indifferent

Ca = *C. albicans*; Ck = *C. krusei*; Cp = *C. parapsilosis*; Ct = *C. tropicalis*; Ef= *E. floccosum*; Mc= *M. canis*; Tm= *T. mentagrophytes*; Tr= *T. rubrum*; DMC = 3,3'-dimethoxycurcumin; d = drug; FCZ = fluconazole; TER = terbinafine.

Inhibitory activity of yeast-hyphae transition assay

Candida species possess an arsenal of virulence factors. Among these, biofilm formation is a relevant barrier to antifungal therapy. In this context, the yeast-to-hyphae transition is a prerequisite for biofilm development by *Candida* species (Ramage *et al.*, 2002) . The transition from planktonic to filamentous cells and its ability to form biofilms are essential virulence strategies of *Candida* species, allowing their adhesion, colonization, and destruction of host tissues (Chen *et al.*, 2020). Therefore, inhibiting yeast-hyphal transition is a way to reduce invasive processes.

In order to investigate the impact of DMC on *Candida* hyphal formation, the morphological changes of *C. albicans* ATCC 90028 were microscopically analyzed. The percentages of single, budding, and developing hyphae cells after the treatment with fluconazole and DMC are presented in Figure 1. The data indicated a significant reduction in hyphal development when cells were treated with DMC at sub-MIC (15.6 μg mL^{-1}), with a mean difference of 5.612, representing 80% reduction compared to untreated cells, where hyphal development was 7%. In contrast, fluconazole exhibited a mean difference of 2.536, representing a reduction of approximately 30%, which was not statistical significant from the non-treated cells. A similar reduction of yeast-to-hyphae transition was observed in another study using curcumin analogs, which also inhibited biofilm formation, highlighting the potential of curcumin and its analogs to overcome biofilm-related drug resistance (Dong *et al.*, 2021).

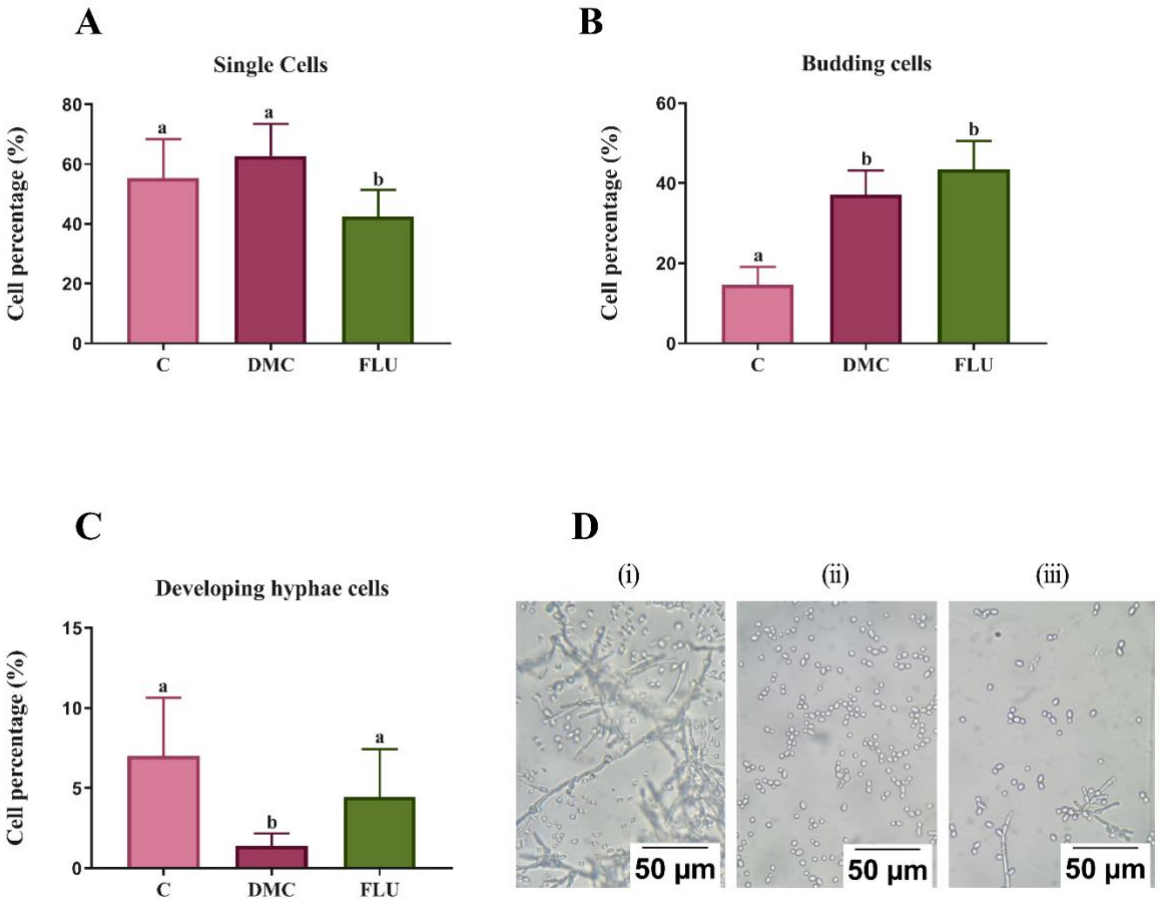

Figure 1. Effect of 3,3'-dimethoxycurcumin and fluconazole on single (**A**), budding (**B**) and developing hyphae cells (**C**) of *C. albicans* ATCC 90028. Non-treated cells (C, pink bar); 3,3'-dimethoxycurcumin (DMC, red bar); fluconazole (FLU, green bar). Cell percentages are referenced to the total cell population (single, budding and developing hyphae cells) in an image, which was set to 100%. Data represents means ± SD of three independent experiments. Statistical analysis was performed by one-way ANOVA and Turkey's test using GraphPad Prism software. Groups with different lowercase letters (a and b) were significantly different ($p \leq 0{\cdot}05$). (**D**) Images taken of *C. albicans*: (i) Control (cells non-treated with DMC or fluconazole); (ii) cells after treatment with a sub-inhibitory concentration of DMC (15.6 µg mL^{-1}); (iii) cells after treatment with a sub-inhibitory concentration of fluconazole (0.25 µg mL^{-1}).

Ergosterol binding and sorbitol protection assays

In order to evaluate the action of DMC on the fungal membrane and cell wall, we performed ergosterol binding and sorbitol protection assays, respectively. Values of MIC were determined in the presence and absence of ergosterol or sorbitol (Table 4).

The ergosterol binding assay indicated that MIC values of DMC were increased from 31.2 µg mL^{-1} (absence of ergosterol) to 250 µg mL^{-1} (presence of ergosterol), evidencing its ability to interact with exogenous ergosterol and reducing its interaction with membrane ergosterol of *C. albicans*, *C. krusei* and *C. tropicalis*. Amphotericin B was used as a positive control due to its ability to complex ergosterol in fungal membranes (Ciesielski *et al.*, 2016). The MIC value for amphotericin B increased 16 and 32 times in the presence of exogenous ergosterol.

Table 4. MIC values (in µg mL^{-1}) of 3,3'-dimethoxycurcumin (DMC) and antifungal drugs in the absence and presence of ergosterol or sorbitol against *Candida* species.

	Absence of ergosterol			Presence of ergosterol			Absence of sorbitol			Presence of sorbitol		
	Ca	**Ck**	**Ct**	**Ca**	**Ck**	**Ct**	**Ca**	**Ck**	**Ct**	**Ca**	**Ck**	**Ct**
DMC	31.2	15.6	31.2	250	125	250	31.2	15.6	31.2	31.2	15.6	31.2
AMB	0.5	0.5	0.5	16.0	16.0	8.0	–	–	–	–	–	–
CPF	–	–	–	–	–	–	0.5	0.2	0.2	15.6	15.6	7.8

Ca = *C. albicans* MIA2876; Ck = *C. krusei* ATCC 6258; Ct = *C. tropicalis* ATCC 750; DMC = 3,3'dimethoxycurcumin; AMB = amphotericin B; CPF = caspofungin; – = not tested.

The sorbitol protection assay aimed to establish the MIC in growth conditions in the presence and absence of sorbitol, a known fungal osmotic protector(Frost *et al.*, 1995). MIC values of DMC were not changed in the presence of sorbitol, indicating no action on the cell wall of *Candida* species. Caspofungin was used as a positive control due to its mechanism of action on cell walls(Hao *et al.*, 2013). MIC values of caspofungin were enhanced 31, 78 and 39 times in the presence of sorbitol for *C. albicans*, *C. krusei* and *C. tropicalis*, respectively. Our study indicated that DMC might target the *Candida* membranes, complexing ergosterol. Despite slight structural differences between DMC and curcumin, both compounds might have similar modes of action. It was reported that curcumin is inducing changes in membrane potential and disruption of the *C. albicans* membrane(Lee e Lee, 2014).

Toxicity against Galleria mellonella assay

In vivo toxicity of DMC was performed against *G. mellonella* larvae. After treatment with the vehicle control (DMSO 10%) and DMC (125 µg mL^{-1}), larval survival was 100% over five days. After 24 h of intra-haemocoelic administration, DMSO 100% solution was able to cause 100% larval lethality. *G. mellonella* has been used as a consolidated model to test the toxicity of compounds and antifungal efficacy (Jemel *et al.*, 2020). In many instances, a significant correlation between larval models and mammalian models has been reached (Harding *et al.*, 2013). Moreover, *G. mellonella* has advantages compared to conventional mammal models, including rapidity and low costs during experimentation (Bokhari *et al.*, 2017).

Limitations and propose avenues for future research

This study marks a significant step in understanding the antifungal properties of curcumin analogs, particularly DMC, against a range of dermatophytes and Candida species. While the findings are promising, it is important to recognize its limitations and identify areas for further research. The differential susceptibility of fungal species to DMC, as observed

with *C. parapsilosis*, highlights the necessity for more in-depth studies into species-specific responses and resistance mechanisms. Additionally, the *in vitro* nature of the study, though pivotal for initial screening, paves the way for *in vivo* investigations to fully assess the therapeutic potential and safety in more complex biological systems. Future studies focusing on the mechanisms of action, especially in the context of drug resistance, will deepen our understanding and guide the development of more effective antifungal strategies. Overall, this research lays a strong foundation for future work, opening new avenues in the fight against fungal infections.

Conclusions

In brief, we have systematically evaluated curcumin and ten analogs against a panel of dermatophyte and *Candida* species. DMC was the most potent compound, with the broadest spectrum of action, including azole-resistant strains. Its synergistic effects with terbinafine, coupled with the ability to impede ergosterol interactions and inhibit hyphal development in *Candida* species, underscore its potential as a treatment for dermatomycosis. The absence of toxicity in *G. mellonella* larvae in our studies reinforces DMC's potential for safe therapeutic application. These results significantly contribute to the field of antifungal research, offering new insights and avenues for developing more effective treatments for widespread fungal infections, potentially altering the landscape of current antifungal treatment strategies.

References

ACHTERMAN, R. R.; WHITE, T. C. Dermatophyte virulence factors: identifying and analyzing genes that may contribute to chronic or acute skin infections. **International Journal of Microbiology**, v. 2012, p. 358305, 2012.

AKABERI, M.; SAHEBKAR, A.; EMAMI, S. A. Turmeric and Curcumin: From traditional to modern medicine. *Em*: **Studies on Biomarkers and New Targets in Aging Research in Iran** . [s.l: s.n.]. v. 1291p. 15–39.

ALALWAN, H. *et al.* The anti-adhesive effect of curcumin on *Candida albicans* biofilms on denture materials. **Frontiers in Microbiology**, v. 8, p. 669, 2017.

ALBUQUERQUE MARANHÃO, F. C. DE *et al.* Mycoses in northeastern Brazil: epidemiology and prevalence of fungal species in 8 years of retrospective analysis in Alagoas. **Brazilian Journal of Microbiology**, v. 50, n. 4, p. 969–978, 2019.

ALI MALAYERI, F.; REZAEI, A.; RAIESI, O. Antifungal agents: Polyene, azole, antimetabolite, other and future agents. **Journal of Basic Research in Medical Sciences**, v. 5, n. 2, p. 48–55, 2018.

APISARIYAKUL, A.; VANITTANAKOM, N.; BUDDHASUKH, D. Antifungal activity of turmeric oil extracted from *Curcuma* longa (Zingiberaceae). **Journal of Ethnopharmacology**, v. 49, n. 3, p. 163–169, 1995.

BAERT, F. *et al.* Updating the taxonomy of dermatophytes of the BCCM/IHEM collection according to the new standard: a phylogenetic approach. **Mycopathologia**, v. 185, p. 161–168, 2020.

BOKHARI, H. *et al. Galleria mellonella* is low cost and suitable surrogate host for studying virulence of human pathogenic *Vibrio cholerae*. **Gene**, v. 628, p. 1–7, 2017.

BRASCH, J.; BECK-JENDROSCHEK, V.; MAHN, V. Photochemical inhibition of *Trichophyton rubrum* by different compoundings of curcumin. **Mycoses**, v. 61, n. 6, p. 393–399, 2018.

CHEN, E. *et al.* Fungal-host interaction: Curcumin modulates proteolytic enzyme activity of *Candida albicans* and inflammatory host response *In Vitro*. **International Journal of Dentistry**, v. 2018, p. 2393146, 2018.

CHEN, H. *et al.* The regulation of hyphae growth in *Candida albicans*. **Virulence**, v. 11, n. 1, p. 337–348, 2020.

CIESIELSKI, F. *et al.* Recognition of membrane sterols by polyene antifungals amphotericin B and natamycin, A (13)C MAS NMR study. **Frontiers in Cell and Developmental Biology**, v. 4, p. 57–68, 2016.

CLSI. Reference method for broth dilution antifungal susceptibility testing of yeasts; approved standard—Third Edition. **CLSI document M27-A3**, v. 28, n. April, 2008a.

CLSI. Reference method for broth dilution antifungal susceptibility testing of filamentous fungi; approved standard—Second Edition. **CLSI document M38-A2**, v. 28, n. April, 2008b.

DONG, H. *et al.* Synergistic antifungal effects of curcumin derivatives as fungal biofilm inhibitors with fluconazole. **Chemical Biology & Drug Design**, v. 97, n. 5, p. 1079–1088, 2021.

FROST, D. J. *et al.* A whole-cell *Candida albicans* assay for the detection of inhibitors towards fungal cell wall synthesis and assembly. **The Journal of Antibiotics**, v. 48, n. 4, p. 306–310, 1995.

HAJIFATHALI, S. *et al.* Investigation of the antifungal effects of curcumin against nystatin-resistant *Candida albicans*. **Dental Research Journal**, v. 20, p. 50, 2023.

HAO, B. *et al.* Caspofungin Kills *Candida albicans* by Causing both cellular apoptosis and necrosis. **Antimicrobial Agents and Chemotherapy**, v. 57, n. 1, p. 326–332, 2013.

HARDING, C. R. *et al.* Use of *Galleria mellonella* as a model organism to study *Legionella pneumophila* Infection. **Journal of Visualized Experiments**, n. 81, 2013.

HOLLAND, L. M. *et al.* Comparative phenotypic analysis of the major fungal pathogens *Candida parapsilosis* and *Candida albicans*. **PLoS Pathogens**, v. 10, n. 9, p. e1004365, 2014.

IGNASIAK, K.; MAXWELL, A. *Galleria mellonella* (greater wax moth) larvae as a model for antibiotic susceptibility testing and acute toxicity trials. **BMC Research Notes**, v. 10, n. 1, p. 428, 2017.

IRACANE, E. *et al.* Identification of an exceptionally long intron in the *HAC1* gene of *Candida parapsilosis*. **mSphere**, v. 3, n. 6, p. e00532-18, 2018.

JEMEL, S. *et al. Galleria mellonella* for the Evaluation of Antifungal Efficacy against Medically Important Fungi, a Narrative Review. **Microorganisms**, v. 8, n. 3, p. 390, 2020.

KUMAR, A. *et al.* Curcumin targets cell wall integrity via calcineurin-mediated signaling in *Candida albicans*. **Antimicrobial Agents and Chemotherapy**, v. 58, n. 1, p. 167–175, 2014.

KUMAR, ANAND *et al.* Fungicidal versus fungistatic therapy of invasive *Candida* infection in non-neutropenic adults: a meta-analysis. **Mycology**, v. 9, n. 2, p. 116–128, 2018.

LEE, W.; LEE, D. G. An antifungal mechanism of curcumin lies in membrane-targeted action within *Candida albicans*. **IUBMB Life**, v. 66, n. 11, p. 780–785, 2014.

LEMES, T. H. *et al.* In vitro antifungal activity of *Candida* culture extracts against *Trichophyton rubrum* and *Trichophyton mentagrophytes*. **Brazilian Journal of Case Reports**, v. 1, n. 4, p. 135–152, 2021.

LEMES, T. H. *et al*. *Candida parapsilosis* culture extracts: in vitro, antagonistic action against *Candida albicans*, *Candida auris* and *Candida parapsilosis*. **Brazilian Journal of Case Reports**, v. 3, n. 1, p. 24–29, 2022.

MARQUES, B. C. *et al.* Methoxychalcones: Effect of methoxyl group on the antifungal, antibacterial and antiproliferative activities. **Medicinal Chemistry**, v. 16, n. 7, p. 881–891, 2019.

MELLO, V. G. *et al.* Virulence factors and antifungal susceptibility in *Candida* species isolated from dermatomycosis patients. **Mycopathologia**, v. 186, n. 1, p. 71–80, 2021.

NAGARGOJE, A. A. *et al.* Quinoline based monocarbonyl curcumin analogs as potential antifungal and antioxidant agents: synthesis, bioevaluation and molecular docking study. **Chemistry and Biodiversity**, v. 17, n. 2, p. e1900624, 2020.

NELSON, K. M. *et al.* The essential medicinal chemistry of curcumin. **Journal of Medicinal Chemistry**, v. 60, n. 5, p. 1620–1637, 2017.

NOUREDDIN, S. A.; EL-SHISHTAWY, R. M.; AL-FOOTY, K. O. Curcumin analogues and their hybrid molecules as multifunctional drugs. **European Journal of Medicinal Chemistry**, v. 182, p. 111631, 2019.

PEREIRA, J. A. *et al.* Antibiofilm and cytotoxic effect of 3,3′-dihydroxycurcumin (DHC) as photosensitizer agent in antimicrobial photodynamic therapy for endodontic purposes. **Photodiagnosis and Photodynamic Therapy**, v. 36, p. 102534,2021.

POLAQUINI, C. R. *et al.* Antibacterial activity of 3,3′-dihydroxycurcumin (DHC) is associated with membrane perturbation. **Bioorganic Chemistry**, v. 90, p. 103031, 2019.

PRYSZCZ, L. P. *et al.* Unexpected genomic variability in clinical and environmental strains of the pathogenic yeast *Candida parapsilosis*. **Genome Biology and Evolution**, v. 5, n. 12, p. 2382–2392, 2013.

RAMAGE, G. *et al.* The filamentation pathway controlled by the Efg1 regulator protein is required for normal biofilm formation and development in *Candida albicans*. **FEMS Microbiology Letters**, v. 214, n. 1, p. 95–100, 2002.

SANCHES, C. V. G. *et al.* Diacetylcurcumin: a new photosensitizer for antimicrobial photodynamic therapy in *Streptococcus mutans* biofilms. **Biofouling**, v. 35, n. 3, p. 340–349, 2019.

SARDI, J. DE C. O *et al.* Unexplored endemic fruit species from Brazil: antibiofilm properties, insights into mode of action, and systemic toxicity of four *Eugenia* spp. **Microbial Pathogenesis**, v. 105, p. 280–287, 2017a.

SARDI, J. DE C. O. *et al.* Antibacterial activity of diacetylcurcumin against *Staphylococcus aureus* results in decreased biofilm and cellular adhesion. **Journal of Medical Microbiology**, v. 66, n. 6, p. 816–824, 2017b.

SHAHZAD, M. *et al.* Utilising polyphenols for the clinical management of *Candida albicans* biofilms. **International journal of antimicrobial agents**, v. 44, n. 3, p. 269–273, 2014.

SPITZER, M.; ROBBINS, N.; WRIGHT, G. D. Combinatorial strategies for combating invasive fungal infections. **Virulence**, v. 8, n. 2, p. 169–185, 17, 2017.

SRIVASTAVA, V.; SINGLA, R. K.; DUBEY, A. K. Emerging virulence, drug resistance and future anti-fungal drugs for *Candida* pathogens. **Current Topics in Medicinal Chemistry**, v. 18, n. 9, p. 759–778, 2018.

TOLEDO, L. DE *et al.* Essential oil of *Cymbopogon* nardus (L.) rendle: a strategy to combat fungal infections caused by *Candida* Species. **International Journal of Molecular Sciences**, v. 17, n. 8, p. 1252, 2016.

3. Design, synthesis and anti-*Candida* activity of diarylideneacetones inspired by curcumin

Carlos R. Polaquini, Janaina C. O. Sardi, **Veridianna C. Pattini**, Margarete T. G. Almeida, Pedro L. Rosalen, Luis O. Regasini. *Preprint* at SSRN (2024).

Abstract

Infections caused by *Candida* species have considerably increased in recent decades. However, the antifungal agents for the treatment of candidiasis are restricted to a few classes of drugs, which have some therapeutic limitations, including high toxicity, reduced efficacy and resistance development. This perspective encouraged us to design, synthesize and evaluate a series of 24 diarylideneacetones inspired by the structure and bioactivity of curcumin, a natural product with recognized antifungal activity. Structure-activity relationship derived from series I and II suggested hydroxyl groups had a key role in the fungitoxicity. Among antifungal compounds, 3-hydroxy-dibenzylideneacetone was the most active against *Candida* species, with Minimum Inhibitory Concentration (MIC) ranging from 7.8 to 31.2 µM. *Candida albicans* and *Candida krusei* were more susceptible to 3-hydroxy-dibenzylideneacetone than fluconazole, which was used as a reference anti-*Candida* drug. 3-Hydroxy-dibenzylideneacetone at sub-MIC was able to reduce *C. albicans* adhesion onto human gingival fibroblasts and human epidermal keratinocytes. 3-Hydroxy-dibenzylideneacetone inhibited *C. albicans* biofilm formation and biofilm maturation when tested at respective MIC and 10 × MIC. Combinations of 3-hydroxy-dibenzylideneacetone and amphotericin B or fluconazole showed synergistic effects against *C. albicans*, with Fractional Inhibitory Concentration Index (FICI) values of 0.5 and 0.2, respectively. Studies on the fungitoxicity of 3-hydroxy-dibenzylideneacetone indicated a dual action, targeting both the membrane and cell wall of *C. albicans*, thereby compromising cellular integrity. Finally, 3-hydroxy-dibenzylideneacetone was more stable than curcumin in phosphate buffer and demonstrated low acute toxicity against *Galleria mellonella* larvae. These findings open new avenues for studying diarylideneacetones as anti-*Candida* prototypes inspired by the structure and bioactivity of curcumin.

Introduction

Incidence of human fungal infections has considerably increased in the last decades. Various factors have led to this escalation, including an increase in invasive surgical procedures and immunocompromised individuals, as well as the indiscriminate use of antifungal drugs (Stamatiades *et al.*, 2018). Among human fungal pathogens, the species of *Candida* are most frequently related to severe infections, mainly *Candida albicans* (Naglik, Richardson e Moyes, 2014). Nevertheless, candidiasis caused by non-albicans *Candida* species, such as *Candida tropicalis*, *Candida glabrata*, *Candida parapsilosis* and *Candida krusei*, has resurged in recent years (Kołaczkowska e Kołaczkowski, 2016). *Candida* pathogenicity is mediated by several virulence factors, including adherence and biofilm formation on host tissues and abiotic surfaces, including medical devices (Staniszewska, 2020). The treatment against candidiasis is mainly restricted to some antifungal drug classes, including azoles, polyenes and echinocandins (Bellmann e Smuszkiewicz, 2017). In this context, some factors have limited the conventional antifungal therapy, including the low efficacy related to resistance and the high toxicity caused by systemic administrations (Fisher *et al.*, 2018).

Curcumin (**1**) is a phytochemical with a broad spectrum of pharmacological activities, highlighting its antifungal activity against *Candida* species (Khan *et al.*, 2012; Lao *et al.*, 2006; Neelofar *et al.*, 2011). *In vivo* investigations revealed that the application of a vaginal cream containing curcumin was able to reduce the infection of *C. albicans* in rats after six days(Fernandes *et al.*, 2018). Moreover, curcumin inhibits virulence factors of *Candida* species, including adhesion (Alalwan *et al.*, 2017), biofilm (Dovigo *et al.*, 2011) and yeast-to-hyphae transition(Sharma *et al.*, 2010) Although curcumin possesses *in vitro* and *in vivo* anti-*Candida* activities, some factors may hinder its clinical use, such as its poor chemical and metabolic stabilities (Nelson *et al.*, 2017). Studies have correlated these limitations with the presence of the β-diketone subunit, which is susceptible to aldo-keto reductases at physiological pH (Heger

et al., 2014; Rosemond *et al.*, 2004). These chemical-biological barriers can be overcome by substituting the β-diketone with a monoketone group (Shetty *et al.*, 2014). In our previous investigations, we successfully designed open and cyclic monoketone analogs of curcumin by molecular simplification, which were more stable and active than curcumin, highlighting compounds with antibacterial (**2**) (Morão *et al.*, 2019) and antiproliferative activities (**3**)(Lima *et al.*, 2018; Silva *et al.*, 2018) (Figure 1).

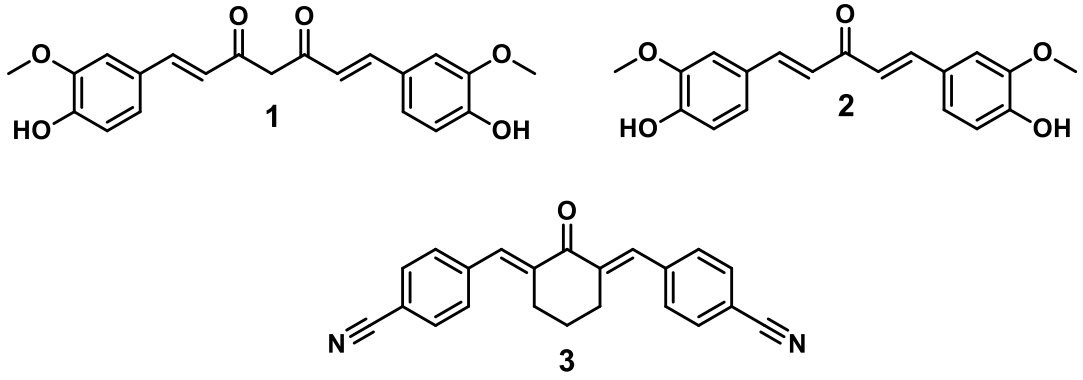

Figure 1. Structure of curcumin (**1**) and its bioactive monoketone analogs (**2** and **3**).

As part of our continuing studies on monocarbonyl analogs of curcumin, we explored a series of 24 diarylideneacetones and their effects against five *Candida* species. The most active compound, 3-hydroxy-dibenzylideneacetone (**17**), was selected for detailed bioassays, including its effect against clinical isolated *Candida* species in combination with fluconazole and amphotericin B. Additionally, we investigated the anti-adhesion and antibiofilm activities as well as preliminary mode of action. In addition, compound **17** was evaluated on chemical stability at physiological pH and *in vivo* toxicity against *Galleria mellonella*.

Material and methods

Design

Our works on antibacterial and antiproliferative monocarbonyl compounds (**2** and **3,** see Figure 1) encouraged us to investigate other monocarbonyl analogs focused on combating *Candida* species. Herein, we designed two series of compounds belonging to diarylideneacetone class. In series I, we explored the relevance of the number and position of hydroxyl and methoxyl groups, which are substituents of the curcumin benzene rings. In series II, we used the most active compound of series I, compound **17**, as a template and evaluated the influence of electron density on its ring B. Two sets of diarylideneacetones of series II were designed, (*i*) analogs with phenyl ring B substituted by electron-withdrawing groups and electron-donating groups and (*ii*) heteroaryl as ring B (Figure 2).

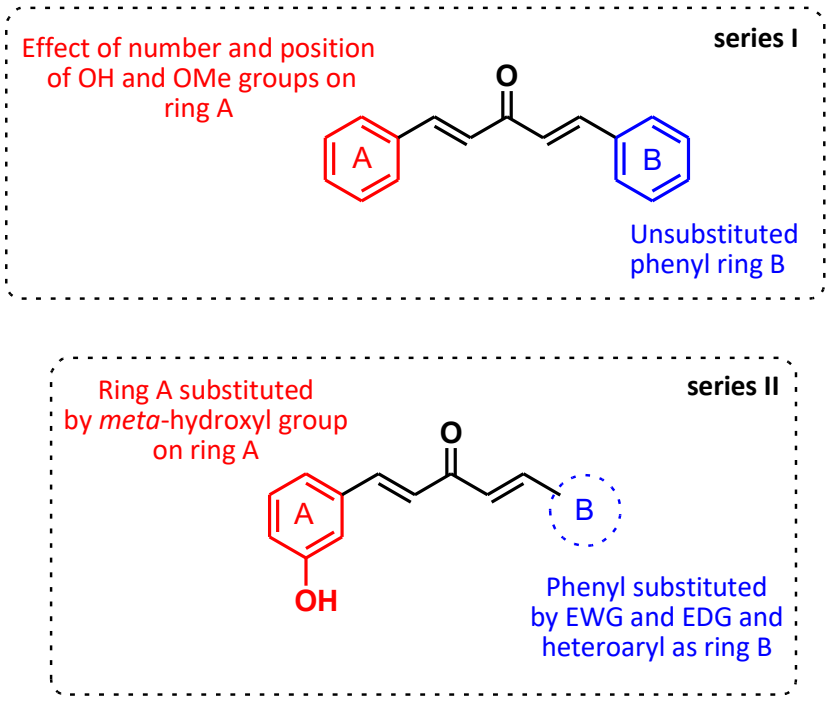

Figure 2. Design of monoketone analogs (diarylideneacetones) of series I and II. EWG = electron-withdrawing groups; EDG = electron-donating groups.

Synthesis

Materials and instruments

All reagents and solvents were purchased from Merck® (Kenilworth, USA). Reactions were monitored using thin-layer chromatography (with fluorescent indicator at 254 nm, Supelco®). Preparative thin-layer chromatography plates of silica-gel with fluorescent indicator at 254 nm (1000 μm, 20 × 20 cm, Analtech®) were used for the purification of compounds. Silica-gel (230−400 mesh, Supelco®) and LH-20 (Sephadex®) (Merck, Kenilworth, USA) were used for column chromatography separations. Melting points were determined in Tecnopon® PFM-IIV apparatus (MS Tecnopon Instrumentação, Piracicaba, Brazil). Nuclear Magnetic Resonance spectra (^{1}H and ^{13}C NMR) were carried out on Bruker Avance III ® spectrometer 14.1 T (600 MHz) (Bruker, Billerica, USA), using $CDCl_3$ or DMSO-d_6 as solvents and tetramethylsilane and residual non-deuterated solvents ($CHCl_3$ and DMSO) were used as internal standards. Chemical shifts (δ) and coupling constants (J) were expressed in ppm and Hz, respectively. Multiplicities were reported as singlets (s), doublets (d) and doublet of doublets (dd).

*Curcumin (**1**) and its monoketone analog (**2**)*

Curcumin was purchased from Merck (Kenilworth, USA). Compound **2** was synthesized, by a reaction between acetone and vanillin, and characterized according to our previous work (Morão *et al.*, 2019).

*Synthesis of compounds **4**–**17***

Compounds **4**–**17** were synthesized in two steps as outlined below, following the methods established in our previous work (Pereira *et al.*, 2021).

Synthesis of benzylideneacetone intermediate

A solution of benzoic aldehyde (80 mmol) in acetone (150 mL) was cooled in an ice bath for 15 min. Acetonic solution of sodium hydroxide (10 mL, 0.5 M) was added and the reaction medium was stirred at room temperature for 3 h. Reaction medium was poured onto crushed ice from deionized water. Crude product was submitted to liquid-liquid extraction with ethyl acetate (4 × 40 mL) and combined organic phases were concentrated under reduced pressure. Benzylideneacetone intermediate was recrystallized in ethanol.

*Synthesis of dibenzylideneacetones **4**–**17***

To a solution of benzylideneacetone intermediate (5.2 mmol) in ethanol (10 mL), the benzaldehyde derivative corresponding to the curcuminoids **4**–**17** substitutes (5.0 mmol) was added (see Table 1 for curcuminoids **4**–**17** substitutes). Catalytic amounts of sulfuric acid were added to the reaction medium and the solution was stirred at room temperature for 48-72 h. Reaction medium was poured onto crushed ice from deionized water to harvest the crude product. Soluble crude product was partitioned with ethyl acetate (3 × 25 mL) and the combined organic phases were concentrated under reduced pressure. Crude products were purified by chromatography column over silica-gel, using mixtures of hexane and ethyl acetate (9:1).

Synthesis of compounds **18**–**20**

Compounds **18**–**20** were synthesized in four steps as outlined below, including the synthesis of benzylideneacetone intermediate previously described.

Protection of hydroxyl groups

A suspension of K_2CO_3 (50 mmol) in dry acetone (25 mL) was cooled in an ice bath for 10 min. The *ortho*-hydroxybenzaldehyde derivative (5 mmol) corresponding to the curcuminoids **18**–**20** substitutes (Table 1) and methoxymethyl chloride (20 mmol) were added. The reaction

mixture was stirred at room temperature for 1 h under N_2 atmosphere. The suspension was diluted with deionized water (25 mL) and the crude product extracted with ethyl acetate (3 × 25 mL). The combined organic layer was concentrated under reduced pressure. Crude products were purified by column chromatography over silica gel using hexane and ethyl acetate as eluents.

Aldol condensation

A solution of respective *ortho*-methoxymethyl-benzaldehyde (2 mmol) and benzylideneacetone intermediate (2.2 mmol) in ethanol (7 mL) was cooled in an ice bath for 10 min. 1 mL of NaOH in ethanol (1 M) was added dropwise to the reaction mixture and stirred at room temperature for 8 h under a N_2 atmosphere. Reaction medium was poured onto crushed ice from deionized water to harvest the crude product. Soluble crude product obtained was partitioned with ethyl acetate (3 × 15 mL), and the combined organic phases were concentrated under reduced pressure. Crude products were purified by column chromatography over silica gel using mixtures of hexane and ethyl acetate as eluents.

*Deprotection of hydroxyl groups and synthesis of compounds **18-20***

A solution of respective methoxymethyl-dibenzylideneacetone (1 mmol) in ethanol (5 mL) and 33% HCl (0.3 mL) was stirred at room temperature for 48 h under N_2 atmosphere. Reaction medium was poured onto crushed ice from deionized water. The mixture obtained from the reaction crude product was partitioned with ethyl acetate (3 × 15 mL), and the combined organic phases were concentrated under reduced pressure. The obtained compounds (**18**-**20**) were purified by preparative thin-layer chromatography on a silica-gel plate using hexane and ethyl acetate (9:1), 0.01% ethanol, and 0.01% acetic acid as eluents.

*Synthesis of analogs **21**–**27***

Compounds **21**–**27** were synthesized in two steps as described below, following the methods established in our previous work (Polaquini *et al.*, 2019).

Synthesis of 3-hydroxybenzylideneacetone intermediate

A solution of 3-hydroxybenzaldehyde (4 mmol) and acetone (1.5 mmol) in ethanol (5 mL) was cooled in an ice bath for 10 min. Catalytic amounts of sulfuric acid dissolved in ethanol (5 mL) were dropwise added to the reaction mixture. The solution was stirred at room temperature for 24 h. Reaction mixture was poured onto crushed ice from deionized water. The crude product was submitted to liquid-liquid extraction with ethyl acetate (3 × 15 mL) and combined organic phases were concentrated under reduced pressure. 3-hydroxybenzylideneacetone intermediate was purified by column chromatography over silica gel using a mixture of hexane and ethyl acetate (3:2) as eluent.

*Synthesis of diarylideneacetones **21**–**27***

A solution of 3-hydroxybenzylideneacetone intermediate (1 mmol) and benzaldehyde derivative or heteroarylcarbaldehyde (1.5 mmol) corresponding to the curcuminoids **21**–**27** substitutes (Table 1) in ethanol (5 mL) was cooled in an ice bath for 10 min. Catalytic amounts of sulfuric acid solubilized in ethanol (5 mL) was added dropwise to the reaction mixture. The solution was stirred at room temperature for 10–48 h. Reaction mixture was poured onto crushed ice from deionized water. The crude product was partitioned with ethyl acetate (3 × 15 mL) and combined phases were concentrated under reduced pressure. Compounds **21**–**27** were purified by gel permeation column chromatography (LH-20) using ethanol as eluent.

Anti-Candida assay

Five strains from American Type Culture Collection (ATCC) were used, including *Candida albicans* ATCC 90028, *Candida tropicalis* ATCC 750, *Candida glabrata* ATCC 90030, *Candida parapsilosis* ATCC 22019 and *Candida krusei* ATCC 6258. Ten clinical *Candida* isolates were used; *C. albicans* 6293, *C. albicans* 6326, *C. tropicalis* 6477, *C. tropicalis* 6559, *C. glabrata* 5136, *C. glabrata* 5361, *C. parapsilosis* 6175, *C. parapsilosis* 6186, *C. krusei* 6473 and *C. krusei* 6347. All clinical isolates were obtained from the collection of Laboratory of Mycology, Department of Dermatological, Infectious and Parasitic Diseases, São José do Rio Preto Medical School, São José do Rio Preto, Brazil(Pattini *et al.*, 2024). Minimum inhibitory concentration (MIC) and minimum fungicidal concentration (MFC) values of 250 to 1.9 μM were determined by the microdilution method according to Clinical & Laboratory Standards Institute (CLSI) protocols. Minor modifications in this protocol and its detailed procedures were reported in our previous works (Pattini *et al.*, 2024; Sardi *et al.*, 2016). Briefly, the designed compounds were prepared in DMSO and tested in concentrations ranging from 250 to 1.9 μM in 10% DMSO and RPMI 1640 medium buffered with MOPS (4-morpholinepropanesulfonic acid, pH 7.0) and 2% glucose. Each aliquot of 100 μL microdilutions in a 96-well microtiter plates was inoculated with 100 μL of standardized fungal suspensions at the concentration of 1×10^6 cells mL^{-1}. Amphotericin B and fluconazole were used as standard antifungal drugs and tested in concentrations ranging from 125 to 0.2 μM in 10% DMSO and the same medium as described above. Three independent assays were performed. MIC value was visually determined as the lowest concentration of the compound that did not produce turbidity. MFC value was defined as the lowest concentration of a compound that allowed no visible growth on solid media. The most active compound, 3-hydroxy-dibenzylideneacetone (**17**), was selected for further studies described below.

Anti-adhesion assay

Effects of 3-hydroxy-dibenzylideneacetone **(17)** against the adhesion of *C. albicans* ATCC 90028 onto human cells was evaluated as previously published (Nani *et al.*, 2020; Sardi, Polaquini, *et al.*, 2017), with minor modifications. Briefly, cell cultures of human epidermal keratinocytes (HaCaT cell line) and human gingival fibroblasts (HGF-1 cell line) were obtained from the Cell Bank of Rio de Janeiro (Brazil). The cells were cultivated in Dulbecco's modified Eagle's medium supplemented with 10% fetal bovine serum (Gibco), penicillin (100 units mL^{-1}), streptomycin (100 μg mL^{-1}), and l-glutamine (200 mM) at 37 °C in a 5% CO_2. HaCat and HGF-1 cells were seeded in a 24-well plates (10^5 cells $well^{-1}$). After the formation of monolayers in the wells, the supernatant was discarded and 500 μL of *C. albicans* ATCC 90028 was added to the wells (10^3 cells $well^{-1}$) in the absence (negative control) or presence of 3-hydroxy-dibenzylideneacetone at sub-inhibitory concentrations (0.25 MIC = 7.8 μM) to maintain the viability of human and fungal cells. The plates were incubated at 37 °C in 5% CO_2 for 2 or 3 h. After incubation, the supernatant containing keratinocytes, fibroblasts and non-adherent yeast cells was discarded. Adherent cells were washed 3 times with sterile phosphate buffered saline (PBS) and then trypsinized. An aliquot of 100 μL of the suspended cells were plated for CFU measurement onto sabouraud dextrose agar (SDA) and incubated at 37 °C in 5% CO_2 for 24 h. Yeast adhesion to keratocytes and fibroblasts were determined in relation to the total number of adherent cells in the untreated control group (negative control). The assays were carried out in triplicates with three independent experiments with separately cultured yeast.

Antibiofilm efficacy of 3-hydroxy-dibenzylideneacetone

The effect of 3-hydroxy-dibenzylideneacetone (**17**) on biofilm formation and on 24 h biofilms of *C. albicans* ATCC 90028 were evaluated as previously described (Sardi *et al.*, 2017a).

Briefly, an aliquot of 100 µL *C. albicans* suspension (10^8 CFU mL^{-1}) in yeast nitrogen base medium (YNB) was added to 96-well plates. The plates were incubated at 37 °C for 2 h to allow *C. albicans* adhesion. The supernatant was removed, and the wells were washed with PBS in order to remove non-adherent cells. The biofilm in formation was treated with 3-hydroxy-dibenzylideneacetone (**17**) at MIC and 10 × MIC (31.2 µM and 312 µM, respectively) in YNB for 24 h at 37 °C. After 24 h, the supernatants were removed, and the biofilms were washed with PBS in order to remove non-adherent cells. The remaining biofilm was homogenized, serially diluted, and plated on SDA. The plates were incubated at 37 °C for 24 h and colonies were counted. The assays were carried out in triplicate with separately grown biofilms. Untreated biofilm was used as a negative control. Amphotericin B at MIC and 10 × MIC, a standard antifungal drug, was used as a positive control.

In order to evaluate the effects of 3-hydroxy-dibenzylideneacetone against 24 h biofilms of *C. albicans*, an aliquot of 100 µL *C. albicans* suspension (10^8 CFU mL^{-1}) in YNB was added to the wells of 96-well plates. The plates were incubated at 37 °C for 24 h to allow biofilm formation. The supernatant was removed, and the biofilms were washed with PBS to remove non-adherent cells. The biofilms were exposed to 3-hydroxy-dibenzylideneacetone (**17)** at MIC and 10 × MIC (31.2 µM and 312 µM, respectively) in YNB for 24 h at 37 °C. After that, the supernatants were removed, and the biofilms were washed in order to remove non-adherent cells. The biofilm was homogenized, serially diluted, and plated on SDA. The plates were incubated at 37 °C for 24 h and colonies were counted. The assays were carried out in triplicates of three independently grown biofilms. Untreated biofilm was used as a negative control and amphotericin B was used as a positive control.

Ergosterol binding and sorbitol protection assays

In order to evaluate the effect of 3-hydroxy-dibenzylideneacetone (**17)** on *C. albicans* membrane ergosterol and cell wall, the ergosterol binding and sorbitol protection assays,

respectively were investigated. MIC values of 3-hydroxy-dibenzylideneacetone (**17)** against *C. albicans* ATCC 90028 in the presence and absence of ergosterol (100 µM) or sorbitol (0.8 µM) were determined by the microdilution technique, as previously described(Sardi *et al.*, 2017a). Briefly, an aliquot of 100 µL RPMI-1640 medium was added to 96-well plates and 3-hydroxy-dibenzylideneacetone was serially diluted at a ratio of two. In order to obtain concentrations ranging between 250 and 1.9 µM. Amphotericin B and caspofungin were used as standard antifungal drugs and tested at the concentrations ranging between 62.5 and 0.03 µM. Three independent assays were performed. The MIC values were visually determined as the lowest concentration of 3-hydroxy-dibenzylideneacetone (**17)** that did not produce any visual turbidity in the wells.

Checkerboard assay

The synergistic efficacy of 3-hydroxy-dibenzylideneacetone (**17)** combined with amphotericin B or fluconazole against *C. albicans* ATCC 90028 were determined as described previously(Sardi *et al.*, 2016). Briefly, antifungal drugs and 3-hydroxy-dibenzylideneacetone were serially diluted two-fold along the X and Y axes of a 96-well plate, respectively. The final concentrations ranged from 125–0.1 µM for fluconazole and amphotericin B and from 125–1.9 µM for 3-hydroxy-dibenzylideneacetone. Checkerboard assay was used to calculate the Fractional Inhibitory Concentration Index (FICI) values, which were used to classify the effects of the combinations as synergistic (FICI < 0.5), additive ($0.5 \geq$ FICI ≥ 1), indifferent ($1 \geq$ FICI > 4) or antagonistic (FICI > 4). The FICI values were calculated and interpreted using the indication of Doern(Doern, 2014).

Acute toxicity assay

Systemic toxicity of 3-hydroxy-dibenzylideneacetone (**17)** against *Galleria mellonella* was determined according to our previous work(Garcia *et al.*, 2021). Briefly, ten larvae (weighing

0.2−0.3 g) were selected for each group. The larvae were chilled on ice for 20 min, and 10 μL of 3-hydroxy-dibenzylideneacetone (2.0, 1.5,1.0, 0.5 and 0.25 mg mL^{-1}) was injected into the hemocoel of each larva via the last left proleg using a 25 μL syringe. All groups were incubated at 37 °C, and their survival was monitored for up to 96 h. The larvae showing high myelinization and absence of movements upon touch were counted as dead. The toxicity was performed in three independent assays. Larvae groups injected with 12.5% DMSO which was used as the solvent or 0.9% saline were used as negative controls**.**

Chemical stability assay

The chemical stability of 3-hydroxy-dibenzylideneacetone (**17)** (at λ_{max} 362 nm) and curcumin (at λ_{max} 426 nm) were analyzed by monitoring their UV–vis absorptions in phosphate buffer (pH 7.4) at 37 °C according to our previous work(Polaquini *et al.*, 2019). Compounds were solubilized in DMSO and evaluated at 35 μM. The spectra were run against blanks containing buffer solution and DMSO.

Results and discussion

Design and synthesis

We designed two series of diarylideneacetones inspired by substitution of β-diketone moiety of curcumin by a monoketone group. Compounds **4**–**17** (series I) and **21**–**27** (series II) were synthesized by concise synthetic routes, with 22–74% and 23–42% overall yields, respectively (Figure 3).

For the synthesis of dibenzylideneacetones *ortho*-substituted by the hydroxyl group of series I (**18**–**20**), we used four steps, including methoxymethyl group (MOM) protection and deprotection reactions (Figure 4). *Ortho*-hydroxyl and carbonyl groups establish a keto-phenolic tautomerism, which was a barrier to aldol condensation reactions, requiring protection

and an alternative synthetic route. Dibenzylideneacetones **18**–**20** were obtained with overall yields ranging from 10 to 21% (Figure 4).

The structures of all analyzed compounds were conclusively verified through melting point assessments and detailed analyses of ^{1}H and ^{13}C NMR spectra, as detailed in the supplementary material (Figures S1-S24). NMR parameters, including chemical shifts (δ), coupling constants (J) and multiplicities, consistently matched those anticipated for the designed structures. . The ^{1}H NMR spectra displayed the pairs of methynic hydrogens α/α' and β/β', which resonated as doublets and indicated the formation of two double carbon-carbon bonds. These doublets presented coupling constants ranging from 15 to 16 Hz, confirming their *trans* configuration. For compounds previously documented in the literature, NMR data were successfully cross-referenced with existing reports (Dai *et al.*, 2015; Deck *et al.*, 2018; Shen *et al.*, 2015; Weber *et al.*, 2005; Yamakoshi *et al.*, 2010; Zhou *et al.*, 2018). Diarylideneacetones **6**, **10**, **12**–**14**, **19**, **20**, **22**–**27** were identified as new compounds (SciFinder ®).

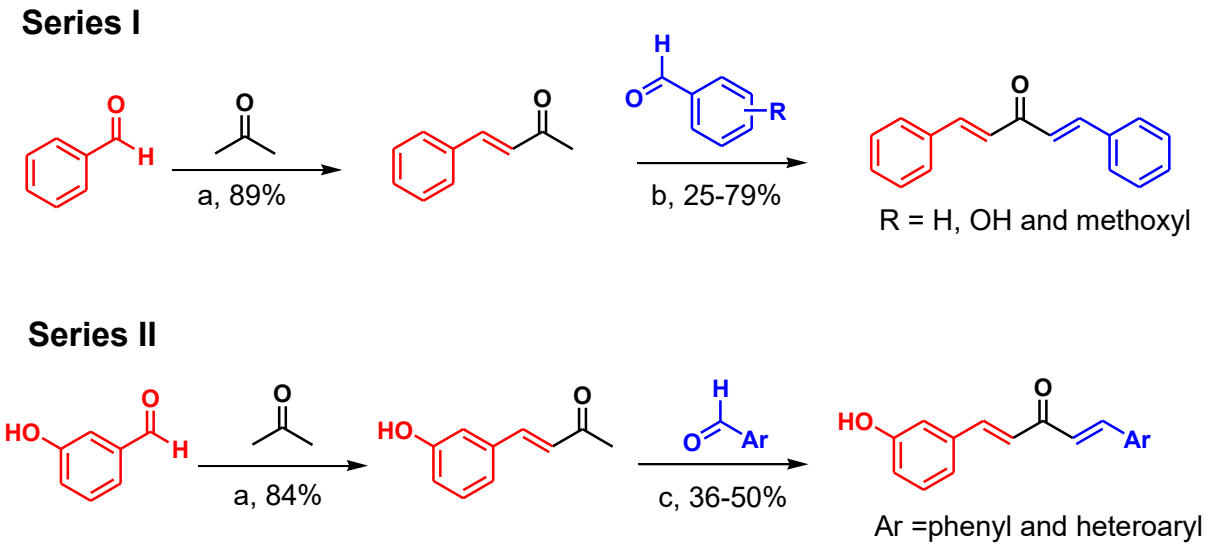

Figure 3. Synthesis of diarylideneacetones of series I and series II. Reagents and conditions: (a) NaOH and room temperature; (b) H_2SO_4, ethanol and room temperature (c) NaOH, ethanol and room temperature. The percentages below the arrows are the yields of the product.

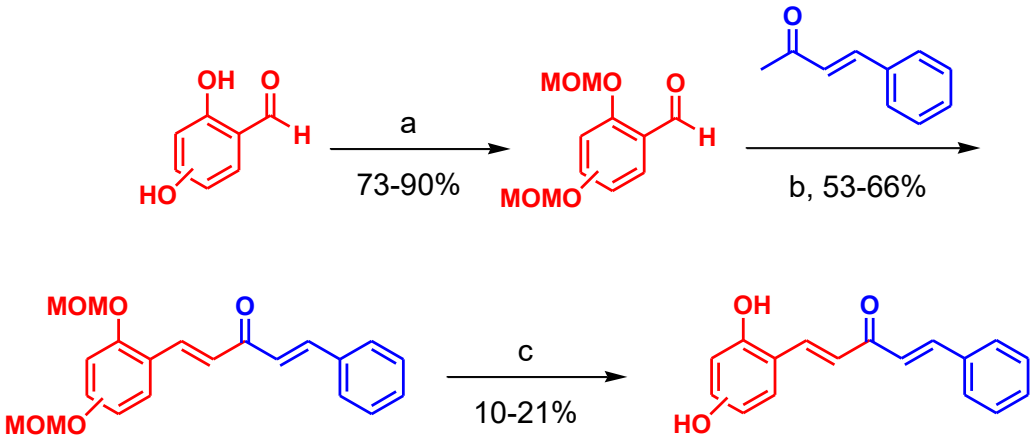

Figure 4. Synthesis of dibenzylideneacetones **18–20**. Reagents and conditions: (**a**) methoxymethyl group, K_2CO_3, dry acetone, N_2 atmosphere and room temperature; (**b**) NaOH, ethanol, N_2 atmosphere and room temperature (**c**) HCl, ethanol, N_2 atmosphere and room temperature. The percentages below the arrows are the yields of the product.

Anti-Candida activity

Anti-*Candida* activity of curcumin and the designed analogs were firstly evaluated against five *Candida* species. The antifungal potency of the compounds was expressed as Minimum Inhibitory Concentration (MIC) and Minimum Fungicidal Concentration (MFC) values in µM (Table 1).

Table 1. Anti-*Candida* activity determined by the MIC and MFC of curcumin (**1**), monoketone analog of curcumin (**2**) and its diarylideneacetone analogs divided in series I (**4**-**20**) and series II (**21**-**27**) expressed as MIC and MFC values in μM.

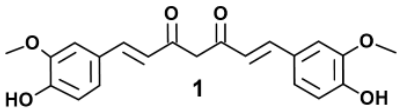

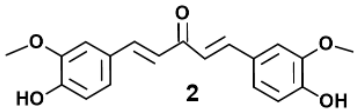

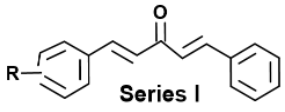

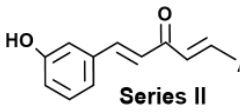

Cpd.	R or Ar	Ca		Ct		Cg		Cp		Ck	
		MIC	MFC	MIC	MFC	MIC	MFC	MIC	MFC	MIC	MFC
1	−	>250	>250	>250	>250	>250	>250	>250	>250	>250	>250
2	−	95.7	192	95.7	192	95.7	192	95.7	192	95.7	192
4	3-OMe, 4-OH	27.8	55.7	27.8	55.7	27.8	55.7	111	223	27.8	55.7
5	H	>250	>250	>250	>250	133	133	>250	>250	133	>250
6	3-OH, 4-OMe	111	223	55.7	111	111	223	55.7	111	27.8	55.7
7	2-OMe	>250	>250	>250	>250	>250	>250	>250	>250	>250	>250
8	3-OMe	237	237	118	237	>250	>250	>250	>250	118	237
9	4-OMe	>250	>250	237	237	>250	>250	>250	>250	237	>250
10	2,3-diOMe	212	212	106	212	>250	>250	>250	>250	106	212
11	2,4-diOMe	>250	>250	>250	>250	>250	>250	>250	>250	>250	>250
12	2,5-diOMe	>250	>250	>250	>250	>250	>250	>250	>250	>250	>250
13	3,4-diOMe	>250	>250	106	212	>250	>250	>250	>250	>250	>250
14	2,4,5-triOMe	>250	>250	>250	>250	>250	>250	>250	>250	>250	>250
15	3,4,5-triOMe	193	193	>250	>250	>250	>250	>250	>250	193	193
16	4-OH	62.3	62.3	125	250	31.2	62.3	62.3	125	31.2	62.3
17	3-OH	31.2	62.3	31.2	62.3	7.8	15.6	31.2	62.3	15.6	31.2
18	2-OH	62.3	62.3	62.3	125	15.6	31.2	62.3	125	62.3	62.3
19	2,3-diOH	58.6	58.6	117	235	29.3	29.3	117	117	58.6	117
20	2,5-diOH	117	235	235	235	58.6	58.6	235	235	117	235
21	3-hydroxyphenyl	58.6	117	14.6	29.3	58.6	58.6	58.6	117	7.1	14.6
22	4-methylphenyl	29.5	59.1	29.5	29.5	54.9	54.9	110	110	59.1	59.1
23	4-chlorophenyl	110	220	>250	>250	237	237	237	237	110	220
24	3,4-dichlorophenyl	>250	>250	>250	>250	>250	>250	>250	>250	>250	>250
25	2-furyl	64.9	64.9	64.9	64.9	250	250	250	250	16.2	16.2
26	3-pyridyl	62.1	62.1	15.5	15.5	62.1	62.1	62.1	124	31.1	62.1
27	4-pyridyl	62.1	124	31.1	62.1	62.1	62.1	15.5	31.1	31.1	62.1
FCZ	−	52.2	−	6.5	−	6.5	−	3.2	−	104	−
AMP B	−	0.5	−	0.5	−	0.5	−	0.3	−	0.5	−

MIC = Minimum Inhibitory Concentration; MFC = Minimum Fungicidal Concentration; Ca = *C. albicans* ATCC 90028; Ct = *C. tropicalis* ATCC 750; Cg = *C. glabrata* ATCC 90030; Cp = *C. parapsilosis* ATCC 22019; Ck = *C. krusei* ATCC 6258; FCZ = fluconazole; AMP B = amphotericin B; − not determined.

Curcumin **(1)** showed MIC values > 250 μM against all *Candida* species. Previous studies found MIC values of curcumin ranging from 678 to 1357 μM against *C. albicans* (ATCC10261 and 44829), *C. tropicalis* (ATCC 750) and *C. glabrata* (ATCC 90030) (Neelofar *et al.*, 2011). However, in this work, curcumin was not evaluated in concentrations higher than 250 μM due to low solubility in the culture medium, which could lead to inaccurate measurements of MIC and MFC values.

The antifungal effect of replacing the β-diketone subunit by a monoketone group was investigated. The MIC of the monoketone analog of curcumin (**2**) was lower than of curcumin, 96 μM versus 250 μM respectively, indicating that the molecular simplification improved the fungitoxicity.

Comparisons between the MIC values of compounds **2** and **4** (an unsymmetrical dibenzylideneacetone with unsubstituted benzene ring B), indicated the relevance of the number of methoxyl and hydroxyl substituents for bioactivity. Compound **4** (MIC = 27.8 μM) demonstrated higher activity against *C. albicans*, *C. tropicalis*, *C. glabrata* and *C. krusei* when compared to **2** (MIC = 95.7 μM) suggesting that the removal of the second pair of *meta*-OMe and *para*-OH substituents on the aromatic ring B improved the antifungal activity. As part of simplification of the molecule, compound **5** (a dibenzylideneacetone with unsubstituted benzene rings A and B) was evaluated. Compound **5** (MIC ≥ 133 μM) was less potent than **4** (27.8 μM ≤ MIC ≤ 111 μM), suggesting that completely removing the methoxyl and hydroxyl substituents decreased the anti-*Candida* activity. Inversion of OH and OMe substitutions, in the *meta* and *para* positions, were also investigated comparing the anti-*Candida* activity of compounds **4** and **6**. The activity of compound **6** against *C. albicans*, *C. tropicalis* and *C. glabrata* were lower than compound **4**. However, it demonstrated comparable efficacy to compound **4** against *C. parapsilosis* and *C. krusei*, suggesting that the inversion of OH and

OMe positions might play a less critical role in the compound's antifungal effectiveness against certain *Candida* species.

Methoxyl and hydroxyl groups displayed a central role on antifungal activity, two sets of methoxyl-dibenzylideneacetones (**7**–**15**) and hydroxy-dibenzylideneacetones (**16**–**20**) of series I were tested. Dibenzylideneacetones mono-(**7**–**9**), di-(**10**–**13**) and trisubstituted (**13**–**15**) by methoxyl groups were weakly active. However, dibenzylideneacetones mono-(**16**–1**8**) and disubstituted (**18**–**20**) by hydroxyl groups showed a higher activity. The comparison between the two sets of compounds indicated that hydroxyl was more relevant to fungitoxicity than the methoxyl group. Monohydroxylated compounds (7.8 μM ≤ MIC ≤ 62.3 μM) showed higher potency than dihydroxylated compounds (29.3 μM ≤ MIC ≤ 235 μM), indicating the number of hydroxyl groups interfered with the bioactivity. Among these analogs, 3-hydroxy-dibenzylideneacetone (**17**) was the most active of series I (7.8 μM < MIC < 31.2 μM) and selected to design the series II, exhibiting higher effect against *C. albicans* than fluconazole.

In series II, we assessed the relevance of electronic density on ring B (see Figure 2) for the anti-*Candida* activity. The compounds substituted by electron-donating groups, **21** (*meta*-OH) and **22** (*para*-Me), exhibited fungitoxicity against *C. albicans*, with MIC values of 58.6 μM and 29.5 μM, respectively. On the other hand, compounds mono- and disubstituted by chlorine (an electron-withdrawing groups), **23** (*para*-Cl) and **24** (*meta*, *para*-diCl) were weakly active. The comparison of bioactivity presented by **21**–**24** suggested that an electron-rich ring B supported fungitoxicity. Also, we evaluated heteroaryl of the benzene ring, which displays six π-electrons and may mimic its resonating system. Compounds **25** (2-furyl), **26** (3-pyridyl) and **27** (4-pyridyl) were active against all *Candida* species. These compounds **23**–**25** were recognized as ring bioisosters of 3-hydroxy-dibenzylideneacetone (**17**) which increases anti-*Candida* activity.

The fungistatic or fungicidal action of compounds was calculated by the ratio of the MFC and MIC values. Fungicidal agents exhibit MFC/MIC ratio values < 4(Sardi *et al.*, 2017a). All antifungal compounds presented MFC/MIC ratios of 1 and 2, indicating they are fungicidal agents against *Candida* species. Among these, 3-hydroxy-dibenzylideneacetone (**17**) displayed the lowest MFC values (15.6 μM ≤ MFC ≤ 62.3 μM) and was selected for assays using clinical isolates. The effects of 3-hydroxy-dibenzylideneacetone against a panel of 10 clinical *Candida* isolates from three anatomic regions, nails (*n* = 7), genital tract (*n* =2) and skin (*n* =1), were expressed as MIC values (Table 2). In contrast to action against reference ATCC strains, 3-hydroxy-dibenzylideneacetone was weakly active against clinical isolates, with MIC values ranging from 62.5 to 250 μM (Table 2).

Table 2. Anti-*Candida* activity of 3-hydroxy-dibenzylideneacetone, fluconazole and amphotericin B against clinical isolates expressed as MIC values in μM

Clinical isolate	Origin	17	FCZ	AMP B
Ca 6293	genital tract	250	3.9	−
Ca 6326	nail	>250	7.8	−
Ct 6477	nail	125	250	−
Ct 6459	skin	125	7.8	−
Cg 5136	genital tract	>250	125	−
Cg 5371	nail	62.5	62.5	−
Cp 6175	nail	125	15.6	−
Cp 6186	nail	>250	7.8	−
Ck 6473	nail	>250	−	0.5
Ck 6347	nail	>250	−	1.0

MIC = minimum inhibitory concentration; Ca = *C. albicans*; Ct = *C. tropicalis;* Cg = *C. glabrata*; Cp = *C. parapsilosis*; Ck = *C. krusei*; 17 = 3-hydroxy-dibenzylideneacetone; FCZ = fluconazole; AMP B = amphotericin B; − not tested.

Effects of compound 17 on C. albicans adhesion to human cells lines

Fungal adhesion onto host cells is the first step in the development of infectious processes(Lipke, 2018). This step is mediated by specific mechanisms, such as the fungal adhesins interacting with receptors on host cells, and non-specific mechanisms, such as *Candida* cell surface hydrophobicity (Höfs, Mogavero e Hube, 2016; Muadcheingka e Tantivitayakul, 2015). Inhibition of *Candida* adhesion may be an efficient strategy to reduce its infection(Oliveira, de *et al.*, 2016). Therefore, the effect of 3-hydroxy-dibenzylideneacetone (**17**) at 0.25 MIC on the adhesion of *C. albicans* onto HaCaT and HGF-1 cells was investigated. Exposing the *C. albicans* for 2 h to 3-hydroxy-dibenzylideneacetone inhibited adhesion onto HaCaT (Figure 5A) and HGF-1 cells (Figure 5B) when compared to the negative control unexposed *C. albicans*. Inhibitory effects of 3-hydroxy-dibenzylideneacetone on keratinocytes and fibroblasts were similar, suggesting that the human cell type did not affect its anti-adhesion activity (Figure 5). Others reported no differences in the *C. albicans* adhesion to human gingival fibroblast and epithelial cells after exposure to nisin Z(Akerey *et al.*, 2009). It was also reported that exposure time of *Candida* species was not relevant to the effects of an ethanol extract of propolis on the *C. albicans*, *C. tropicalis*, *C. parapsilosis*, *C. krusei* and *C. glabrata* adhesion to HaCaT cells (Nani *et al.*, 2020).

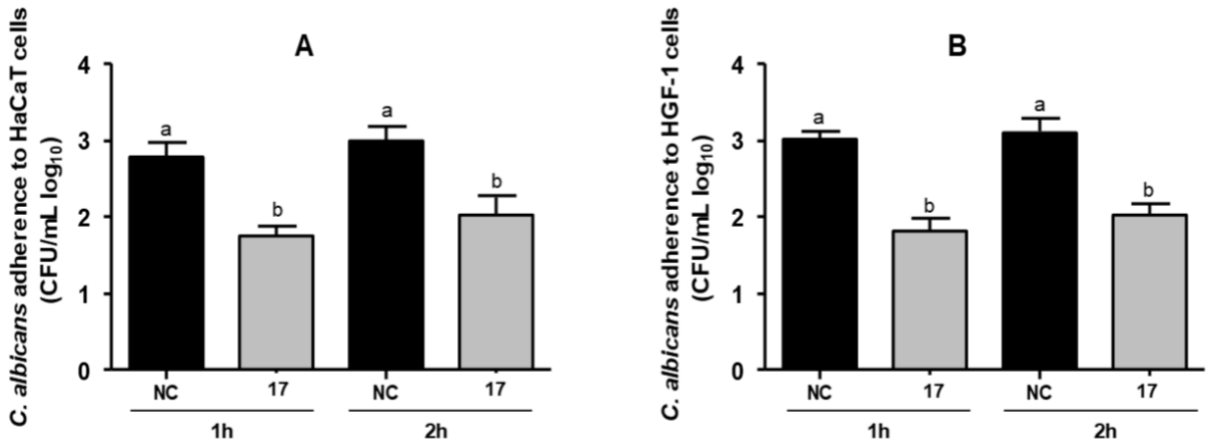

Figure 5. Effects (mean ± SD) of 3-hydroxy-dibenzylideneacetone (**17**) on the *C. albicans* ATCC 90028 adhesion onto (**A**) human keratinocyte cells (HaCaT) and (**B**) human gingival fibroblast cells (HGF-1). **NC** = negative control (untreated *C. albicans*). Letters a and b indicated statistical difference between treatments ($p < 0.05$; ANOVA with Tukey's post hoc test).

Evaluation of compound 17 on C. albicans biofilms

The ability to form biofilms on biotic and abiotic surfaces is a crucial step of *Candida* main virulence factor of *Candida* infections(Nobile e Johnson, 2015). *C. albicans* biofilm formation has various steps, including initial adhesion (0−2 h), germination, micro-colony formation, filamentation, monolayer development, proliferation (2−24 h) and biofilm maturation (24−48 h)(Gulati e Nobile, 2016). 3-Hydroxy-dibenzylideneacetone and amphotericin B were evaluated for their ability to inhibit biofilm formation and maturation (Figure 6). 3-Hydroxy-dibenzylideneacetone at MIC and 10 × MIC inhibited the *C. albicans* biofilm formation when compared to biofilms exposed to PBS (negative control). The inhibitory effects of 3-hydroxy-dibenzylideneacetone on the biofilm formation were very similar to the amphotericin B effects (Figure 6A). 3-Hydroxy-dibenzylideneacetone at MIC and 10 × MIC values reduced the biofilm maturation when a 24 h biofilm was exposed for 24 h to the inhibitory compounds

compared to the negative control. However, its inhibitory effects on the *C. albicans* 24 h biofilm were weaker than the amphotericin B effects (Figure 6B).

It has been reported that a mixture of curcumin-piperine presented antibiofilm effect at values ranging from 64–1024 µg mL^{-1} and 256–2048 µg mL^{-1} for minimum biofilm inhibitory concentration and minimum eradicating concentration, respectively(Tsopmene *et al.*, 2024). In another study, a curcumin-sophorolipid nanocomplex was able to inhibit *C. albicans* adhesion, biofilm development and filamentation at sub-inhibitory concentration(Rajasekar *et al.*, 2021). On the other hand, there are no reports on the effect of curcumin analogs against *Candida* biofilms, which were only exploited as antibiofilm agents against bacterial species, including *Staphylococcus aureus*, *Streptococcus mutans*, *Enterococcus faecalis*, *Lactobacillus casei*, *Actinomyces israelii* and *Fusarium nucleatum* (Pereira *et al.*, 2021; Sanches *et al.*, 2019; Santos *et al.*, 2021; Sardi *et al.*, 2017b).

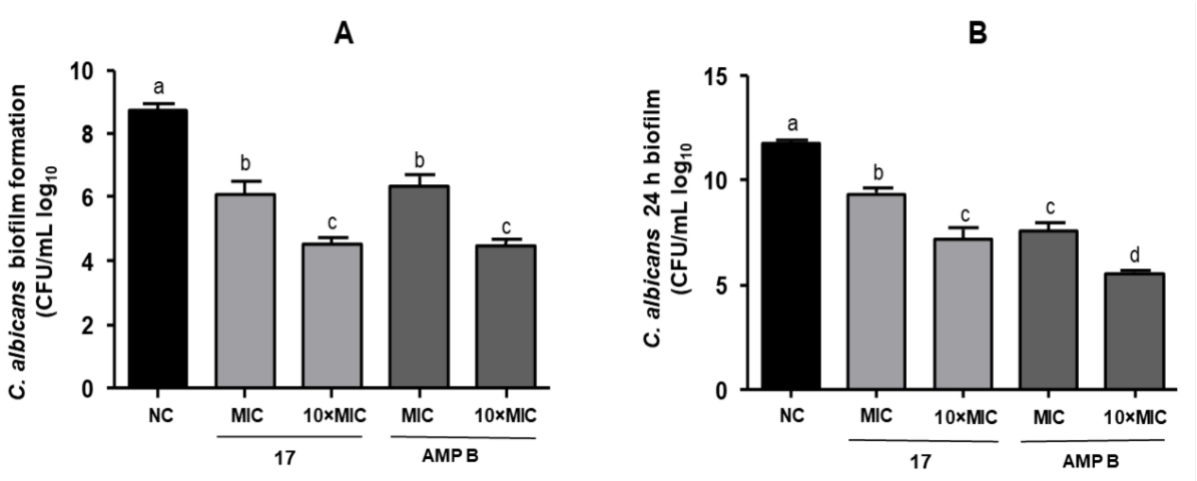

Figure 6. (**A**) Effects of 3-hydroxy-dibenzylideneacetone on 24 h biofilm formation (**B**) and exposing 24 h biofilms to 3-hydroxy-dibenzylideneacetone. Different letters above the bars denote statistical differences when compared to each other. Data compared to negative control (unexposed biofilm) where $P < 0.05$ – One-way ANOVA with Tukey's Post hoc test.

Ergosterol binding and sorbitol protection assays

In order to investigate the action of 3-hydroxy-dibenzylideneacetone on fungal membrane and cell wall, ergosterol binding and sorbitol protection assays, respectively were investigated. Values of MIC were determined in the presence and absence of ergosterol or sorbitol (Table 3). Adding ergosterol revealed that MIC values of 3-hydroxy-dibenzylideneacetone were enhanced from 31.2 μM (absence of ergosterol) to 125 μM (presence of ergosterol), evidencing its ability to interact with exogenous ergosterol and reducing its interaction with membrane ergosterol. Amphotericin B was used as a positive control due to its ability to complex with ergosterol, causing membrane disruption (Ciesielski *et al.*, 2016). Its MIC value was increased by 62 times by exogenous ergosterol.

Adding sorbitol showed that MIC values of 3-hydroxy-dibenzylideneacetone changed from 31.2 μM to 250 μM, indicating its action on the cell wall of *C. albicans.* Sorbitol is an osmotic protector which stabilizes fungal cells with a damaged cell wall. In this context, disruptors of fungal cell walls have their potency reduced in the presence of sorbitol (Frost *et al.*, 1995; Leite *et al.*, 2014). Caspofungin was used as positive control and its MIC values ranged from 0.05 to 1.8 in the presence of sorbitol. Altogether, our data indicated a dual effect of 3-hydroxy-dibenzylideneacetone on *C. albicans*, targeting the membrane and the cell wall. In spite of structural differences between 3-hydroxy-dibenzylideneacetone and curcumin, both compounds act at the same targets. The action of curcumin on *C. albicans* cytoplasmic membrane, including its ability to induce changes in membrane potential and disruption was described previously (Lee e Lee, 2014). The disruptor activity of curcumin on the cell wall of *C. albicans* is targeting the calcineurin signaling pathway (Kumar *et al.*, 2014).

Table 3. MIC values (in μM) of 3-hydroxy-dibenzylideneacetone and antifungal drugs in the absence and presence of ergosterol or sorbitol against *C. albicans* ATCC 90028.

Compound	Ergosterol		Sorbitol	
	Absence	Presence	Absence	Presence
17	31.2	125	31.2	250
amphotericin B*	0.5	31.2	–	–
caspofungin*	–	–	0.05	1.8

– not determined; * positive controls.

Checkerboard assay

The treatment against fungal infections using drug combination may enhance its efficacy, mitigate the adverse effect of antifungals and reduce the emergence of resistant strains(Sun, Zhang e Li, 2012). The effects of 3-hydroxy-dibenzylideneacetone against *C. albicans* in combination with amphotericin B (a polyene) and fluconazole (an azole). Combinations of 3-hydroxy-dibenzylideneacetone with amphotericin B and fluconazole displayed synergistic effects with FICI values of 0.5 and 0.2, respectively. The synergic combinations might be related to the mechanism of action of 3-hydroxy-dibenzylideneacetone**.** As amphotericin B and fluconazole cause direct and indirect fungal membrane damage, respectively, the action of 3-hydroxy-dibenzylideneacetone against this target resulted in a potentiated effect against *C. albicans* (Bongomin *et al.*, 2018; Nakagawa *et al.*, 2016; Sagatova *et al.*, 2015).

Acute toxicity assay

Galleria mellonella has been used as an alternative animal model in order to assess the *in vivo* toxicity of antifungal agents(Kavanagh e Sheehan, 2018). 3-Hydroxy-dibenzylideneacetone was injected into the larvae in doses ranging from 12.5 to 100 mg kg^{-1}. Larvae survival percentage was monitored up to 96 h (Figure 7). Larvae groups treated with saline (negative control) or DMSO (vehicle control) showed 100% and 90% survival, respectively. The

administration of 3-hydroxy-dibenzylideneacetone at doses 25 mg kg^{-1} and 50 mg kg^{-1} resulted in ≥ 60% survival. However, *G. mellonella* groups treated with 3-hydroxy-dibenzylideneacetone at doses 75 mg kg^{-1} and 100 mg kg^{-1} showed ≤ 50% survival. From these results, the 3-hydroxy-dibenzylideneacetone dose required in order to kill 50% of the larvae (LD_{50}) was estimated to be 75 mg kg^{-1} (or 300 µmol kg^{-1}) after 96 h of treatment(Merigo *et al.*, 2017). *G. mellonella* larvae treated with curcumin showed 80% survival at 2.85 µmol kg^{-1} after 96 h(Merigo *et al.*, 2017). 3-Hydroxy-dibenzylideneacetone at 12.5 mg kg^{-1} (50 µmol kg^{-1}), the lowest dose assessed in our study, showed 100% survival after 96 h. The comparison between larvae survival percentage values suggested that 3-hydroxy-dibenzylideneacetone was less toxic than curcumin, which is recognized as safe for humans in high doses (12 g day^{-1})(James *et al.*, 2015; Lao *et al.*, 2006).

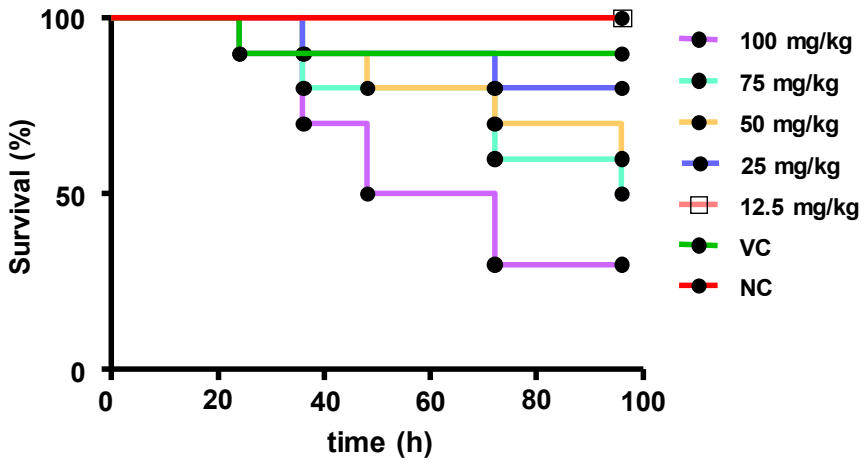

Figure 7. Acute toxicity of 3-hydroxy-dibenzylideneacetone against *G. mellonella.* Larvae groups treated with 0.9% saline (NC) and 12.5% DMSO (VC) were used as negative control.

Chemical stability assay

The poor stability of curcumin under physiological conditions is a central obstacle to its clinical use(Nelson *et al.*, 2017). In order to assess the ability of 3-hydroxy-dibenzylideneacetone to

overcome this limitation, we investigated its stability at pH 7.4 and 37 °C by monitoring the decrease in UV–vis absorption for 24 h (Figure 8). The initial concentrations of 3-hydroxy-dibenzylideneacetone and curcumin were reduced by 17% and 55%, respectively. This comparison suggested that 3-hydroxy-dibenzylideneacetone was more stable than curcumin, demonstrating that the replacement of the β-diketone with a monoketone group improved the chemical stability.

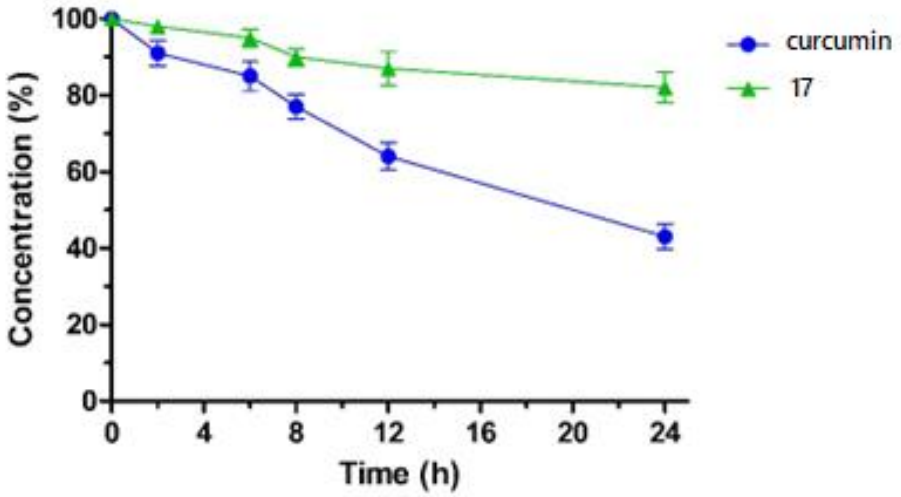

Figure 8. Chemical stability of 3-hydroxy-dibenzylideneacetone (**17)** and curcumin at pH 7.4 and 37 °C by monitoring the decrease in their maximum absorbance for 24 h. Data were represented as means ± SEMs and expressed as percentages.

Conclusion

We designed, synthesized and tested a series of 24 diarylideneacetones against *Candida* species. Structure-activity relationship suggested the hydroxyl group plays a key role on the fungitoxicity. 3-Hydroxybenzilideneacetone (**17**) was the most active compound and was selected for additional biological and chemical assays. The adhesion of *C. albicans* onto human keratinocytes and gingival fibroblasts was reduced by sub-MIC concentration of 3-hydroxy-dibenzylideneacetone. In addition, 3-hydroxy-dibenzylideneacetone had an inhibitory effect against *C. albicans* biofilm formation and biofilm maturation. The anti-*Candida* activity of 3-

hydroxy-dibenzylideneacetone is related to a dual mode of action, including effects on the fungal membrane and cell wall. The combinations of 3-hydroxy-dibenzylideneacetone and amphotericin B or fluconazole exhibited synergistic effects against *C. albicans*, which can be explained by the effect of 3-hydroxy-dibenzylideneacetone disrupting the cell membrane. Acute toxicity using *G. mellonella* as an animal model indicated a low percentage of larval mortality. Moreover, preliminary investigations of chemical stability indicated that 3-hydroxy-dibenzylideneacetone is more stable than curcumin at pH 7.4 and 37 ºC. Our results demonstrated that the replacement of the β-diketone by a monoketone group improved anti-*Candida* activity and chemical stability, corroborating the potential of diarylideneacetones as good substitutes for curcumin. Finally, 3-hydroxy-dibenzylideneacetone can be considered useful as an antifungal prototype, adjuvant to fluconazole and amphotericin B against *Candida* infections.

References

AKEREY, B. *et al. In vitro* efficacy of nisin Z against *Candida albicans* adhesion and transition following contact with normal human gingival cells. **Journal of Applied Microbiology**, v. 107, n. 4, p. 1298–1307, 2009.

ALALWAN, H. *et al.* The anti-adhesive effect of curcumin on *Candida albicans* biofilms on denture materials. **Frontiers in Microbiology**, v. 8, p. 669, 2017.

BELLMANN, R.; SMUSZKIEWICZ, P. Pharmacokinetics of antifungal drugs: practical implications for optimized treatment of patients. **Infection**, v. 45, n. 6, p. 737–779, 2017.

BONGOMIN, F. *et al.* A systematic review of fluconazole resistance in clinical isolates of *Cryptococcus* species. **Mycoses**, v. 61, n. 5, p. 290–297, 2018.

CIESIELSKI, F. *et al.* Recognition of membrane sterols by polyene antifungals amphotericin B and natamycin, A 13C MAS NMR Study. **Frontiers in Cell and Developmental Biology**, v. 4, 2016.

DAI, F. *et al.* Insights into the importance for designing curcumin-inspired anticancer agents by a prooxidant strategy: The case of diarylpentanoids. **Free Radical Biology and Medicine**, v. 85, p. 127–137, 2015.

DECK, L. M. *et al.* Activation of anti-oxidant Nrf2 signaling by enone analogues of curcumin. **European Journal of Medicinal Chemistry**, v. 143, p. 854–865, 2018.

DOERN, C. D. When does 2 plus 2 equal 5? A review of antimicrobial synergy testing. **Journal of Clinical Microbiology**, v. 52, n. 12, p. 4124–4128, 2014.

DOVIGO, L. N. *et al.* Susceptibility of clinical isolates of *Candida* to photodynamic effects of curcumin. **Lasers in Surgery and Medicine**, v. 43, n. 9, p. 927–934, 2011.

FERNANDES, L. DE S. *et al.* Formulation, stability study and preclinical evaluation of a vaginal cream containing curcumin in a rat model of vulvovaginal candidiasis. **Mycoses**, v. 61, n. 10, p. 723–730, 2018.

FISHER, M. C. *et al.* Worldwide emergence of resistance to antifungal drugs challenges human health and food security. **Science**, v. 360, n. 6390, p. 739–742, 2018.

FROST, D. J. *et al.* A whole-cell *Candida albicans* assay for the detection of inhibitors towards fungal cell wall synthesis and assembly. **The Journal of Antibiotics**, v. 48, n. 4, p. 306–310, 1995.

GARCIA, M. A. R. *et al.* Design, synthesis and antibacterial activity of chalcones against MSSA and MRSA planktonic cells and biofilms. **Bioorganic Chemistry**, v. 116, p. 105279, 2021.

GULATI, M.; NOBILE, C. J. Candida albicans biofilms: development, regulation, and molecular mechanisms. **Microbes and Infection**, v. 18, n. 5, p. 310–321, 2016.

HEGER, M. *et al.* The molecular basis for the pharmacokinetics and pharmacodynamics of curcumin and its metabolites in relation to cancer. **Pharmacological Reviews**, v. 66, n. 1, p. 222–307,. 2014.

HÖFS, S.; MOGAVERO, S.; HUBE, B. Interaction of *Candida albicans* with host cells: virulence factors, host defense, escape strategies, and the microbiota. **Journal of Microbiology**, v. 54, n. 3, p. 149–169, 2016.

JAMES, M. I. *et al.* Curcumin inhibits cancer stem cell phenotypes in ex vivo models of colorectal liver metastases, and is clinically safe and tolerable in combination with FOLFOX chemotherapy. **Cancer Letters**, v. 364, n. 2, p. 135–141, 2015.

KAVANAGH, K.; SHEEHAN, G. The Use of *Galleria mellonella* larvae to identify novel antimicrobial agents against fungal species of medical Interest. **Journal of Fungi**, v. 4, n. 3, p. 113, 2018.

KHAN, N. *et al.* Anticandidal activity of curcumin and methyl cinnamaldehyde. **Fitoterapia**, v. 83, n. 3, p. 434–440, 2012.

KOŁACZKOWSKA, A.; KOŁACZKOWSKI, M. Drug resistance mechanisms and their regulation in non- *albicans Candida* species. **J. Antimicrob. Chemother.**, v. 71, n. 6, p. 1438–1450, 2016.

KUMAR, A. *et al.* Curcumin targets cell wall integrity via calcineurin-mediated signaling in *Candida albicans*. **Antimicrobial Agents and Chemotherapy**, v. 58, n. 1, p. 167–175, 2014.

LAO, C. D. *et al.* Dose escalation of a curcuminoid formulation. **BMC Complementary and Alternative Medicine**, v. 6, n. 1, p. 10,2006.

LEE, W.; LEE, D. G. An antifungal mechanism of curcumin lies in membrane-targeted action within *Candida albicans*. **IUBMB Life**, v. 66, n. 11, p. 780–785, 2014.

LEITE, M. C. A. *et al.* Evaluation of antifungal activity and mechanism of action of citral against *Candida albicans*. **Evidence-Based Complementary and Alternative Medicine**, v. 2014, p. 378280, 2014.

LIMA, F. *et al.* The curcumin analog CH-5 exerts anticancer effects in human osteosarcoma cells via modulation of transcription factors p53/Sp1. **International Journal of Molecular Sciences**, v. 19, n. 7, p. 1909, 2018.

LIPKE, P. What we do not know about fungal cell adhesion molecules. **Journal of Fungi**, v. 4, n. 2, p. 59, 2018.

MERIGO, E. *et al.* Effect of different wavelengths and dyes on *Candida albicans* : In vivo study using Galleria mellonella as an experimental model. **Photodiagnosis and Photodynamic Therapy**, v. 18, p. 34–38, 2017.

MORÃO, L. G. *et al.* A simplified curcumin targets the membrane of *Bacillus subtilis*. **MicrobiologyOpen**, v. 8, n. 4, p. e00683, 2019.

MUADCHEINGKA, T.; TANTIVITAYAKUL, P. Distribution of *Candida albicans* and *non-albicans Candida* species in oral candidiasis patients: Correlation between cell surface hydrophobicity and biofilm forming activities. **Archives of Oral Biology**, v. 60, n. 6, p. 894–901, 2015.

NAGLIK, J. R.; RICHARDSON, J. P.; MOYES, D. L. *Candida albicans* pathogenicity and epithelial Immunity. **PLoS Pathogens**, v. 10, n. 8, p. e1004257, 2014.

NAKAGAWA, Y. *et al.* The structure of the bimolecular complex between amphotericin B and ergosterol in membranes Is stabilized by face-to-face Van der Waals interaction with their rigid cyclic cores. **Biochemistry**, v. 55, n. 24, p. 3392–3402, 2016.

NANI, B. D. *et al.* Anti-inflammatory and anti- *Candida* effects of Brazilian organic propolis, a promising source of bioactive molecules and functional food. **Journal of Agricultural and Food Chemistry**, v. 68, n. 10, p. 2861–2871, 2020.

NEELOFAR, K. *et al.* Curcumin as a promising anticandidal of clinical interest. **Canadian Journal of Microbiology**, v. 57, n. 3, p. 204–210, 2011.

NELSON, K. M. *et al.* The essential medicinal chemistry of curcumin. **Journal of Medicinal Chemistry**, v. 60, n. 5, p. 1620–1637, 2017.

NOBILE, C. J.; JOHNSON, A. D. *Candida albicans* biofilms and human disease. **Annual Review of Microbiology**, v. 69, n. 1, p. 71–92, 2015.

OLIVEIRA, H. C. DE *et al.* Peptides derived from a phage display library inhibit adhesion and protect the host against infection by *Paracoccidioides brasiliensis* and *Paracoccidioides lutzii*. **Frontiers in Pharmacology**, v. 7, 2016.

PATTINI, V. C. *et al.* Antifungal activity of 3,3'-dimethoxycurcumin (DMC) against dermatophytes and *Candida* species. **Letters in Applied Microbiology**, v. 77, n. 3, 2024.

PEREIRA, J. A. *et al.* Antibiofilm and cytotoxic effect of 3,3′-dihydroxycurcumin (DHC) as photosensitizer agent in antimicrobial photodynamic therapy for endodontic purposes. **Photodiagnosis and Photodynamic Therapy**, v. 36, p. 102534, 2021.

POLAQUINI, C. R. *et al.* Antibacterial activity of 3,3′-dihydroxycurcumin (DHC) is associated with membrane perturbation. **Bioorganic Chemistry**, v. 90, p. 103031, 2019.

RAJASEKAR, V. *et al.* A curcumin-sophorolipid nanocomplex inhibits *Candida albicans* filamentation and biofilm development. **Colloids and Surfaces B: Biointerfaces**, v. 200, p. 111617, 2021.

ROSEMOND, M. J. C. *et al.* Enzymology of a carbonyl reduction clearance pathway for the HIV integrase inhibitor, S-1360: role of human liver cytosolic aldo-keto reductases. **Chemico-Biological Interactions**, v. 147, n. 2, p. 129–139, 2004.

SAGATOVA, A. A. *et al.* Structural insights into binding of the antifungal drug fluconazole to *Saccharomyces cerevisiae* lanosterol 14α-demethylase. **Antimicrobial Agents and Chemotherapy**, v. 59, n. 8, p. 4982–4989, 2015.

SANCHES, C. V. G. *et al.* Diacetylcurcumin: a new photosensitizer for antimicrobial photodynamic therapy in *Streptococcus mutans* biofilms. **Biofouling**, v. 35, n. 3, p. 340–349, 2019.

SANTOS, V. R. *et al.* Cytotoxicity and effects of curcumin and cinnamaldehyde hybrids on biofilms of oral pathogens. **Biofouling**, v. 37, n. 6, p. 591–605, 2021.

SARDI, J. DE C. O. *et al.* Synthesis, antifungal activity of caffeic acid derivative esters, and their synergism with fluconazole and nystatin against *Candida* spp. **Diagnostic Microbiology and Infectious Disease**, v. 86, n. 4, p. 387–391, 2016.

SARDI, J. DE C. O. *et al.* Unexplored endemic fruit species from Brazil: antibiofilm properties, insights into mode of action, and systemic toxicity of four *Eugenia* spp. **Microbial Pathogenesis**, v. 105, p. 280–287, 2017a.

SARDI, J. DE C. O. *et al.* Antibacterial activity of diacetylcurcumin against *Staphylococcus aureus* results in decreased biofilm and cellular adhesion. **Journal of Medical Microbiology**, v. 66, n. 6, p. 816–824, 1 jun. 2017b.

SHARMA, M. *et al.* Antifungal curcumin induces reactive oxygen species and triggers an early apoptosis but prevents hyphae development by targeting the global repressor *TUP1* in *Candida albicans*. **Bioscience Reports**, v. 30, n. 6, p. 391–404, 2010.

SHEN, T. *et al.* A curcumin derivative that inhibits vinyl carbamate-induced lung carcinogenesis *via* activation of the Nrf2 protective response. **Antioxidants & Redox Signaling**, v. 23, n. 8, p. 651–664, 2015.

SHETTY, D. *et al.* Eliminating the heart from the curcumin molecule: monocarbonyl curcumin mimics (MACs). **Molecules**, v. 20, n. 1, p. 249–292, 2014.

SILVA, G. *et al.* Curcumin analog CH-5 suppresses the proliferation, migration, and invasion of the human gastric cancer cell line HGC-27. **Molecules**, v. 23, n. 2, p. 279, 2018.

STAMATIADES, G. A. *et al.* Fungal infections in patients with inflammatory bowel disease: A systematic review. **Mycoses**, v. 61, n. 6, p. 366–376, 2018.

STANISZEWSKA, M. Virulence Factors in *Candida* species. **Current Protein & Peptide Science**, v. 21, n. 3, p. 313–323, 2020.

SUN, L.; ZHANG, C.; LI, P. Characterization, antibiofilm, and mechanism of action of novel PEG-stabilized lipid nanoparticles loaded with terpinen-4-ol. **Journal of Agricultural and Food Chemistry**, v. 60, n. 24, p. 6150–6156, 2012.

TSOPMENE, U. J. *et al.* Antibiofilm activity of curcumin and piperine and their synergistic effects with antifungals against *Candida albicans* clinical isolates. **Scientifica**, v. 2024, p. 2025557, 2024.

WEBER, W. M. *et al.* Anti-oxidant activities of curcumin and related enones. **Bioorganic & Medicinal Chemistry**, v. 13, n. 11, p. 3811–3820, 2005.

YAMAKOSHI, H. *et al.* Structure–activity relationship of C5-curcuminoids and synthesis of their molecular probes thereof. **Bioorganic & Medicinal Chemistry**, v. 18, n. 3, p. 1083–1092, 2010.

ZHOU, J. *et al.* Antimicrobial evaluation and action mechanism of pyridinium-decorated 1,4-pentadien-3-one derivatives. **Bioorganic & Medicinal Chemistry Letters**, v. 28, n. 10, p. 1742–1746, 2018.

Supporting Information

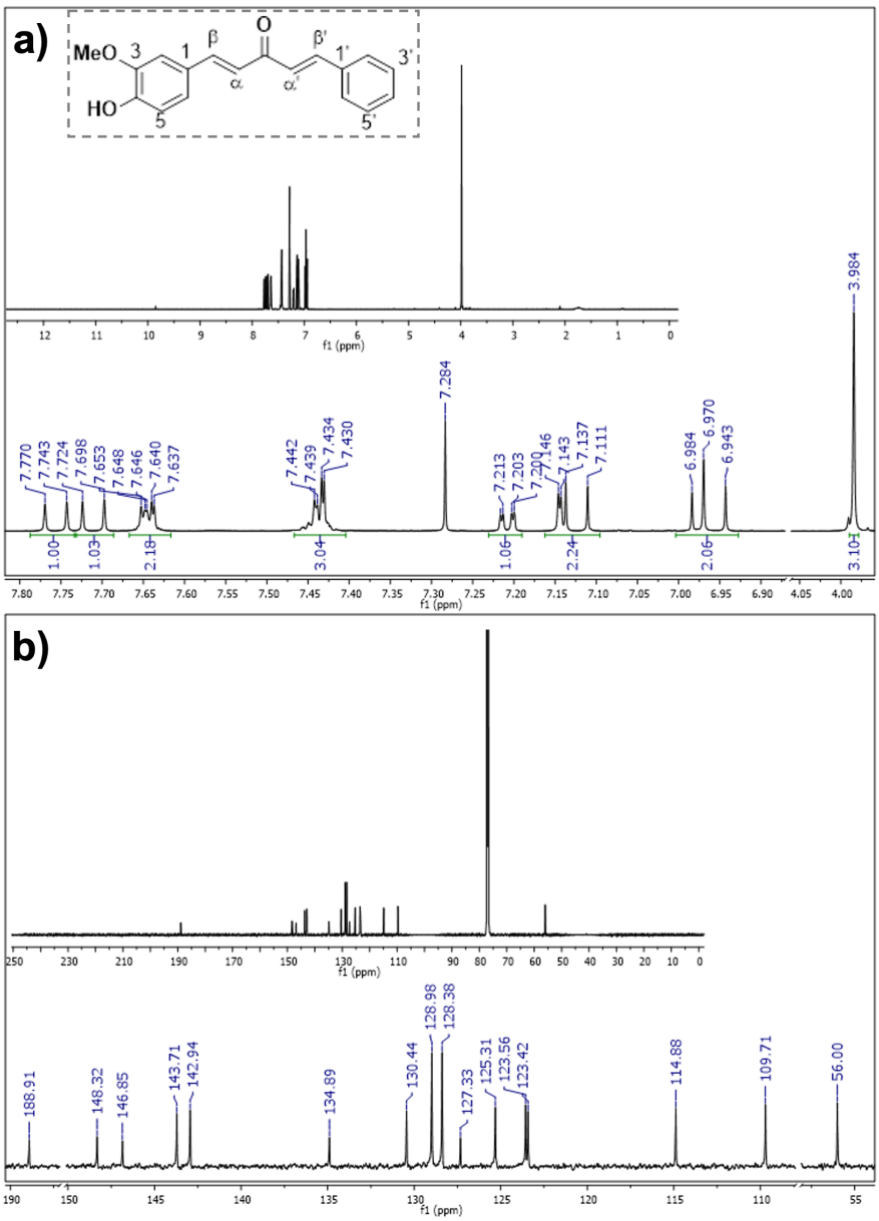

Figure S1. NMR spectra of Compound **4** (1*E*,4*E*)-1-(4-hydroxy-3-methoxyphenyl)-5-phenylpenta-1,4-dien-3-one.(Weber *et al.*, 2005) a) ^{1}H NMR spectrum at 600 MHz. b) ^{13}C NMR spectrum at 150 MHz.

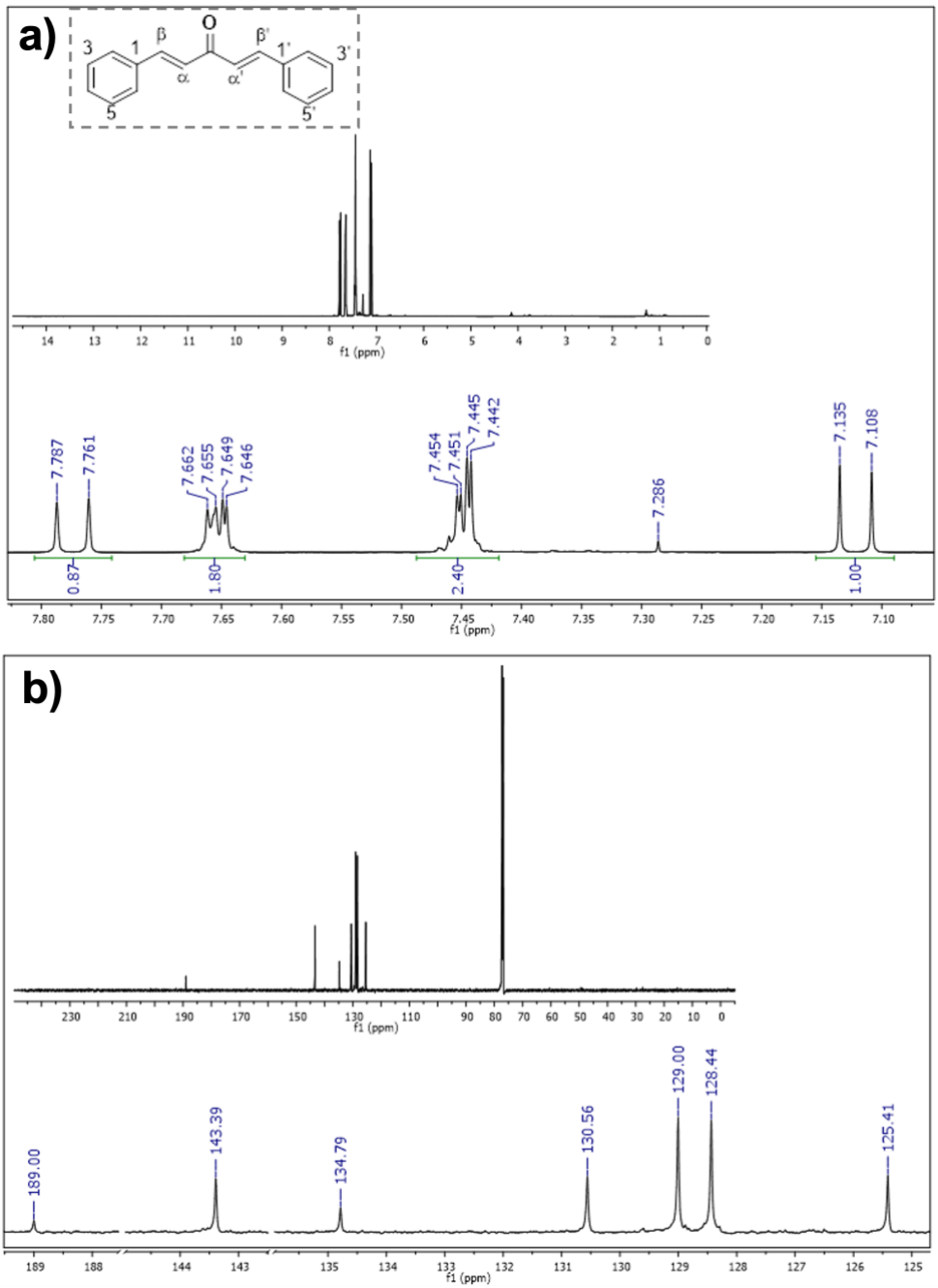

Figure S2. NMR spectra of Compound **5:** (1*E*,4*E*)-1,5-diphenylpenta-1,4-dien-3-one.(Dai *et al.*, 2015) a) ^{1}H NMR spectrum at 600 MHz. b) ^{13}C NMR spectrum at 150 MHz.

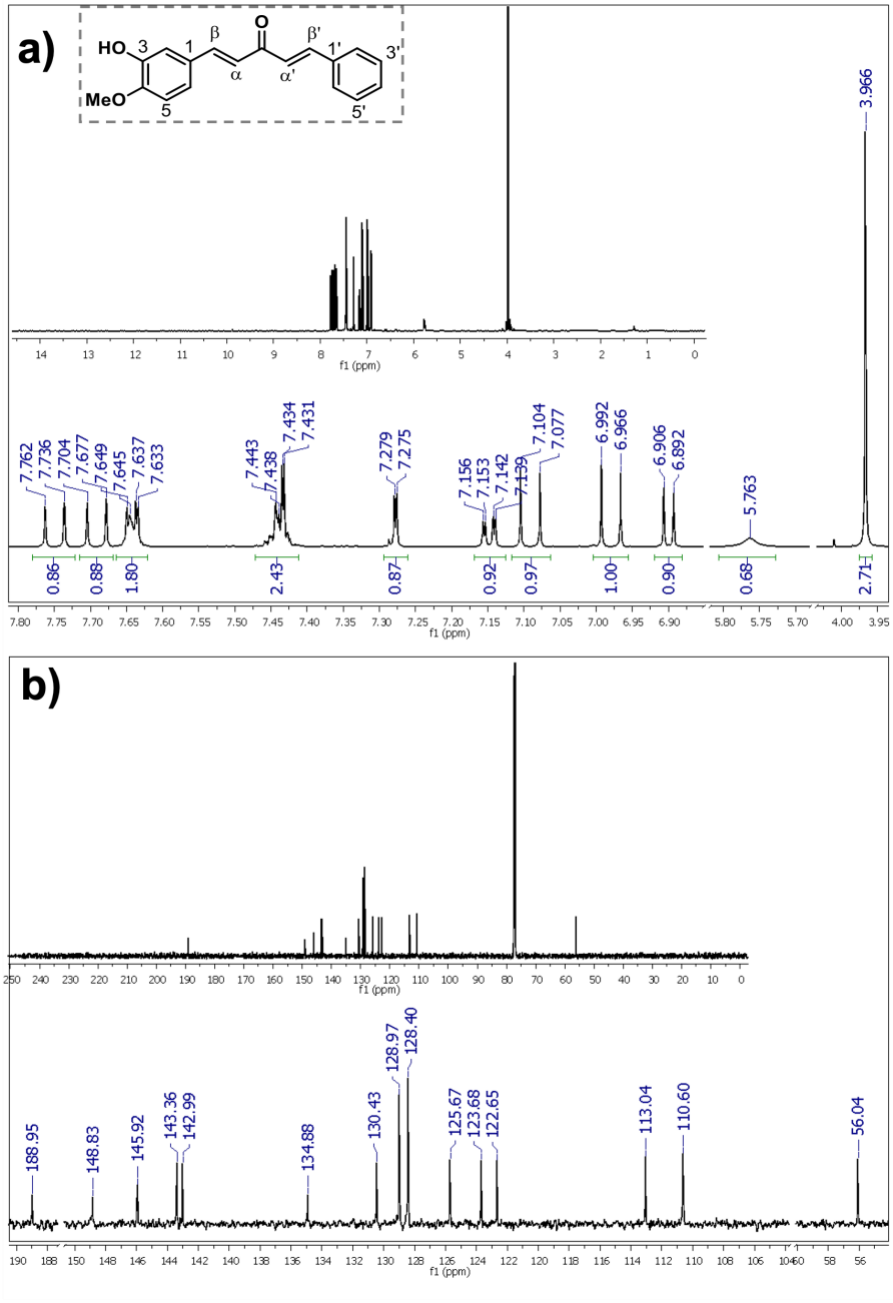

Figure S3. NMR spectra of Compound **6:** (1*E*,4*E*)-1-(3-hydroxy-4-methoxyphenyl)-5-phenylpenta-1,4-dien-3-one. a) ^{1}H NMR spectrum at 600 MHz. b) ^{13}C NMR spectrum at 150 MHz.

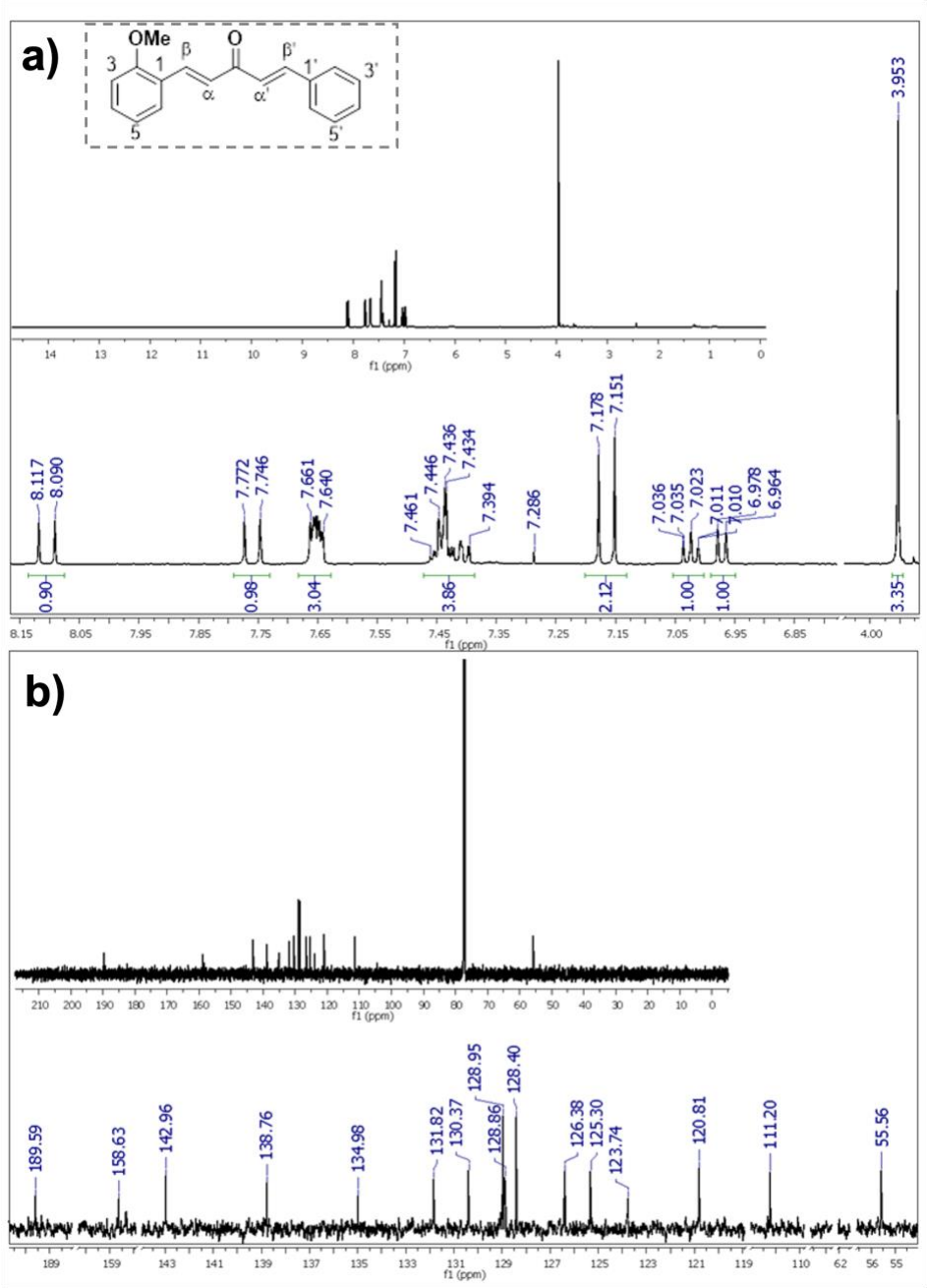

Figure S4. NMR spectra of Compound **7:** (1*E*,4*E*)-1-(2-methoxyphenyl)-5-phenylpenta-1,4-dien-3-one.(Dai *et al.*, 2015; Shen *et al.*, 2015) a) ^{1}H NMR spectrum at 600 MHz. b) ^{13}C NMR spectrum at 150 MHz.

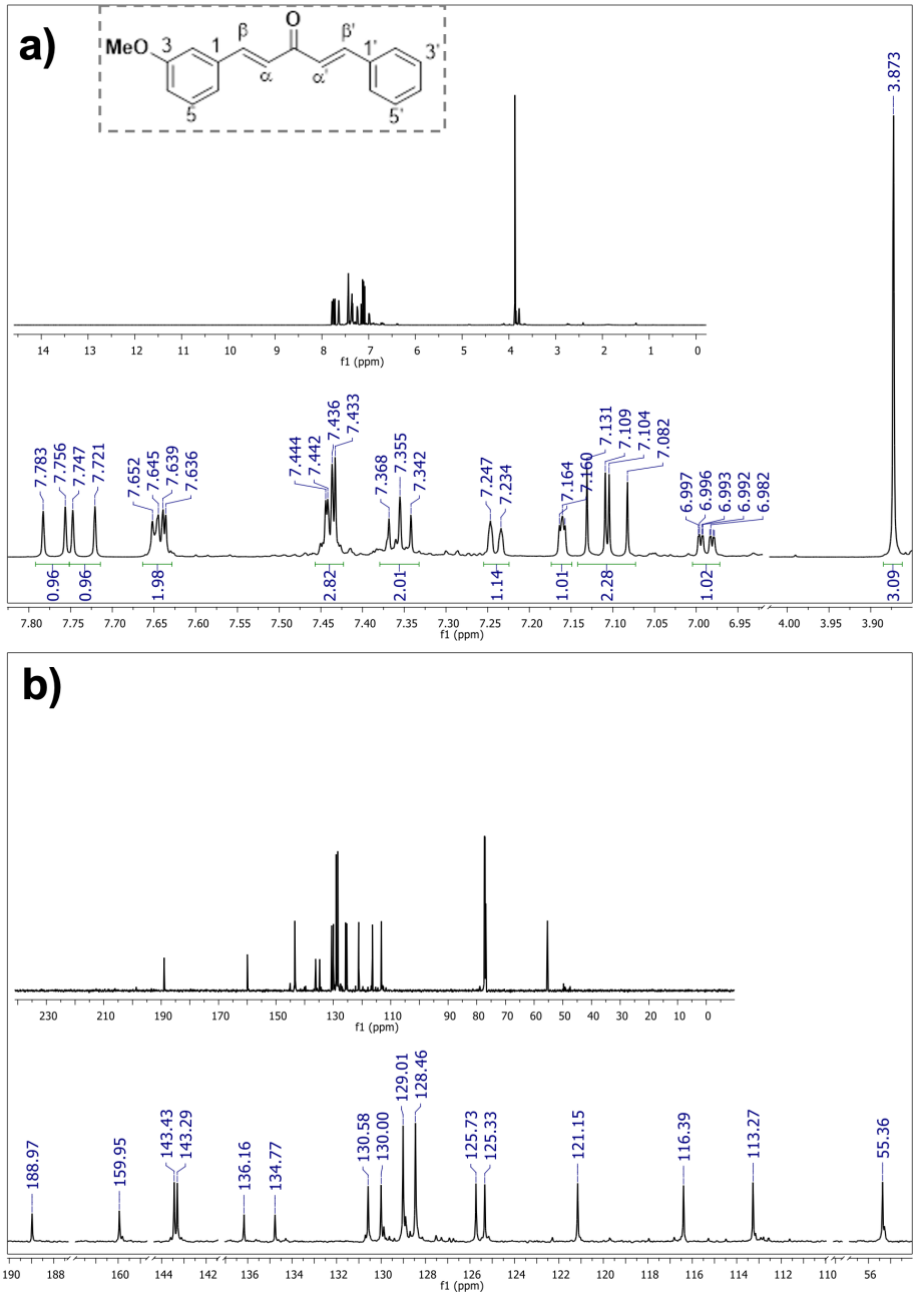

Figure S5. NMR of Compound **8:** (1*E*,4*E*)-1-(3-methoxyphenyl)-5-phenylpenta-1,4-dien-3-one.(Dai *et al.*, 2015) a) ^{1}H NMR spectrum at 600 MHz. b) ^{13}C NMR spectrum at 150 MHz.

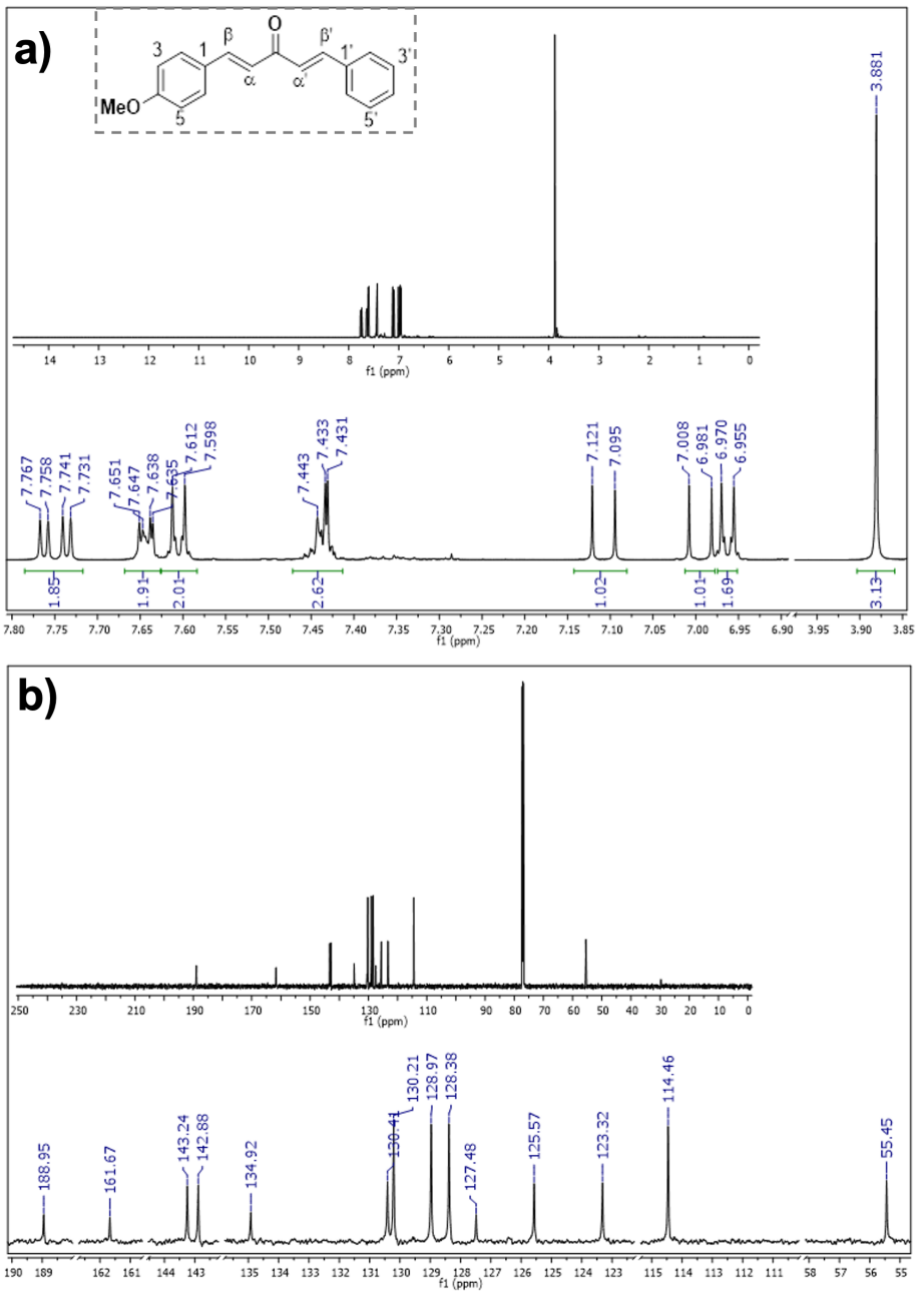

Figure S6. NMR of Compound **9:** (1*E*,4*E*)-1-(4-methoxyphenyl)-5-phenylpenta-1,4-dien-3-one. a) ^{1}H NMR spectrum at 600 MHz. b) ^{13}C NMR spectrum at 150 MHz.

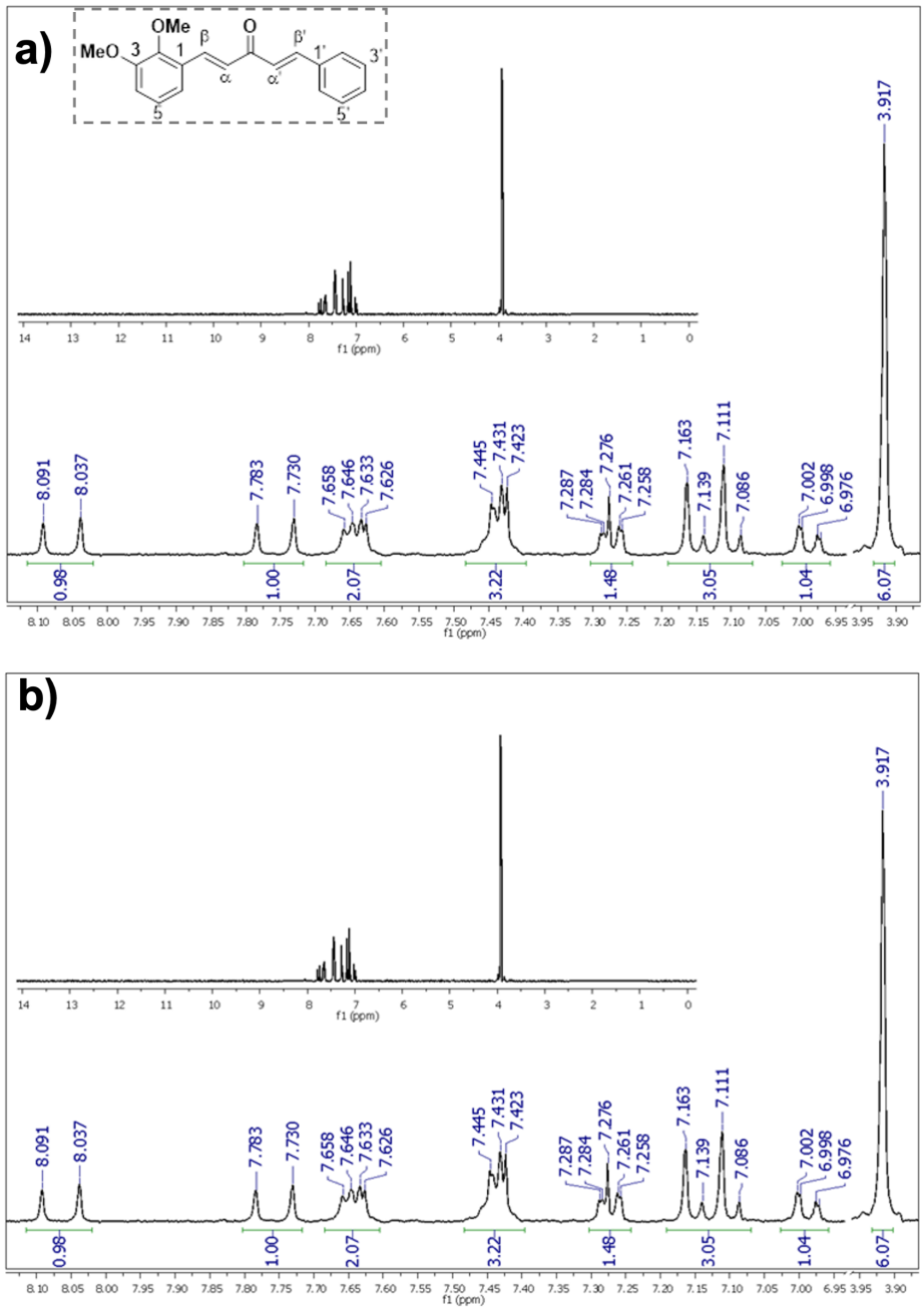

Figure S7. NMR of Compound **10:** (1*E*,4*E*)-1-(2,3-dimethoxyphenyl)-5-phenylpenta-1,4-dien-3-one. a) ^{1}H NMR spectrum at 600 MHz. b) ^{13}C NMR spectrum at 150 MHz.

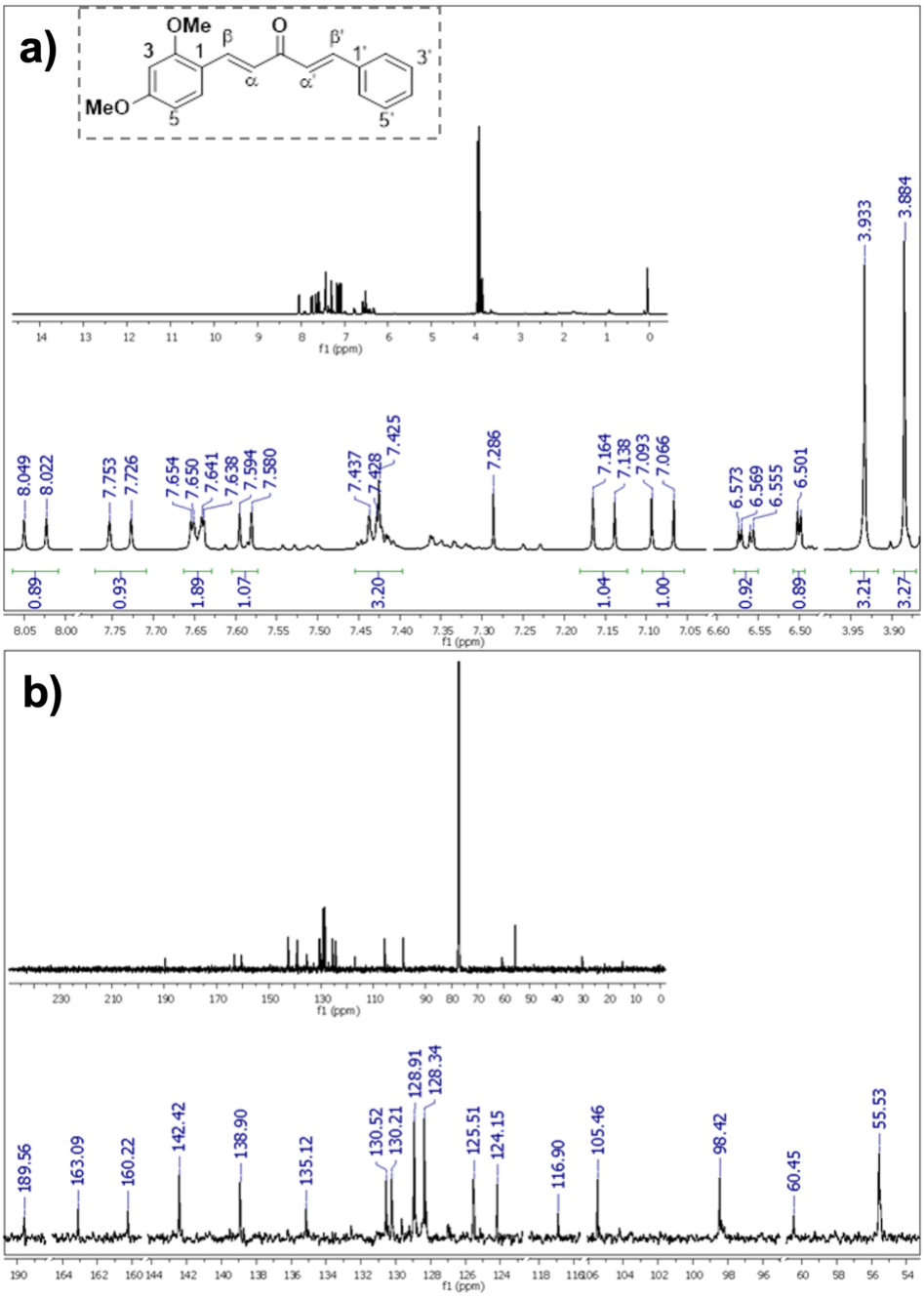

Figure S8. Compound **11:** (1*E*,4*E*)-1-(2,4-dimethoxyphenyl)-5-phenylpenta-1,4-dien-3-one. a) ^{1}H NMR spectrum at 600 MHz. b) ^{13}C NMR spectrum at 150 MHz.

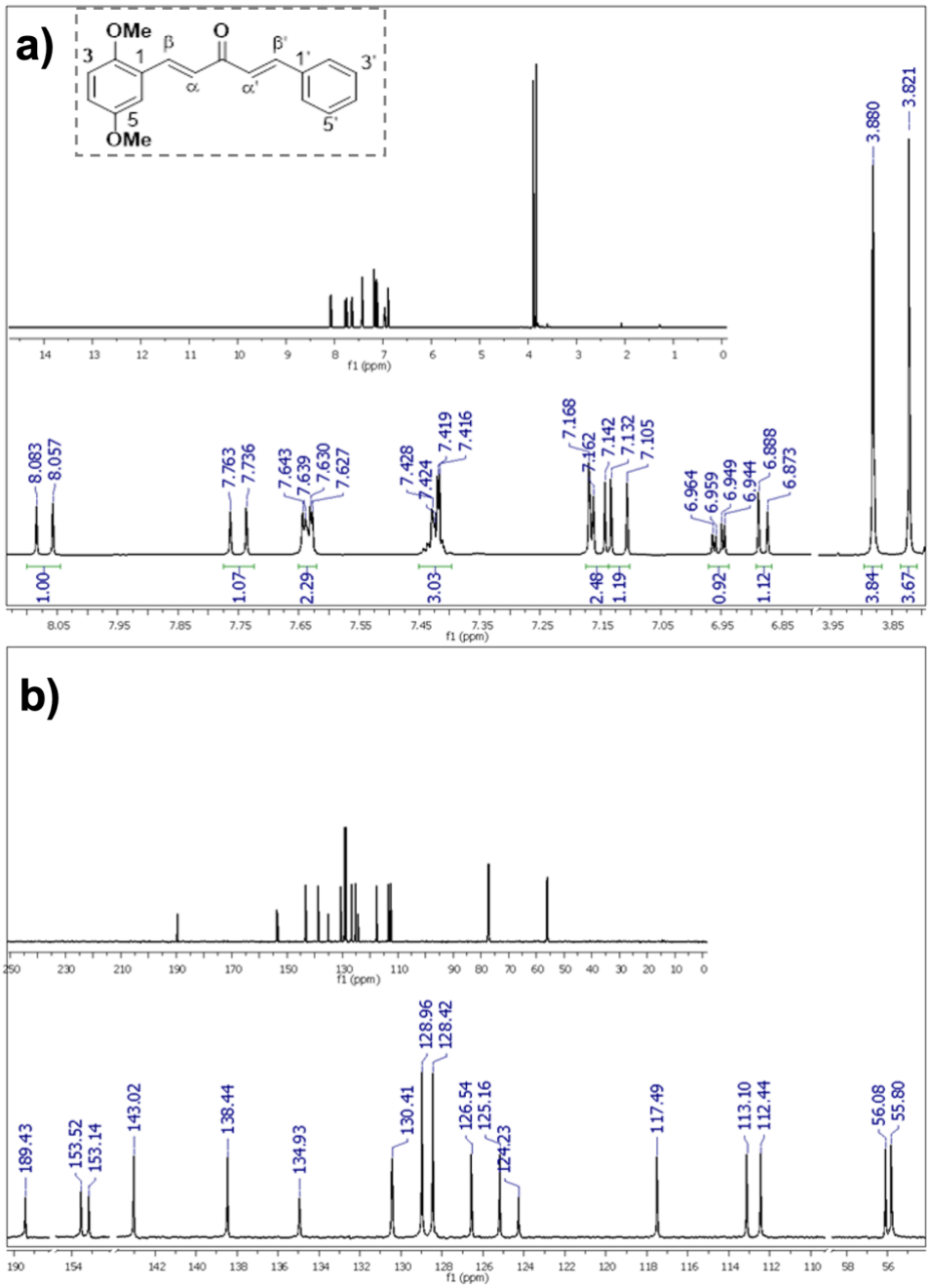

Figure S9. Compound **12:** (1*E*,4*E*)-1-(2,5-dimethoxyphenyl)-5-phenylpenta-1,4-dien-3-one. a) ^{1}H NMR spectrum at 600 MHz. b) ^{13}C NMR spectrum at 150 MHz.

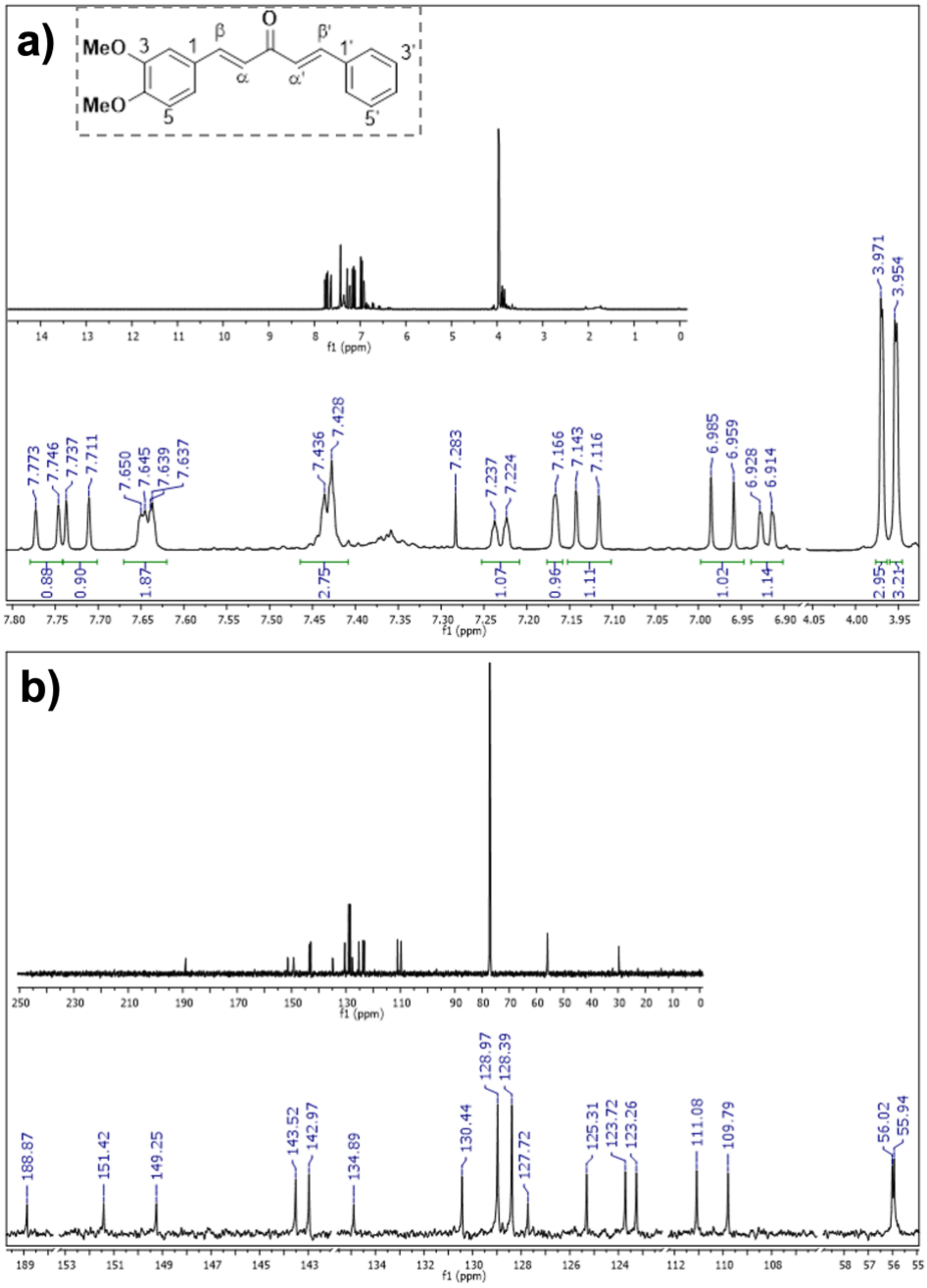

Figure S10. Compound **13:** (1*E*,4*E*)-1-(3,4-dimethoxyphenyl)-5-phenylpenta-1,4-dien-3-one. a) ^{1}H NMR spectrum at 600 MHz. b) ^{13}C NMR spectrum at 150 MHz.

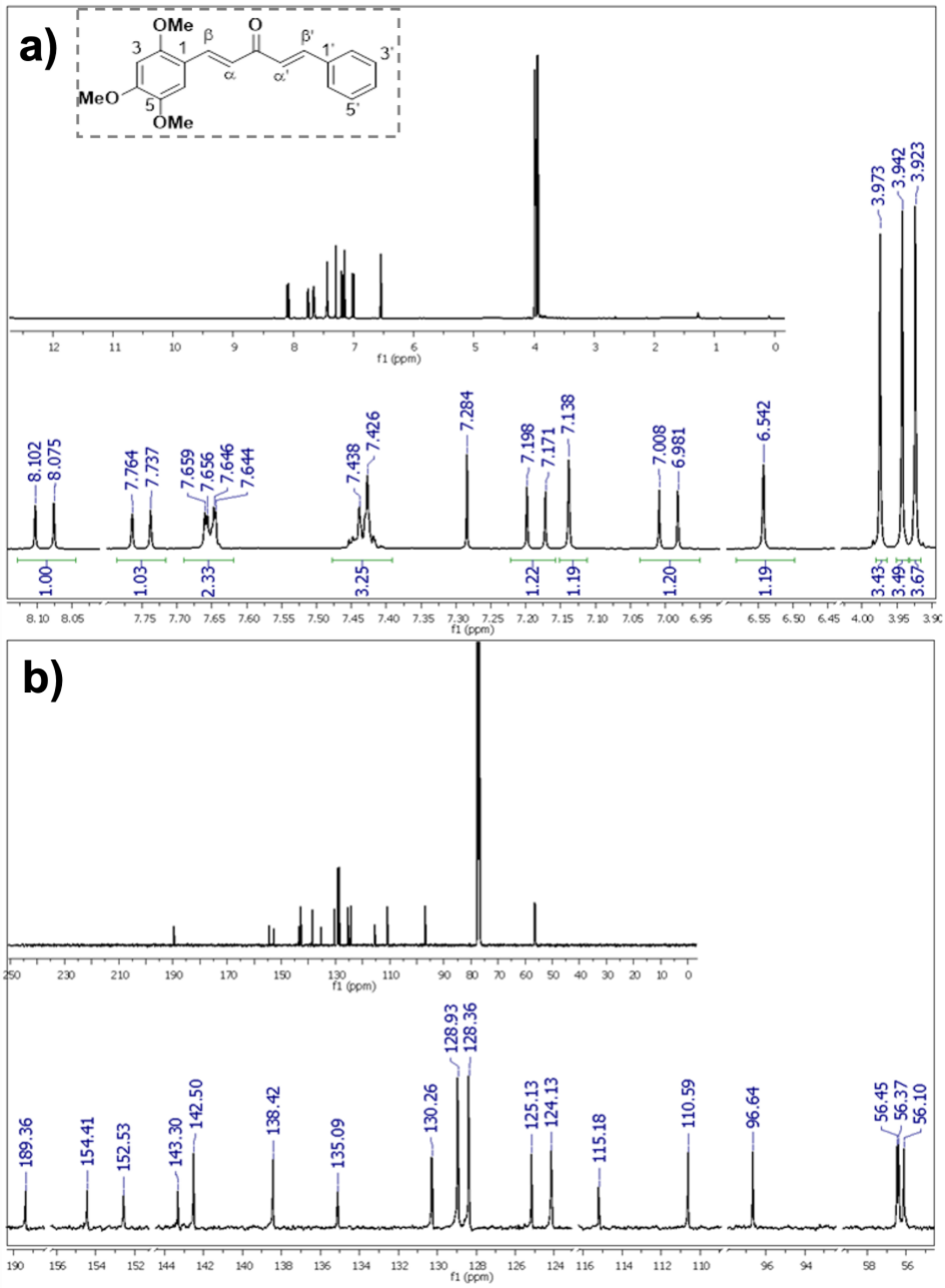

Figure S11. Compound **14:** (1*E*,4*E*)-1-(2,4,5-trimethoxyphenyl)-5-phenylpenta-1,4-dien-3-one. a) ^{1}H NMR spectrum at 600 MHz. b) ^{13}C NMR spectrum at 150 MHz.

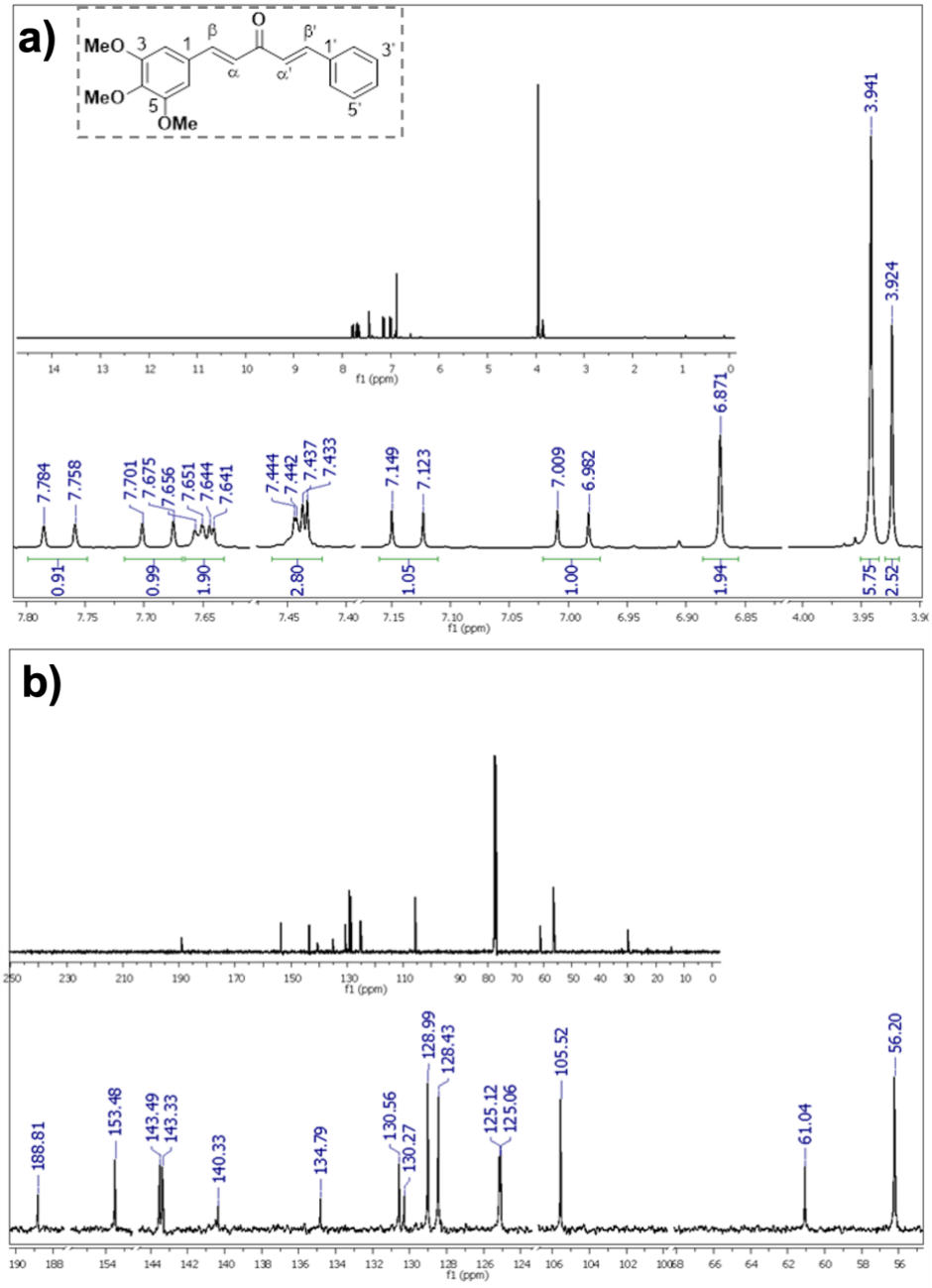

Figure S12. Compound **15:** (1*E*,4*E*)-1-(3,4,5-trimethoxyphenyl)-5-phenylpenta-1,4-dien-3-one.(Yamakoshi *et al.*, 2010) a) ^{1}H NMR spectrum at 600 MHz. b) ^{13}C NMR spectrum at 150 MHz.

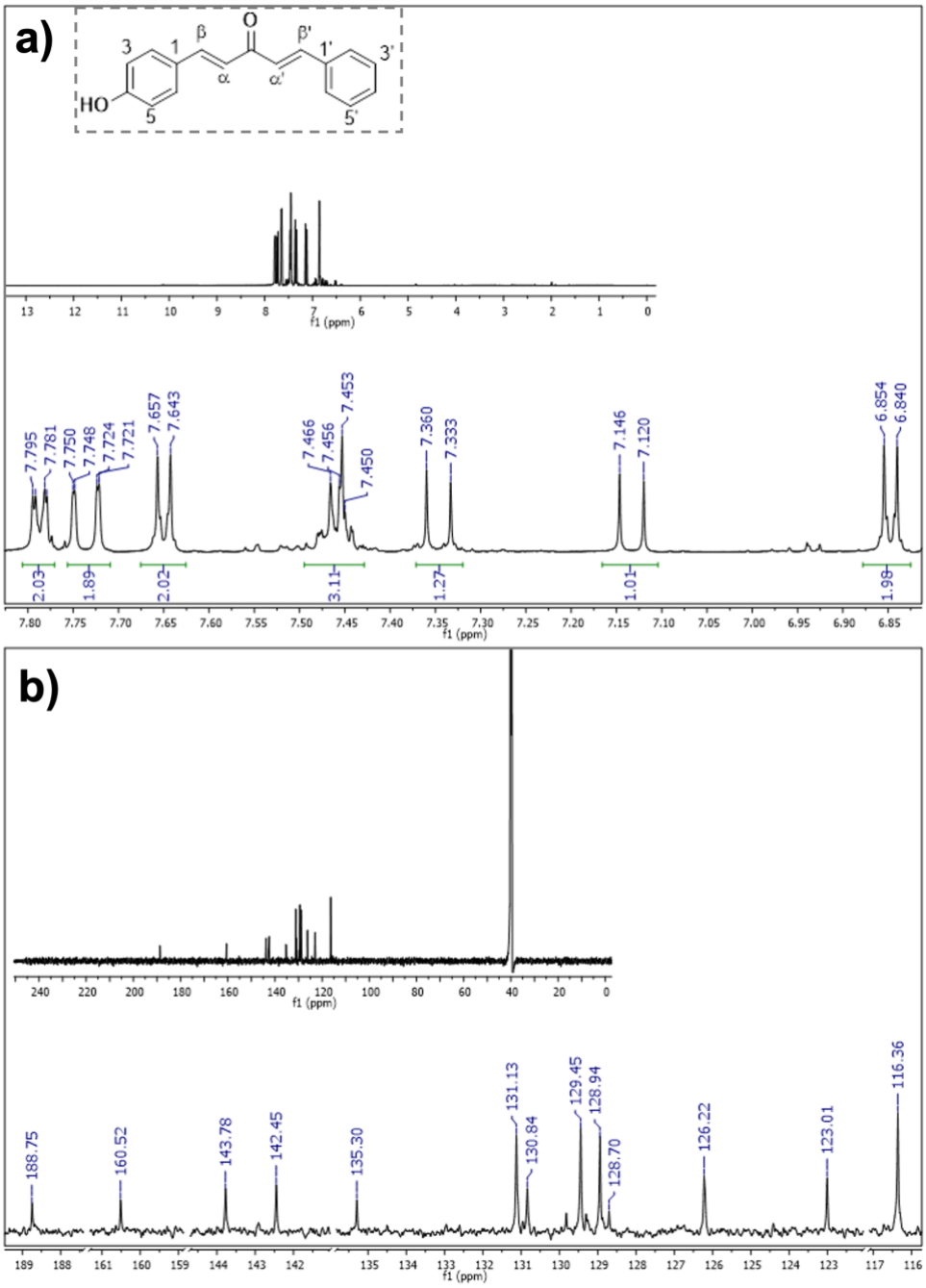

Figure S13. Compound **16:** (1*E*,4*E*)-1-(4-hydroxyphenyl)-5-phenylpenta-1,4-dien-3-one.(Zhou *et al.*, 2018) a) ^{1}H NMR spectrum at 600 MHz. b) ^{13}C NMR spectrum at 150 MHz.

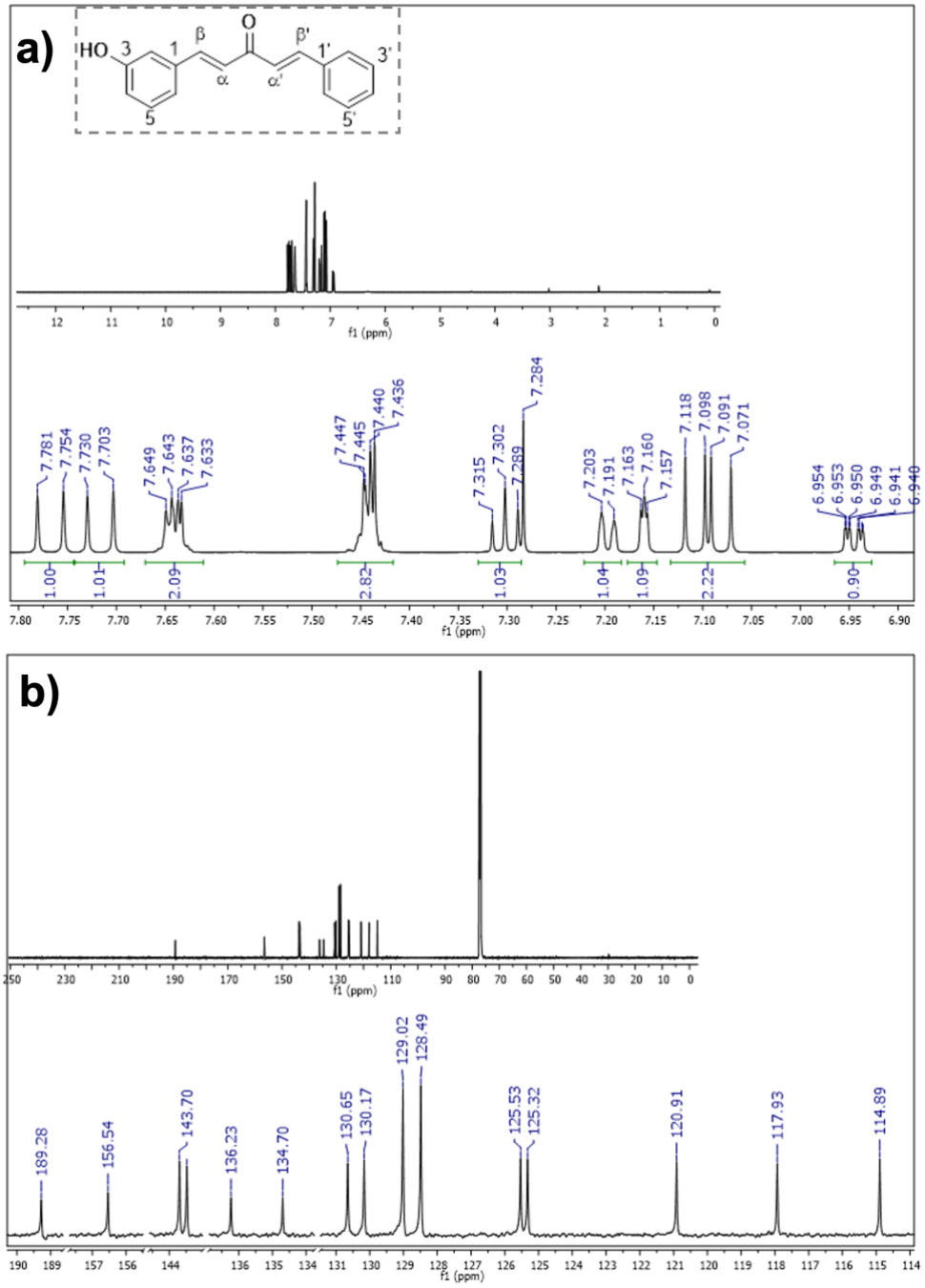

Figure S14. Compound **17:** (1*E*,4*E*)-1-(3-hydroxyphenyl)-5-phenylpenta-1,4-dien-3-one. (Dai *et al.*, 2015; Shen *et al.*, 2015) a) ^{1}H NMR spectrum at 600 MHz. b) ^{13}C NMR spectrum at 150 MHz.

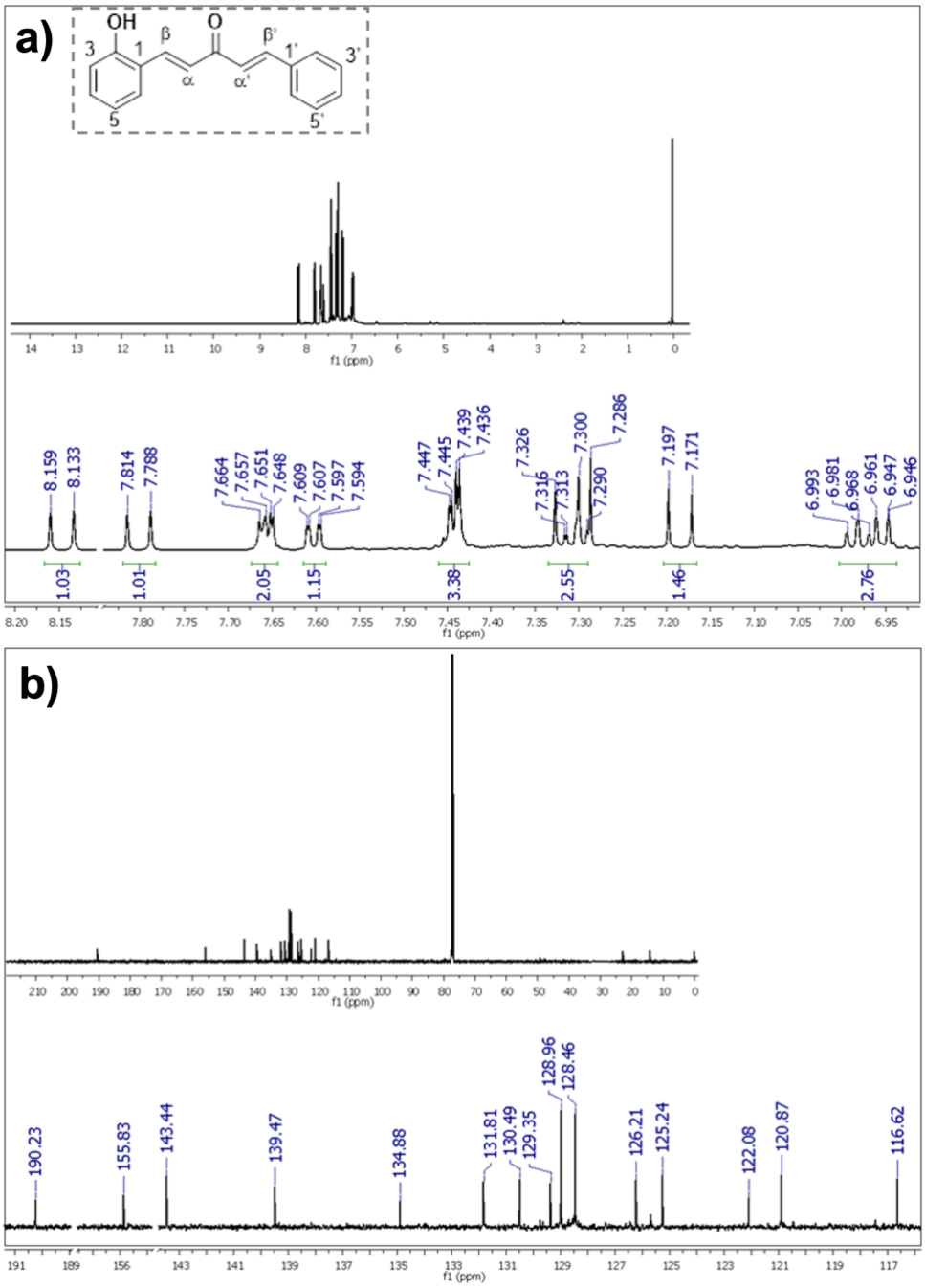

Figure S15. Compound **18:** (1*E*,4*E*)-1-(2-hydroxyphenyl)-5-phenylpenta-1,4-dien-3-one. (Dai *et al.*, 2015; Shen *et al.*, 2015) a) ^{1}H NMR spectrum at 600 MHz. b) ^{13}C NMR spectrum at 150 MHz.

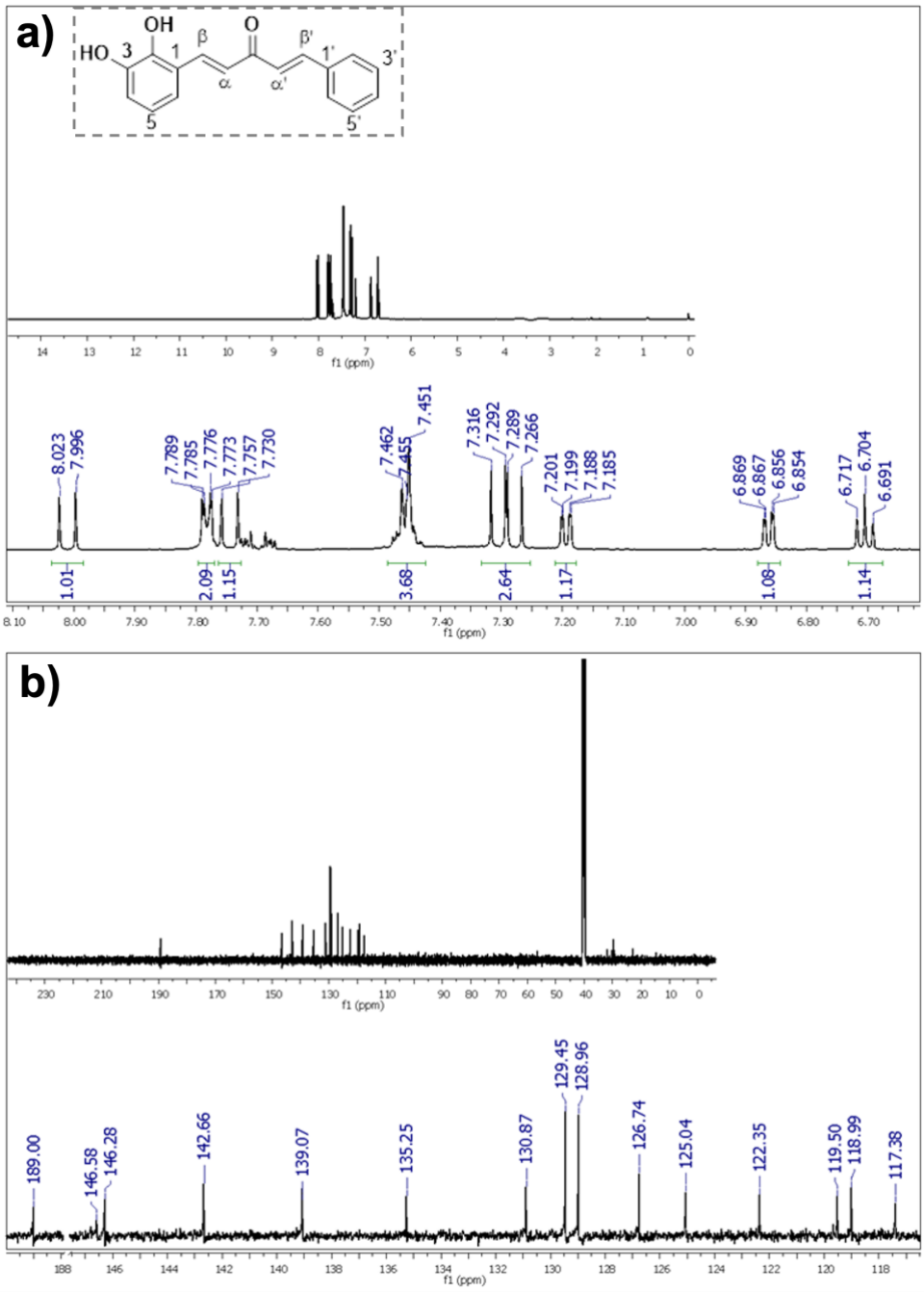

Figure S16. Compound **19:** (1*E*,4*E*)-1-(2,3-dihydroxyphenyl)-5-phenylpenta-1,4-dien-3-one. a) ^{1}H NMR spectrum at 600 MHz. b) ^{13}C NMR spectrum at 150 MHz.

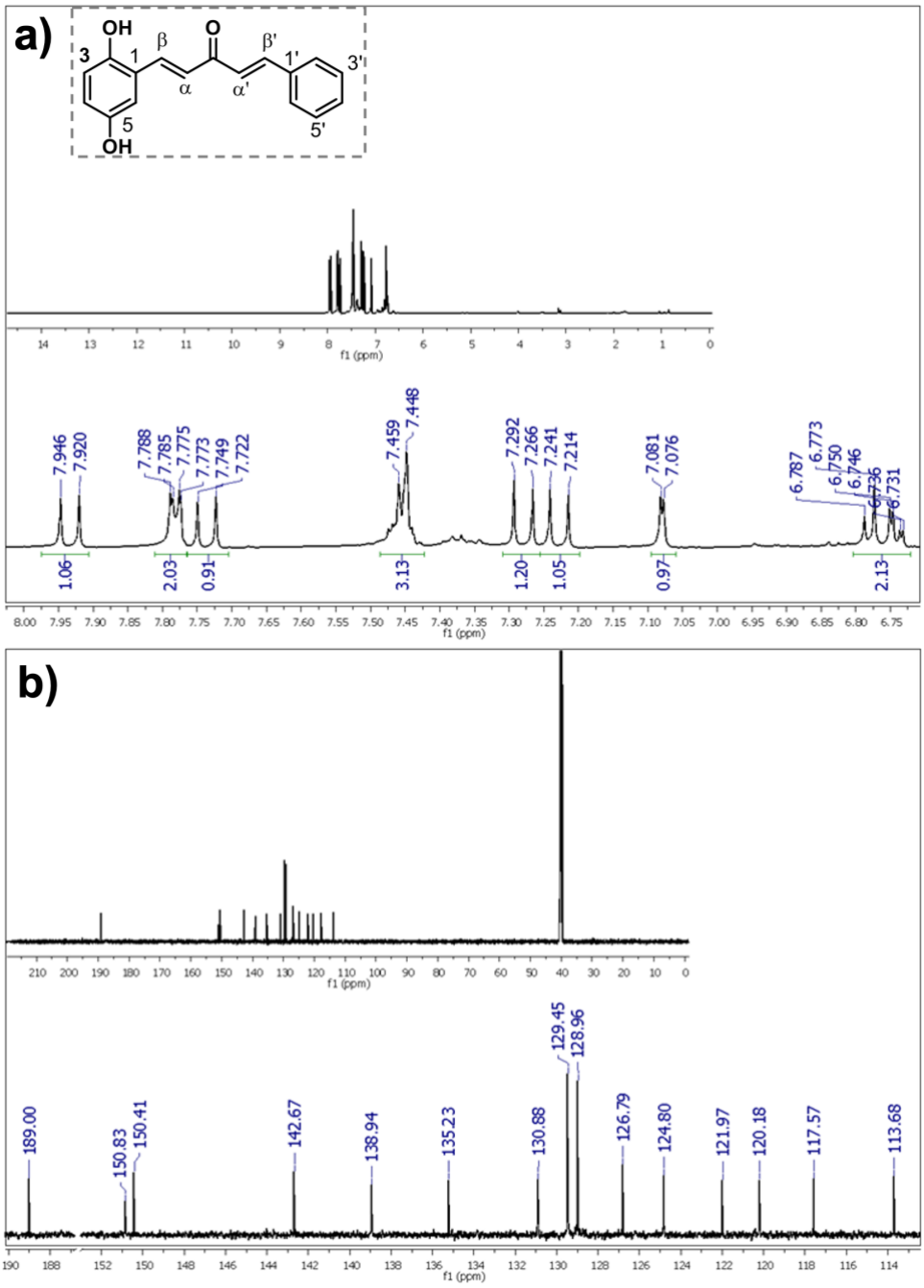

Figure S17. Compound **20:** (1*E*,4*E*)-1-(2,5-dihydroxyphenyl)-5-phenylpenta-1,4-dien-3-one. a) ^{1}H NMR spectrum at 600 MHz. b) ^{13}C NMR spectrum at 150 MHz.

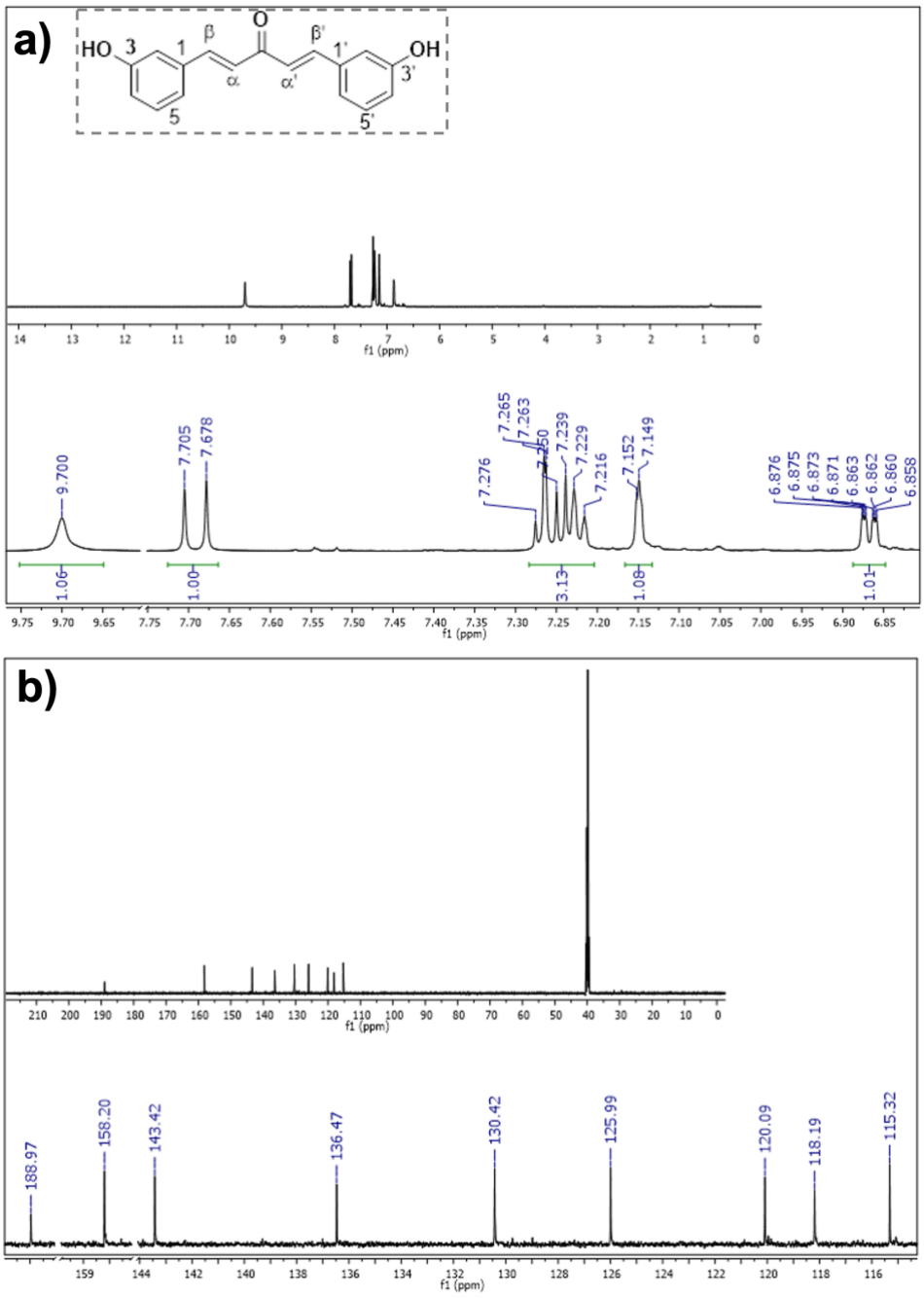

S18. Compound **21:** (1*E*,4*E*)-1,5-*bis*(3-hydroxyphenyl)penta-1,4-dien-3-one.(Dai *et al.*, 2015; Deck *et al.*, 2018) a) ^{1}H NMR spectrum at 600 MHz. b) ^{13}C NMR spectrum at 150 MHz.

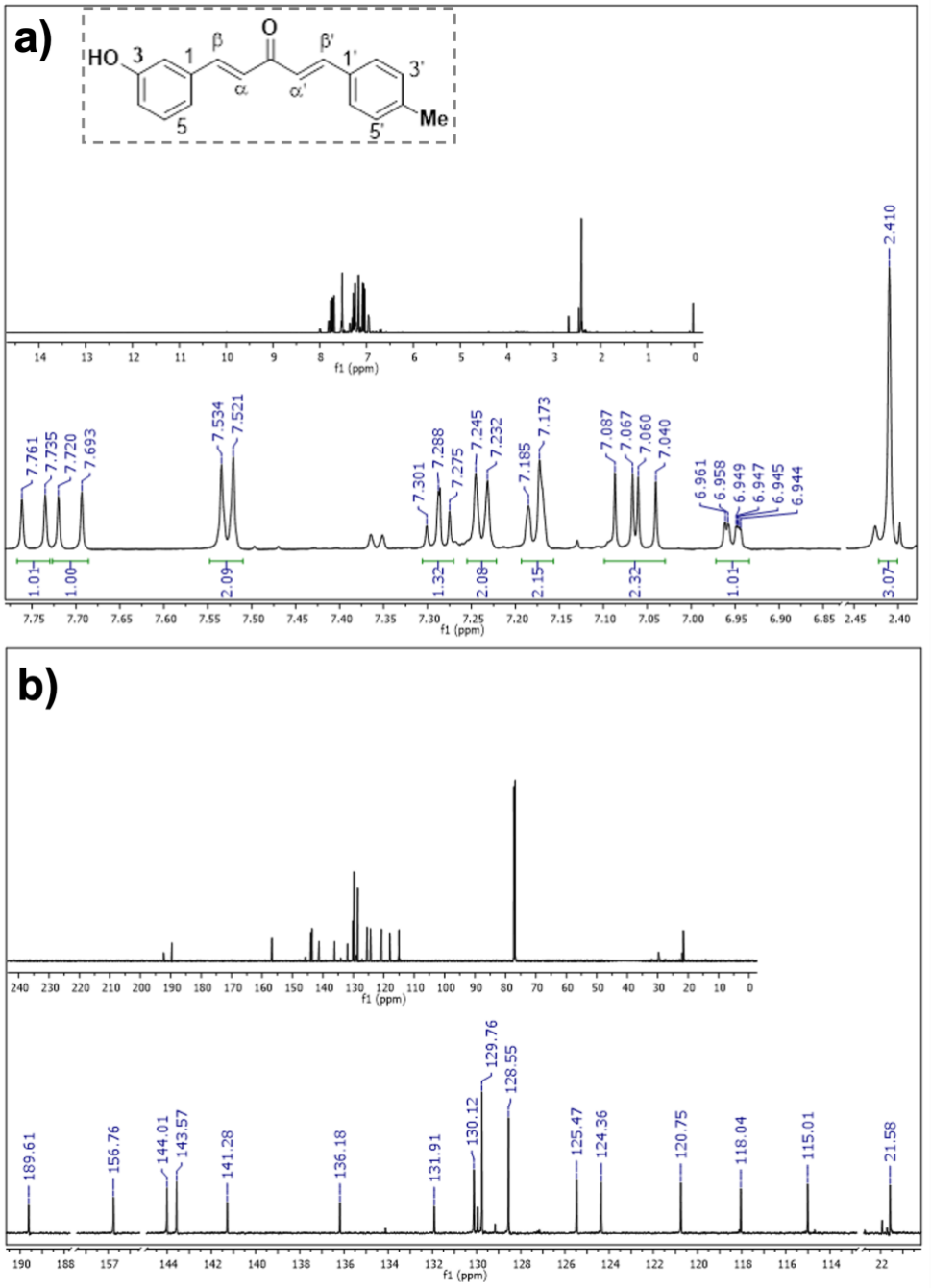

S19. Compound **22:** (1*E*,4*E*)-1-(3-hydroxyphenyl)-5-(4-methylphenyl)penta-1,4-dien-3-one. a) ^{1}H NMR spectrum at 600 MHz. b) ^{13}C NMR spectrum at 150 MHz.

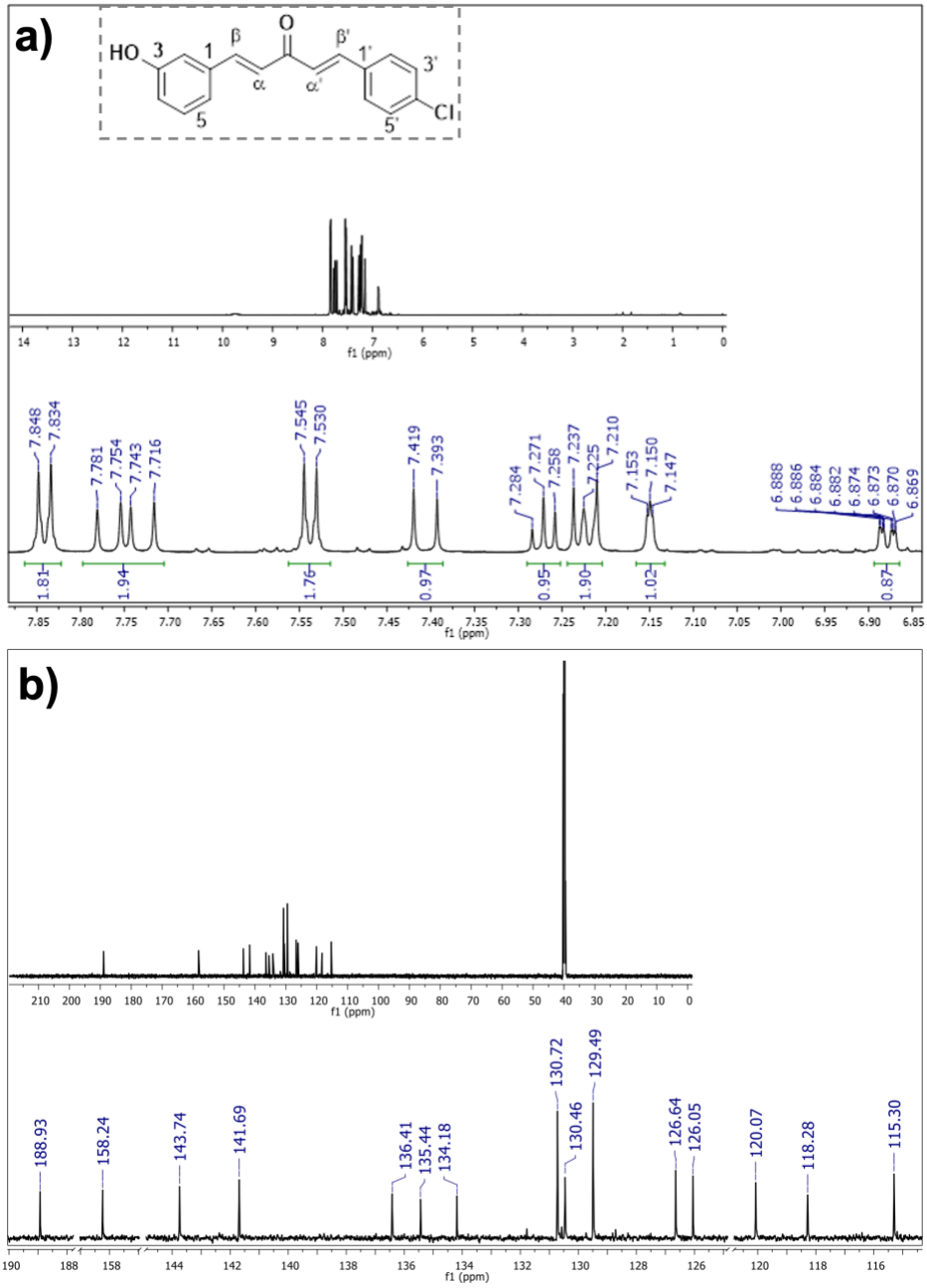

Figure S20. Compound **23:** (1*E*,4*E*)-1-(4-chlorophenyl)-5-(3-hydroxyphenyl)penta-1,4-dien-3-one. a) ^{1}H NMR spectrum at 600 MHz. b) ^{13}C NMR spectrum at 150 MHz.

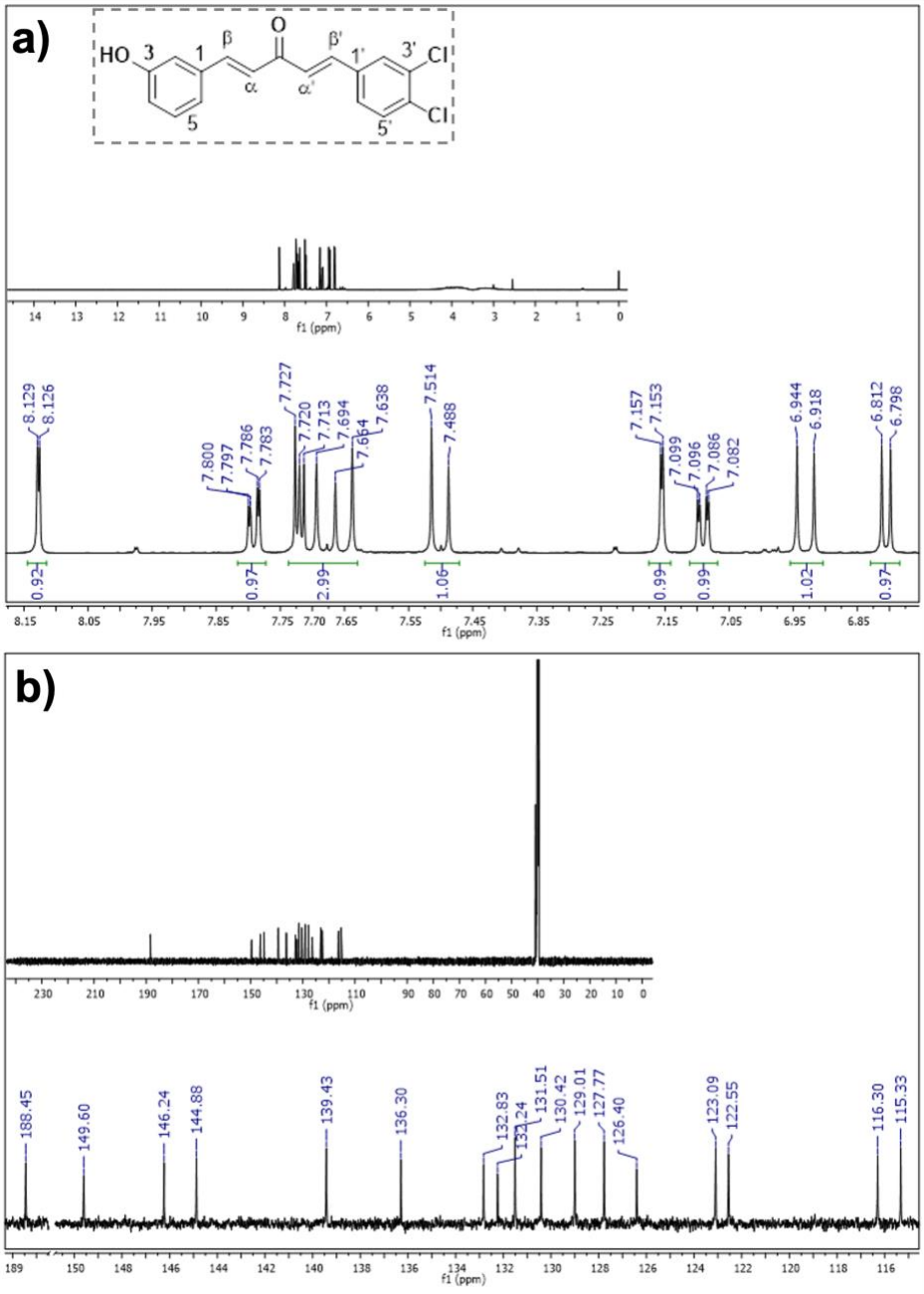

Figure S21. Compound **24:** (1*E*,4*E*)-1-(3,4-dichlorophenyl)-5-(3-hydroxyphenyl)penta-1,4-dien-3-one. a) ^{1}H NMR spectrum at 600 MHz. b) ^{13}C NMR spectrum at 150 MHz.

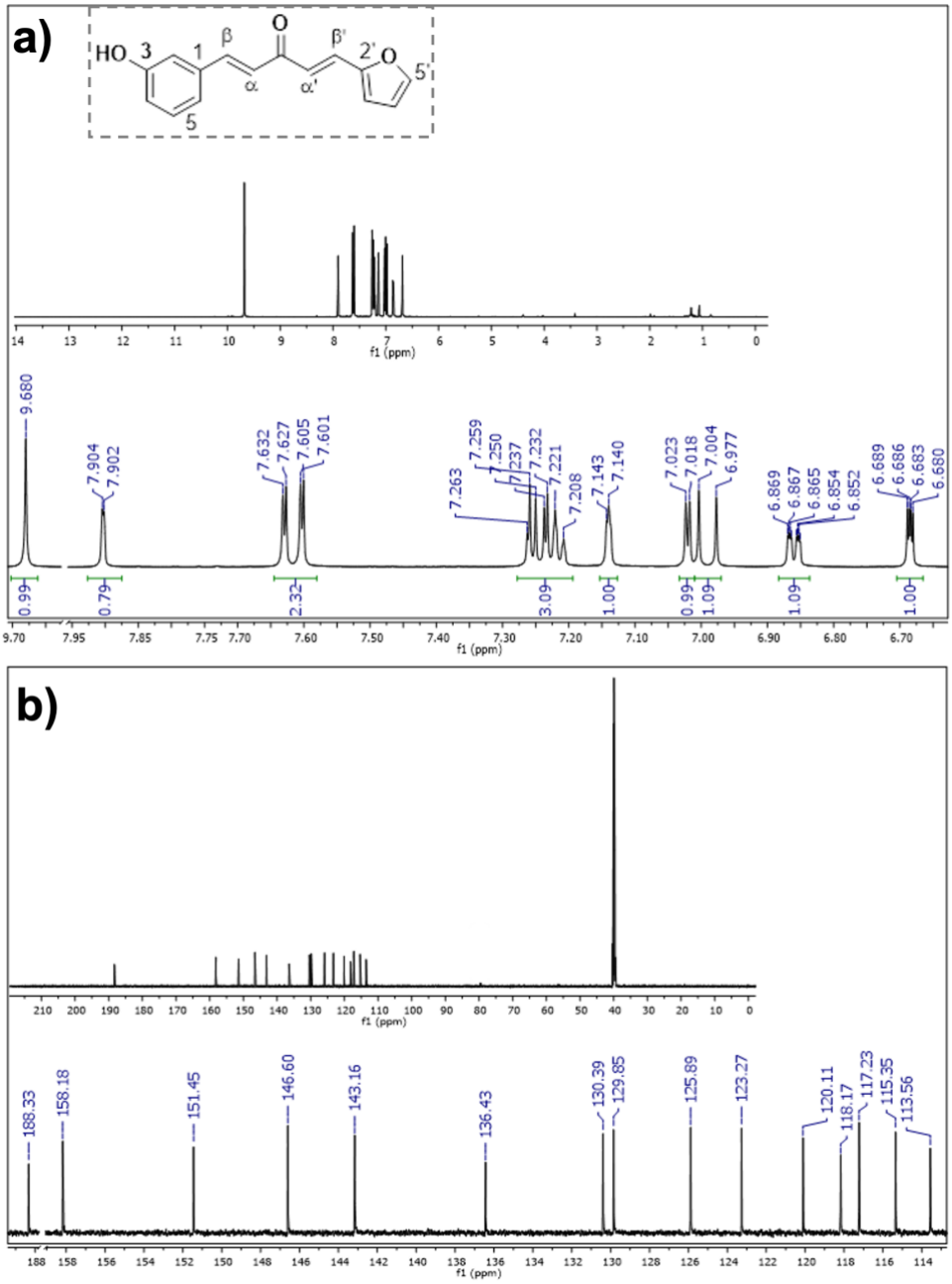

Figure S22. Compound **25:** (1*E*,4*E*)-1-(furan-2-yl)-5-(3-hydroxyphenyl)penta-1,4-dien-3-one. a) ^{1}H NMR spectrum at 600 MHz. b) ^{13}C NMR spectrum at 150 MHz.

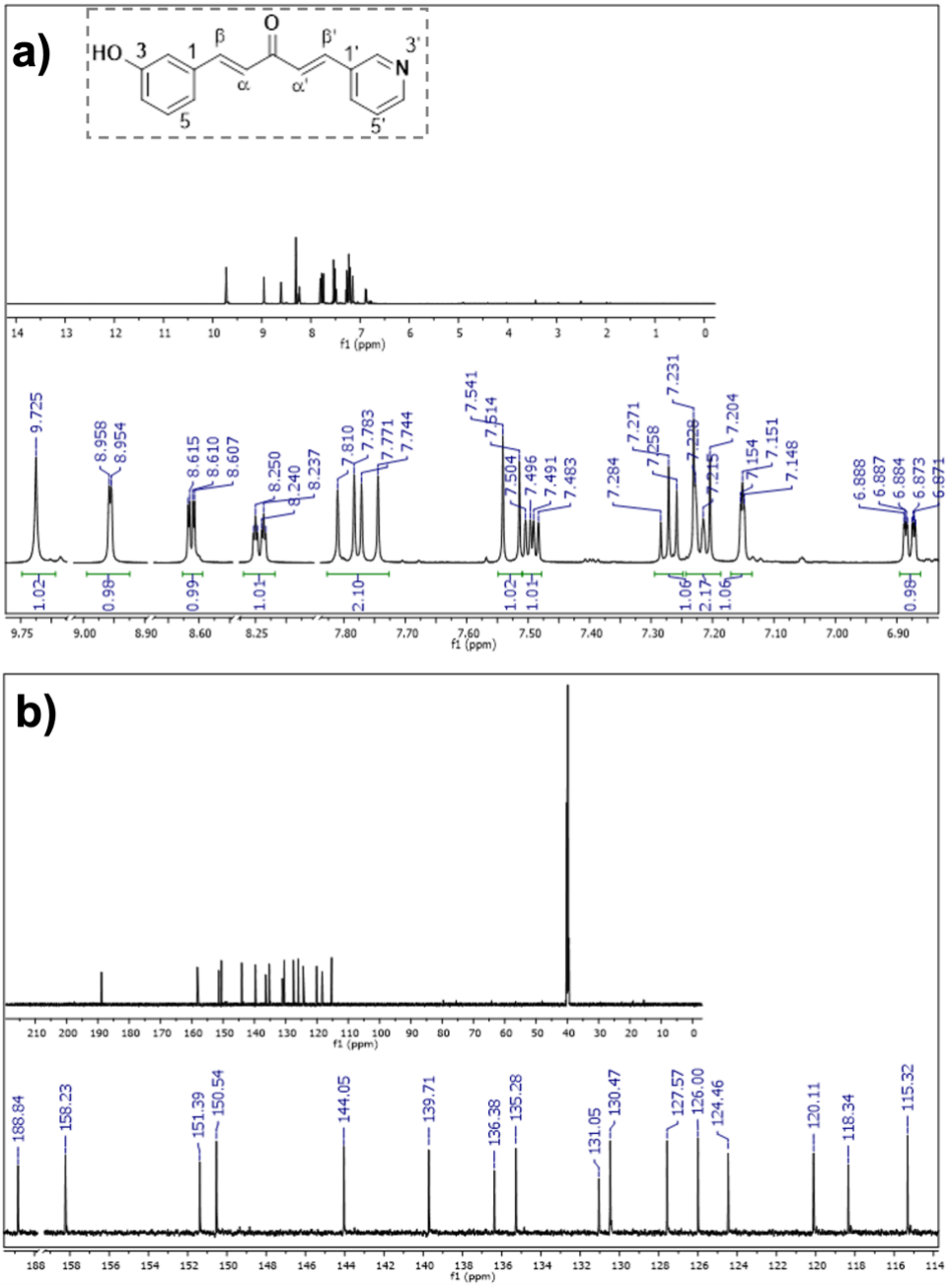

Figure S23. Compound **26:** (1*E*,4*E*)-1-(3-hydroxyphenyl)-5-(pyridin-3-yl)penta-1,4-dien-3-one. a) ^{1}H NMR spectrum at 600 MHz. b) ^{13}C NMR spectrum at 150 MHz.

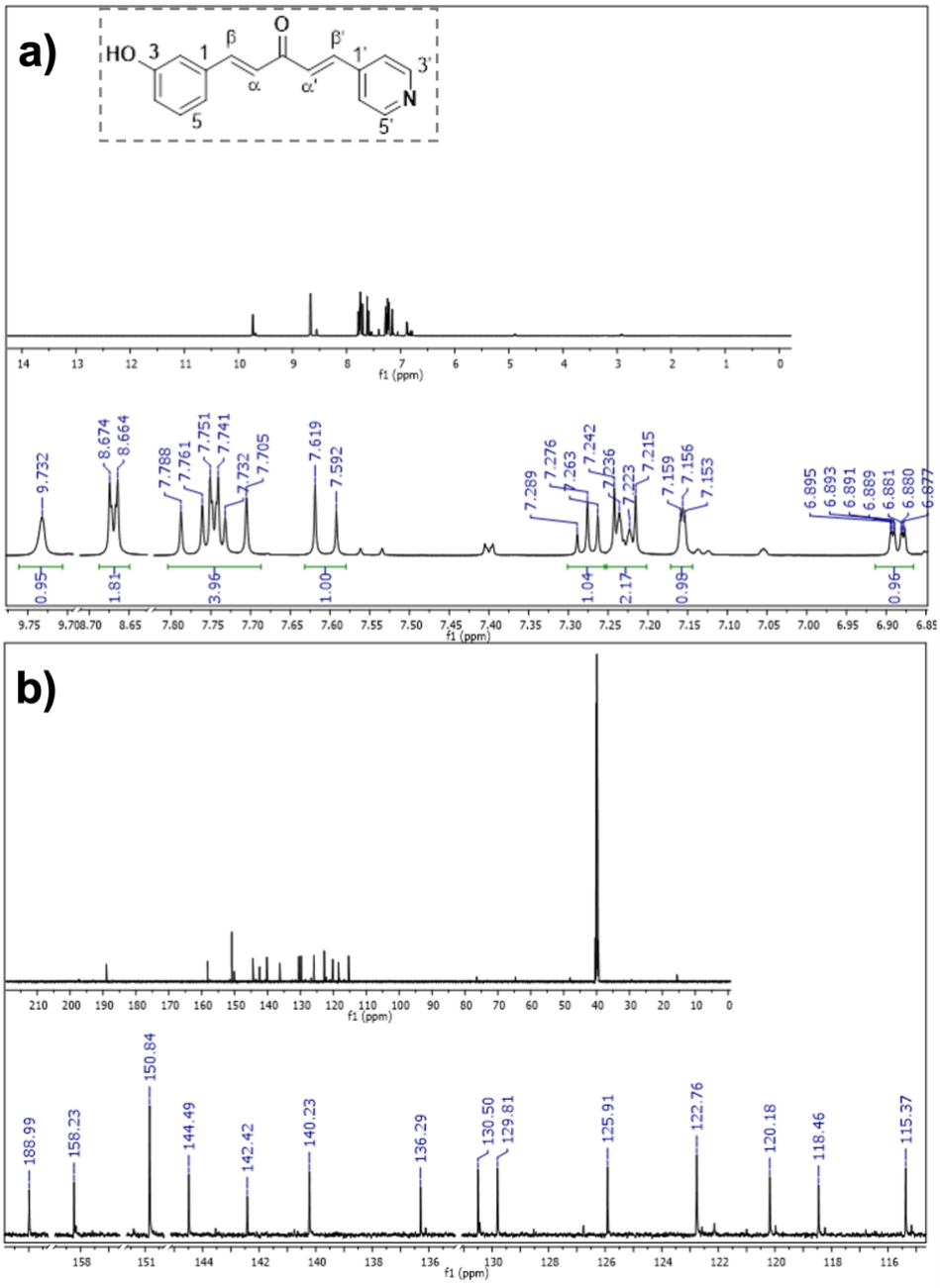

Figure S24. Compound **27:** (1*E*,4*E*)-1-(3-hydroxyphenyl)-5-(pyridin-4-yl)penta-1,4-dien-3-one. a) ^{1}H NMR spectrum at 600 MHz. b) ^{13}C NMR spectrum at 150 MHz.

References

DAI, F. *et al.* Insights into the importance for designing curcumin-inspired anticancer agents by a prooxidant strategy: The case of diarylpentanoids. **Free Radical Biology and Medicine**, v. 85, p. 127–137, 2015.

DECK, L. M. *et al.* Activation of anti-oxidant Nrf2 signaling by enone analogues of curcumin. **European Journal of Medicinal Chemistry**, v. 143, p. 854–865, 2018.

SHEN, T. *et al.* A curcumin derivative that inhibits vinyl carbamate-induced lung carcinogenesis *via* activation of the Nrf2 protective response. **Antioxidants & Redox Signaling**, v. 23, n. 8, p. 651–664, 2015.

WEBER, W. M. *et al.* Anti-oxidant activities of curcumin and related enones. **Bioorganic & Medicinal Chemistry**, v. 13, n. 11, p. 3811–3820, 2005.

YAMAKOSHI, H. *et al.* Structure–activity relationship of C5-curcuminoids and synthesis of their molecular probes thereof. **Bioorganic & Medicinal Chemistry**, v. 18, n. 3, p. 1083–1092, 2010.

ZHOU, J. *et al.* Antimicrobial evaluation and action mechanism of pyridinium-decorated 1,4-pentadien-3-one derivatives. **Bioorganic & Medicinal Chemistry Letters**, v. 28, n. 10, p. 1742–1746, 2018.

Submitted to Journal of Applied Microbiology

4. Monocarbonyl Curcuminoid Coating: A multifunctional coating with anti-adhesion, fungal-killing, and anti-biofilm formation of *Candida albicans*

Veridianna Camilo Pattini, Leticia Ribeiro de Assis, Margarete Tereza G. de Almeida, Luis Octavio Regasini and Henny C. van der Mei

Abstract

Biofilms can be life-threatening in *Candida albicans* infections associated with medical devices. This study aimed to evaluate the effectiveness of 2-hydroxy-dibenzylideneacetone, a monocarbonyl curcuminoid as an antibiofilm coating against *C. albicans*. Polystyrene and glass were used to study the influence of a curcuminoid coating on surface hydrophobicity and biofilm formation. Coated and uncoated surfaces were characterized using FTIR and water contact angle measurements to evaluate the coating. FTIR analysis indicated successful coating on both surfaces. AFM data showed that the curcuminoid coating on polystyrene decreased the adhesion strength of *C. albicans*, while the coating on glass did not significantly alter the adhesion strength. Although, the curcuminoid coating inhibited *C. albicans* adhesion by 66% under flow conditions on glass. The curcuminoid coating decreased the hyphal growth 86% on polystyrene and 65% on glass surfaces. Additionally, biofilm formation was reduced by 48% on coated polystyrene surfaces, but was similar for coated and uncoated glass. Gene expression revealed downregulation of adhesion and biofilm-related genes (*HWP1, ALS3, ALS5*) during the different stages of biofilm formation. Exposure of a 48 h biofilm to curcuminoid showed a decrease in the metabolic activity of the biofilm. This study underscores the potential of a curcuminoid coating to prevent *C. albicans* adhesion, hinder biofilm formation, and reduce metabolic activity of mature biofilms, highlighting its potential use as an antifouling coating against *Candida*-associated infections.

Introduction

Biofilms are life-threatening in medical-related infections, particularly when associated with medical devices, such as intravascular and urinary catheters, dental implants, and orthopedic implants (Srivastava, Chandra e Kumar, 2019). Once attached to the surfaces, these microbial clusters induce metabolic, phenotypic, and genotypic alterations, leading to increased microbial resistance to antimicrobial agents when compared to planktonic cells (Singh, Gaur e Maurya, 2019). *Candida albicans* emerges as the most frequent opportunistic fungus among nosocomial infections, accounting for 15% of sepsis and 40% of bloodstream infections in clinical settings, being one of the most prevalent causative agents of bloodstream infections associated with vascular devices in hospital settings (Magill *et al.*, 2014; Pfaller e Diekema, 2007). Hence, the elimination of biofilms presents a challenge within the medical field.

Currently, studies are focused on exploring surface modifications to create antifouling materials for medical devices and implants by an antimicrobial coating or an antimicrobial releasing coating to prevent or disrupt the adhesion of microorganisms and inhibit biofilm formation on medical devices and implants (Abreu *et al.*, 2013; Campoccia, Montanaro e Arciola, 2013). Antifungal agents such as amphotericin B (Alves *et al.*, 2019), fluconazole (Naderi *et al.*, 2020), and caspofungin (Lamont-Friedrich *et al.*, 2021) have demonstrated promising outcomes. However, their persistent application on surfaces can contribute to the selection and emergence of novel resistant strains. Consequently, innovative strategies are being explored to develop antimicrobial biomaterials that do not rely on antibiotic release (Afewerki *et al.*, 2020).

Curcumin has shown promising potential as an antimicrobial product to coat materials with applications, from the food industry (Manohar *et al.*, 2015) to the healthcare sector, in wound-dressings (Gaydhane, Kanuganti e Sharma, 2020) and coatings on medical devices, such as surgical sutures which showed faster healing and less inflammation of the wound in a mouse

model (Sunitha S *et al.*, 2017). Multilayer curcumin-loaded coatings have exhibited sustained release and strong antibacterial effects, confirming their suitability for orthopedic implants (Virk *et al.*, 2019). Additionally, a coating mixture of curcumin, chlorhexidine, and silver has proven effective for urinary catheters, demonstrating prevention and inhibition of bacterial colonization, along with lubricious properties (Modak S. M. *et al.*, 2019). However, problems associated with stability of curcumin under physiological conditions prevent its clinical use (Nelson *et al.*, 2017). The β-diketone moiety replacement in the curcumin by a monocarbonyl has overcome this limitation and improved its bioactivities.(Shetty *et al.*, 2014) The antifungal effect of monocarbonyl curcumin analogs have been little explored. Only a few papers describe their antifungal activity, in which they only searched a preliminary susceptibility assay against planktonic yeast cells (Nagargoje *et al.*, 2020a; Nagargoje *et al.*, 2020b)

Understanding the mechanisms of action of monocarbonyl curcuminoids as antifungal agents and exploring their potential as a coating on materials can lead to innovative approaches in combating *Candida* biofilm-associated infections. According to former literature, there are no investigations focused on coating surfaces with monocarbonyl curcumin analogs. Therefore, here it is investigated if monocarbonyl curcuminoids can be used as a coating on the surface in order to avoid biofilm formation.

Material and methods

Curcumin and monocarbonyl curcuminoids

Curcumin and all reagents and solvents were purchased from Merck (Kenilworth, USA). The synthesis of monoketone curcuminoids **A**–**G** (Table 1) was performed using the procedures described by Polaquini *et al.*(Polaquini *et al.*, 2024, 2021). The structures of the compounds were confirmed by ^{1}H and ^{13}C NMR spectral data analyses (Figures S1–S7).

Table 1. Structures of curcuminoids **A**−**G**

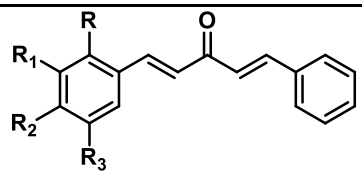

Monocarbonyl curcuminoid	Code	R	R_1	R_2	R_3	References
3,5-dimethoxy-4-hydroxy-dibenzylideneacetone	**A**	H	OCH_3	OH	OCH_3	This paper
3-methoxy-4-hydroxy- dibenzylideneacetone	**B**	H	OCH_3	OH	H	Polaquini *et al*., 2020; Weber *et al*., 2005.
3-hydroxy-4-methoxy- dibenzylideneacetone	**C**	H	OH	OCH_3	H	Polaquini *et al*., 2024
2-hydroxy- dibenzylideneacetone	**D**	OH	H	H	H	Dai *et al*., 2015; Shen *et al*., 2015
3-hydroxy- dibenzylideneacetone	**E**	H	OH	H	H	Polaquini *et al*., 2020; Polaquini *et al*., 2024; Dai *et al*., 2015; Shen *et al*., 2015
4-hydroxy- dibenzylideneacetone	**F**	H	H	OH	H	Polaquini *et al*., 2020; Zhou *et al*., 2018
2,5-dihydroxy- dibenzylideneacetone	**G**	OH	H	H	OH	Polaquini *et al*., 2024

Fungal strains, harvesting, and culture conditions

Reference strains, including *C. albicans* ATCC 10231*, Candida krusei* ATCC 40147*, Candida auris* CBS 1913 and clinical isolates of systemic infection of *Candida* spp. from the collection of the Laboratory of Mycology, Department of Dermatological, Infectious, and Parasitic Diseases, São José do Rio Preto Medical School (FAMERP), São José do Rio Preto, Brazil, were used for the susceptibility tests. The strains were grown on Sabouraud Dextrose Agar (Difco Laboratories, Detroit, MI, USA) and yeast colonies from the agar were suspended in phosphate-buffered saline (PBS, 5 mM K_2HPO_4, 5 mM KH_2PO_4 and 0.15 M NaCl, pH 7.0) to a concentration of 3×10^6 mL^{-1}, as determined in a Bürker-Türk counting chamber.

To prepare yeast suspensions for the adhesion and atomic force microscopy experiments, one colony from the agar plate was transferred into a 10 mL yeast nitrogen base

(YNB, Difco Laboratories, Detroit, MI, USA) and grown for 24 h at 30 °C. This pre-culture was inoculated in 190 mL YNB (1:20) and the main culture was grown for 16 h at 30 °C. Yeast was harvested by centrifugation for 5 min at 4000 × g and resuspended in 10 mL PBS, this was repeated three times to remove all traces of growth medium. Finally, yeast was resuspended in PBS to a concentration of 3×10^6 mL^{-1}, as determined in a Bürker-Türk counting chamber.

Susceptibility assay to determine the most active curcuminoids

To select the most active curcuminoid, the susceptibility profile of *Candida* spp. against the curcuminoids was measured by determining the Minimum Inhibitory Concentrations (MIC) and Minimum Fungicidal Concentrations (MFC), according to the Clinical Laboratory Standard Institute (CLSI) document M27-A3,(CLSI, 2008) with some minor modifications. Briefly, the yeast suspension was diluted to 3×10^3 mL^{-1} in RPMI-1640 medium (Rosen Park Media Institute, Sigma-Aldrich, St. Louis, MO, USA) and 100 µL of the yeast suspension was added to a 96 wells polystyrene plate containing 100 µL RPMI-1640 medium with different concentrations of the curcuminoids (500–7.8 µg mL^{-1}). RPMI-1640 medium was the negative control and yeasts suspension without curcuminoids was the positive control. The plates were incubated at 30 °C for 24 h. The MIC value was determined as the lowest concentration with no visible growth. To determine MFC, an aliquot of 10 µL from each well without visible growth was plated on Sabouraud Dextrose Agar and incubated at 30 °C for 24 h. The MFC was defined as the lowest concentration of the curcuminoid showing no colonies on the agar plates. The experiment was performed in triplicate with separately cultured yeast. The most active compound, 2-hydroxy-dibenzylideneacetone (**D**), was selected for further studies described below.

Coating surfaces with curcuminoid D

Hydrophobic polystyrene and hydrophilic glass were used as model materials. Sterile 12, 48, and 96-well polystyrene flat-bottom microtiter plates were purchased from CELLSTAR®

(Greiner Bio-one, Frickenhausen, Germany), and microscope glass slides from Epredia (Thermo Scientific, Portsmouth, NH, USA). All glass disks were cleaned by sonication for 5 min in 2% RBS 35 detergent (Omnilabo International BV, The Netherlands), rinsed with tap water, washed in methanol (Merck, Darmstadt, Germany), and washed with sterile demineralized water.

The curcuminoid **D** was diluted at 2 mg mL^{-1} in YNB + DMSO (10%). For coating the polystyrene wells plates, 100 µL of the curcuminoid solution was added to each well in a 96 wells plate, 400 µL for 48 wells plate, and 800 µL for 12 wells plate. Glass slides (25 × 75 mm) were exposed to 5 mL of the curcuminoid solution and the smaller glass slides (15 × 15 mm) to 800 µL of the curcuminoid solution. The glass disks (8 mm in diameter) were exposed to 400 µL of the curcuminoid solution. All surfaces were exposed for 24 h at 25 ºC, followed by thorough washing with PBS buffer to remove unbound curcuminoid.

Surface characterization of curcuminoid coatings

The chemical structure of curcuminoid **D** coated on polystyrene and glass surfaces was determined using Fourier transform infrared (FTIR) spectroscopy. FTIR spectra were measured on an Agilent Cary 600 series FTIR spectrometer (Agilent Technologies, St. Clara, CA, USA). FTIR spectra were recorded over the wavenumber range of 4000 and 400 cm^{-1} with a resolution of 4 cm^{-1} and 32 scans were measured and averaged.

Water contact angles were measured to determine the hydrophilicity of the curcuminoid-coated and uncoated polystyrene and glass slides. Water contact angle measurements were carried out using the sessile drop technique with ultrapure water. Ultrapure water droplets of 2 µL were placed on the surfaces and observed using an Olympus BX-41 microscope objective lens. The images were digitally captured using a 1.4-megapixel CCD camera and the contact angle was measured with an image analysis software program (MATLAB, MathWorks, Natick, MA, USA). The reported water contact angles are means of

five measurements performed on different areas of each sample surface in three separate experiments.

Evaluation of the antifungal activity of curcuminoid D

The influence of curcuminoid-coating on C. albicans adhesion in a parallel plate flow chamber

The adhesion of *C. albicans* ATCC 10231 was monitored on uncoated and curcuminoid **D** coated glass slides on the bottom plate of a parallel plate flow chamber, as described previously.(Busscher e Mei, Van Der, 2006) The adhesion of *C. albicans* (10^6 cells mL^{-1}) in PBS was observed with a phase-contrast microscope (Olympus BH-2) equipped with a 10× ultra-long working distance objective (Olympus ULWD-CD Plan 40 PL), connected to a CCD-MXRi camera (Basler A101F, Basler AG, Germany). After 4 h of flowing (share rate of 15 s^{-1}) the yeast suspension through the flow chamber, images were taken at 10 different locations on each sample. The yeast suspension was drained to determine the adhesion strength of the yeasts using an air-liquid interface over the adhering yeast and the flow chamber was filled again with PBS to take images at 10 different locations. The number of adhering yeasts obtained on the curcuminoid coating was compared to the uncoated glass.

Image analysis was done using software based on the Matlab Image Processing Toolkit (The Math Works, MA, USA). Live images were acquired after the summation of 15 consecutive images (time interval 1 s) to enhance the signal-to-noise ratio and to eradicate flowing yeast from the analysis. The experiments were done in triplicate with separately cultured yeasts.

Adhesion strength of yeasts on curcuminoid-coated surfaces

The adhesion forces of *C. albicans* ATCC 10231 on uncoated and curcuminoid **D** coated polystyrene and glass were measured using atomic force microscopy, as described previously.(Carniello *et al.*, 2020) Before each measurement, cantilevers (Bruker, Billerica,

MA, USA) were calibrated using the thermal tuning method and spring constants were always close to the producer's specification of 0.06 N m^{-1}. The yeast probe was prepared by immobilizing a yeast cell to a NP-0 tipless cantilever coated with poly-L-lysine (Sigma-Aldrich, St. Louis, MO, USA) using electrostatic attraction. Yeast probes were used immediately after the preparation. All adhesion forces were performed in PBS and at room temperature under a loading force of 5 nN and at three randomly chosen spots on uncoated and curcuminoid-coated polystyrene and glass. The experiments were performed in duplicate with separately cultured yeasts.

The influence of curcuminoid-coating on hyphal development of C. albicans

The hyphal development was performed on uncoated and coated polystyrene 12 wells plate and glass slides (15 × 15 mm). In each well with or without glass slides and with or without a curcuminoid **D** coating, 800 µL *C. albicans* (10^4 cells mL^{-1}) in YNB were added and incubated for 3.5 h with shaking (80 rpm) at 37 °C. After 3.5 h, the hyphal development was analyzed using an inverted microscope (Rebel, RBLTEW31) equipped with an iPad Pro 2 MP CMOS color camera. Three pictures of each well were taken in each experiment. The experiment was performed in triplicate with separately cultured yeasts.

The efficacy of curcuminoid-coating on biofilm formation

The biofilm formation was performed on uncoated and coated polystyrene 48 wells plate and glass disks (8 mm in diameter). In each well with or without a glass disk and with or without a curcuminoid coating, 400 µL *C. albicans* (10^6 cells mL^{-1}) in PBS was added and incubated at 37 ºC under shaking at 80 rpm for 2 h. After 2 h, the PBS was removed, and 400 µL of Sabouraud Dextrose Broth was added to the wells. The plate was incubated under the same conditions for 48 h. The culture medium was refreshed after 24 h. After 48 h, the colony forming units (CFU) were determined by removing the growth medium, washing the biofilm carefully

twice with 400 µL PBS to remove non-attached cells. After washing, the glass disks were removed from the 48-well plate and transferred to a clean well and 400 µL of PBS was added. The plate was sealed with parafilm and sonicated for 5 min to detach the biofilm from the polystyrene and glass disk surfaces. After sonication, the biofilm was suspended using a pipette. Sequential dilutions were performed and three 10 µL aliquots from each well were plated on Sabouraud Dextrose Agar and incubated at 30 °C for 24 h, after which the colonies were counted. The experiment was performed in triplicate with separately cultured yeasts.

In order to evaluate the therapeutic effect of curcuminoid **D**, 100 µL of *C. albicans* (10^6 cells mL^{-1}) in PBS was added in each well of a polystyrene 96 wells plate and incubated at 37 ºC under shaking at 80 rpm for 2 h. After 2 h, the PBS was removed, and 100 µL of Sabouraud Dextrose broth was added to the wells. The plate was incubated under the same conditions for 48 h and the culture medium was refreshed after 24 h. After 48 h and removal of the culture medium, curcuminoid **D** diluted in Sabourand Dextrose broth and 10% DMSO, was added into the wells with the biofilm at different concentrations (0, 31.2, 62.5, 156, and 312 µg mL^{-1}) and incubated under the same conditions for 24 h. All data were expressed relative to biofilms exposed to only growth medium. After incubation, the growth medium was removed, and the biofilms were washed with PBS to remove non-adhered cells. The metabolic activity of the biofilms was determined with 3-(4,5-dimethylthiazol-2-yl)-2,5-diphenyl tetrazolium bromide (MTT), a yellow dye, which is reduced by cellular enzymes to the blue formazan. Briefly, 100 µL of MTT solution (1 mg ml^{-1} in PBS) was added to each well of a 96 wells plate with a biofilm and incubated at 37 °C for 4 h, protected from light. After 4 h, the MTT solution was removed, and the plates were air dried and 100 µL of 2-propanol was added to dissolve the MTT-formazan product. 100 µL of the propanol-solubilized product was transferred to a new 96-well plate and the optical density was measured at 570 nm on a microplate reader.

Confocal laser scanning microscopy (CLSM, Leica) was used to visualize 48 h biofilms of *C. albicans* ATCC 10231 grown on curcuminoid coated and uncoated polystyrene and glass surfaces. After 48 h, biofilms were washed with PBS and stained with the LIVE/DEAD™ Yeast Viability Kit (Invitrogen, ThermoFisher Scientific, The Netherlands). The Kit was provided with two stains: FUN-1 and Calcofluor White M2R. Upon excitation, FUN-1 shows green fluorescent membrane structures and red fluorescent metabolically active intravacuolar structures, and Calcofluor white stains cell walls blue fluorescent. Staining was done according to the manufacturer's instructions, after which excess stain was removed by washing two times with PBS, and biofilms were immersed in 3 mL PBS. CLSM images were collected using a Leica TCS SP2 CLSM with a 40x water objective using 580 nm excitation and emission filter settings of 365–510 (blue, cell wall), 510–560 nm (green, membrane), and 560–610 nm (red, metabolically active intravacuolar structures). Images were taken over the depth of a biofilm in sequential z-intervals of 2 µm. Subsequently, the stacks of images acquired were color-coded and quantitatively analyzed using fully open-source and free software (Fiji/ImageJ).

Analysis of the influence of curcuminoid-coatings on the gene expression of C. albicans biofilms

The analysis of gene expression was performed under different stages of biofilm formation such as hyphal development, 2 h and 48 h biofilm in order to evaluate the inference of the curcuminoid **D** coating with the genes responsible for adhesion, aggregation, and hyphal development of *C. albicans*. The genes analyzed were: *ALS1* (agglutinin-like sequence 1), *ALS3* (agglutinin-like sequence 3), *ALS5* (agglutinin-like sequence 5), and *HWP1* (hyphal cell wall protein 1) and *Actin 1* was used as the household gene.

The different stages of biofilm formed on coated and uncoated polystyrene surfaces were suspended in PBS prepared in ultrapure water (DNA/RNA free) and subjected to centrifugation for 2 min at 12,000 × g and the supernatant was discarded from the pellet. RNA

was extracted from the yeasts using the Ribopure RNA Purification Kit, Yeast (Invitrogen, Thermo Fisher Scientific, Groningen, The Netherlands) according to the manufacturer's instructions. Traces of genomic DNA were removed using the DNA-free kit (Invitrogen, Thermo Fisher Scientific, Groningen, The Netherlands). The amount and quality of extracted RNA was based on the 260/280-nm ratio measured using the NanoDrop ND-1000 (NanoDrop Technologies LLC, Thermo Fisher Scientific, Wilmington, DE, USA). A mixture of 200 ng RNA, 4 µL 5 × iScript reaction mixture, and 1 µL iScript reverse transcriptase, in a total volume of 20 µL (Iscript; Bio-Rad, Hercules, CA), was used for cDNA synthesis according to the manufacturer's instructions. Real-time reverse transcription-quantitative PCR (RT-qPCR) was performed in a 384-well plate (HSP-3905; Bio-Rad Laboratories, Foster City, CA, USA) with the primer sets for the selected genes (see Table S1 in the supplementary material). The following thermal conditions were used for all RT-qPCRs: 95 °C for 3 min and 40 cycles of 95 °C for 15 s and 60 °C for 45 s.

The absolute C_t values from all the RT-qPCR assays were used to calculate the expression ratios of the genes in *C. albicans* cells formed on curcuminoid coated glass and polystyrene surfaces compared to uncoated counterparts. The values obtained were normalized using the household *ACT1* (encoding beta-actin) gene as a reference. The data were expressed in relation to the gene expression of the positive control (biofilms formed on uncoated surfaces). Gene expression was assessed in triplicate experiments with separately grown cultures.

Statistical analysis

Statistical analysis was performed using GraphPad Prism Software (version 8.2 for Windows, La Jolla, California, USA). Data are the mean of three biologically independent experiments ± standard deviation (SD). Statistically significant differences between the experimental groups were determined by one-way analysis of variance (ANOVA) or Student's *t*-test. A *P*-value of ≤ 0.05 was considered statistically significant.

Results

Minimum inhibitory concentration (MIC) and minimum fungicidal concentration (MFC) of curcuminoids

The anti-*Candida* activities of curcumin and unsymmetrical monocarbonyl analogs (Curcuminoids **A-G**) were evaluated against six *Candida* strains (Table 2). Out of seven curcumin analogs, six compounds completely inhibited the growth of at least one *Candida* strain at concentrations below 250 μg mL^{-1} (Table 2). The hydroxyl group position was particularly relevant for fungitoxicity, compounds with hydroxyl groups at the carbons 2' (**D**) and 3' (**E**) exhibited higher anti-*Candida* activity compared to their regioisomer at carbon 4' (**F**) position. This pattern was also observed in methoxylated-hydroxylated curcuminoids, as curcuminoid **C**, with hydroxyl at position 3’ and methoxyl at position 4’, which inhibited three strains. On the other hand, curcuminoid **B** with methoxyl and hydroxyl at position 3’ and 4’, respectively, did not inhibit growth of any strain at concentrations below 250 μg mL^{-1}.

Curcuminoid **D** had the lowest MIC and MFC values from all curcuminoids derivatives investigated. Based on these results, curcuminoid **D** was selected for further experiments.

Table 2. Antifungal activity of curcuminoids against planktonic *Candida* species determined by MIC and MFC.

Compounds	R	*C. albicans* ATCC 10213		*C. albicans* CA1		*C. krusei* ATCC 40147		*C. auris* CBS 10913		*C. auris* CAU 491	
		MIC ($\mu g\ mL^{-1}$)	MFC ($\mu g\ mL^{-1}$)	MIC ($\mu g\ mL^{-1}$)	MFC ($\mu g\ mL^{-1}$)	MIC ($\mu g\ mL^{-1}$)	MFC ($\mu g\ mL^{-1}$)	MIC ($\mu g\ mL^{-1}$)	MFC ($\mu g\ mL^{-1}$)	MIC ($\mu g\ mL^{-1}$)	MFC ($\mu g\ mL^{-1}$)
Curcumin	-	>250	>250	62.5–125	>125	31.2–62.5	125	31.2	125	31.2	125
A	**3,5-OMe, 4-OH**	>250	>250	250	>250	125–250	>250	125-250	250	125–250	>250
B	**3-OMe, 4-OH**	>250	>250	>250	>250	>250	>250	>250	>250	>250	>250
C	**3-OH, 4-OMe**	>250	>250	>250	>250	250	250	125	125	250	>250
D	**2-OH**	7.8–15.6	15.6	125	>250	31.2	62.5	15.6–31.2	31.2–62.5	31.2	125
E	**3-OH**	31.2–62.5	62.5–125	250–500	>250	250–500	>250	250	>250	125	250
F	**4-OH**	>250	125	>250	>250	>250	>250	250	>250	250	>250
G	**2,5-OH**	>250	>250	>250	>250	250	>250	250	250	250	>250

MIC = the lowest concentration of the substance that inhibited visible yeasts growth

MFC= the lowest concentration of the substances at which 99.9% of the yeasts were killed.

Characterization of the curcuminoids coated surfaces

The chemical structure of curcuminoid **D** coated on polystyrene and glass surfaces were determined using Fourier transform infrared (FT-IR) spectroscopy (Figure 1).

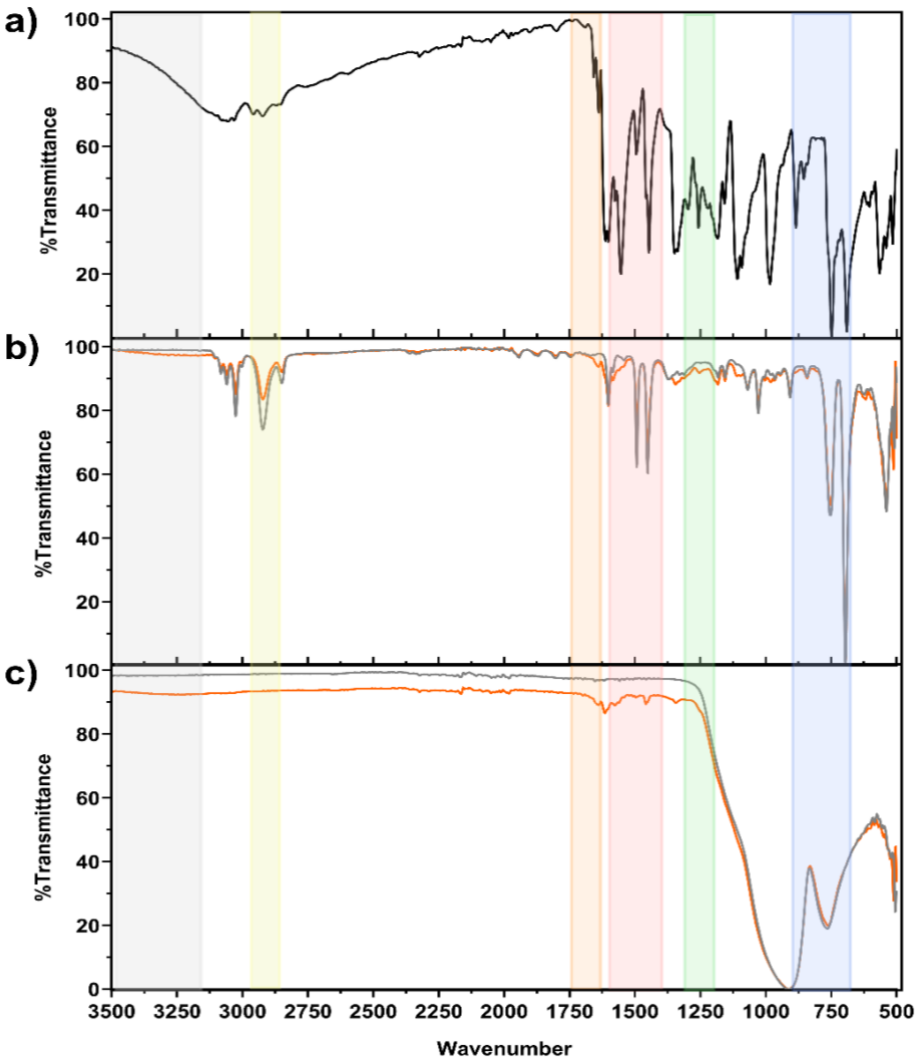

Figure 1. The FTIR spectra of curcuminoid **D** powder and coatings on polystyrene and glass. (**a**) powder mixed in a KBr tablet, (**b**) uncoated and coated polystyrene, and (**c**) uncoated and coated glass. The spectrum with the grey line corresponds to the uncoated surfaces and the orange to the curcuminoid-coated surfaces. The colored regions correspond to special bands in curcuminoid **D**.

The FTIR spectrum of curcuminoid **D** (Figure 1a) showed a broad band between 3500–3200 cm^{-1} indicative of the O-H stretching (grey band) in the phenol group; the region between 3100–3000 cm^{-1} was attributed to C-H stretching (yellow band) in the aromatic ring; the region between 1750–1650 cm^{-1} for the conjugated C=O stretching (orange band); between 1600–1400 cm^{-1} the C=C stretching (red band) of the aromatic ring; between 1300–1200 cm^{-1} the C-O stretching (green band); and between 900–675 cm^{-1} the C-H bending (blue band) in the aromatic ring. This FTIR spectrum confirmed the chemical structure of curcuminoid **D**.

The spectrum of coated and uncoated polystyrene (Figure 1b) demonstrated several prominent peaks characteristic of the polymer structure, including sharp peaks corresponding to the aromatic C-H stretching vibrations (3080–3020 cm^{-1}), the aliphatic C-H stretching region (2920–2850 cm^{-1}), peaks associated with the aromatic ring C=C bonds (1600 cm^{-1} and 1493 cm^{-1}), aromatic C-H bonds (1452 cm^{-1}), bending vibrations of the aliphatic C-H bonds from the ethyl groups (1375 cm^{-1}), and sharp peaks in the region of aromatic C-H out-of-plane bending (760–690 cm^{-1}). The spectrum of coated and uncoated glass exhibited two broad bands (Figure 1c), the Si-O-Si stretching region (1100–1000 cm^{-1}) and around 800 cm^{-1} the Si-O stretching, which are the characteristic features of silica-based glass. Additionally, small peaks present in the coated samples at 1750–1650 cm^{-1} (orange band), at 1600–1400 cm^{-1} (red band), and 1300–1200 cm^{-1} (green band) indicate the presence of the curcuminoid **D** coating on both polystyrene and glass samples.

The wettability of the coated surfaces was determined by measuring the water contact angles. After 24 h of coating with curcuminoid **D**, the hydrophilic glass became more hydrophobic (from 0 to 51 ± 11 degrees), while the hydrophobic polystyrene did not change (from 90 ± 1 to 87 ± 3 degrees).

Adhesion strength of yeasts on curcuminoid-coated surfaces

The adhesion strength of *C. albicans* on curcuminoid-coated and uncoated polystyrene and glass surfaces was determined using AFM. The AFM data (Figure 2) indicated that the curcuminoid **D** coating on polystyrene caused a significant twofold decrease in the adhesion force of *C. albicans* after 2 s in contact with the surface compared with uncoated polystyrene. The adhesion force on polystyrene, was threefold higher than on glass, but for the curcuminoid **D** coated polystyrene and glass the adhesion forces became very similar.

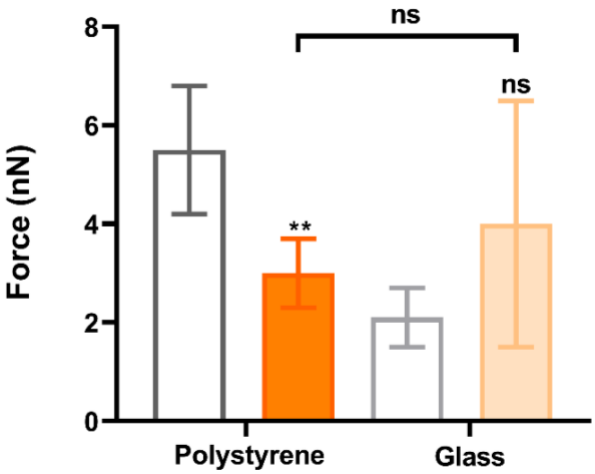

Figure 2. The effect of curcuminoid **D** coating on *C. albicans* ATCC 10231 adhesion strength on uncoated and curcuminoid-coated polystyrene and glass after 2 s contact. The grey bars are the uncoated surfaces and the orange curcuminoid-coated surfaces. Data represents means ± SD of three independent experiments. Statistical analysis was performed by one-way ANOVA and statistical significance differences between yeast adhesion strength on curcuminoid-coated and uncoated surfaces are indicated with asterisks, ** $P \leq 0.01$.

C. albicans adhesion on the curcuminoid coated glass in a parallel plate flow chamber

The adhesion of *C. albicans* on curcuminoid **D** coated and uncoated glass slides was evaluated in a parallel plate flow chamber. The cell adhesion on the curcuminoid-coated glass was reduced by 66% before an air-liquid interface and by 86% after an air-liquid interface when compared to the control (uncoated glass) (Figure 3).

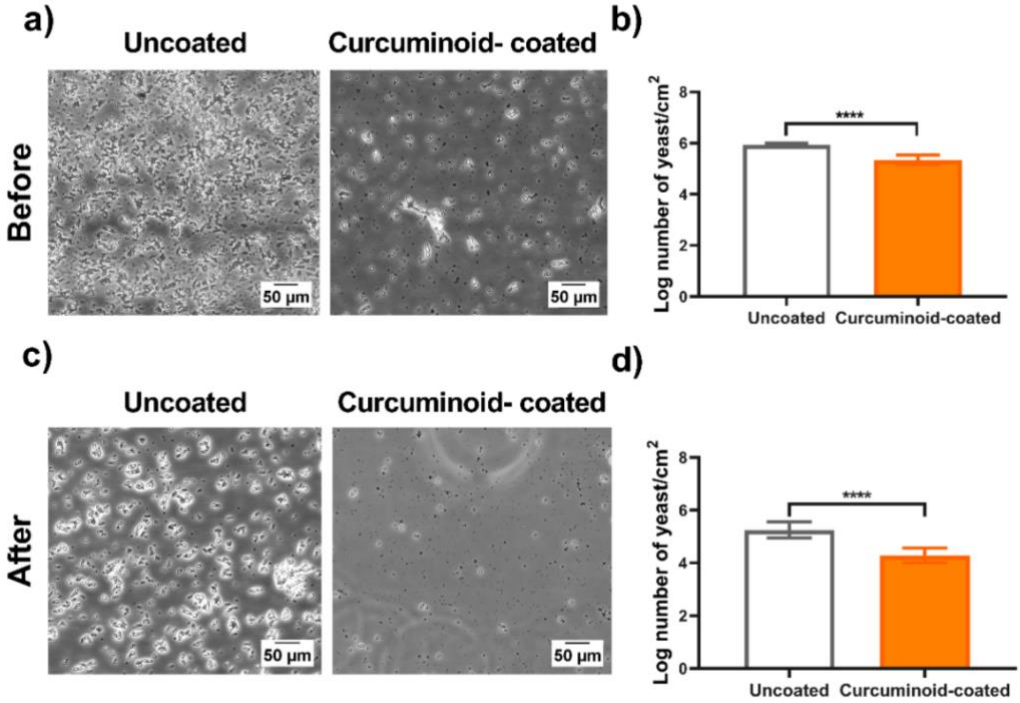

Figure 3. The effect of curcuminoid **D** coating on glass on the adhesion of *C. albicans* ATCC 10231 in a parallel plate flow chamber before **(a, b)** and after an air-liquid interface **(c, d)**. Data represents means ± SD of three independent experiments. Statistical analysis was performed by Student's t-test and statistical significance between yeast density on curcuminoid-coated and uncoated surfaces are indicated with asterisks, **** $P \leq 0.0001$.

Effect of the curcuminoid D coating on C. albicans hyphal development

Curcuminoid **D** coating on polystyrene and glass slides inhibited the hyphal development of *C. albicans*, reducing hyphal length by 65% and 86%, respectively (Figure 4). Longer hyphae were observed on polystyrene surfaces than on glass. On polystyrene, the average hyphal length was 75 µm, compared to 27 µm on the curcuminoid coated polystyrene and on glass the average hyphal length was 50 µm, and 7 µm on coated glass.

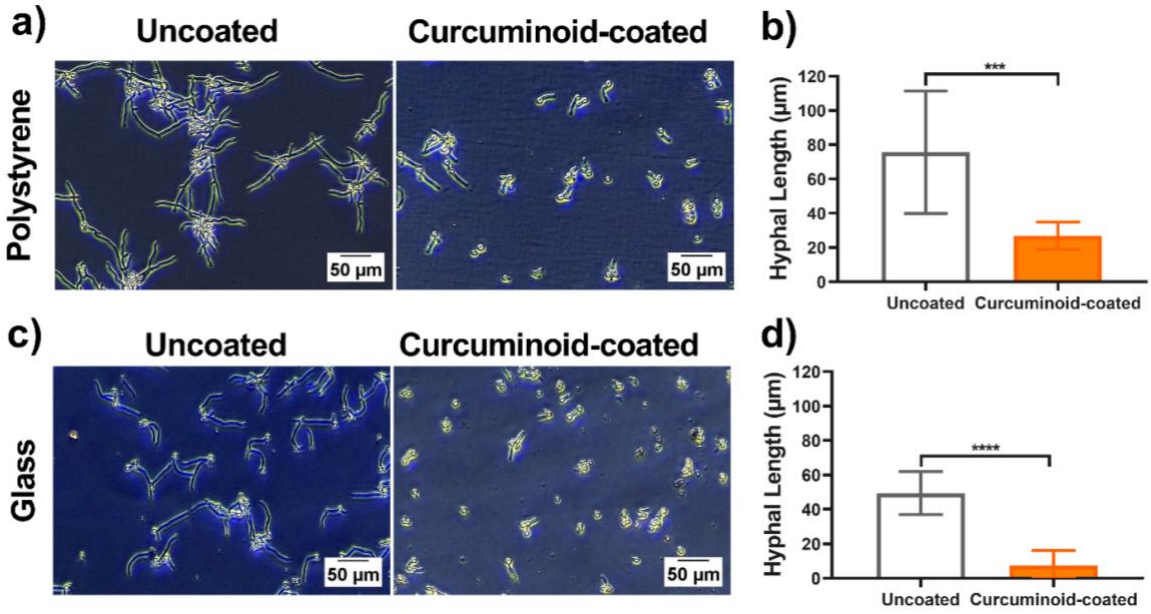

Figure 4. Effect of curcuminoid **D** coating on polystyrene (**a, b**) and glass (**c, d**) on the development of the hyphal length of *C. albicans* ATCC 10231. Data represents means ± SD of three independent experiments. Statistical analysis was performed by Student's t-test and statistical significance between hyphal development length on curcuminoid-coated and uncoated surfaces are indicated with asterisks, *** $P \leq 0.001$ and **** $P \leq 0.0001$.

Evaluation of curcuminoid-coating on C. albicans biofilm formation

CLSM images and CFU counting (Figure 5) indicated that curcuminoid **D** coating on polystyrene significantly inhibited the 48 h biofilm formation of *C. albicans*, however, it did not affect the biofilm formation on glass.

The curcuminoid **D** coating inhibited the formation of the cell membrane and the cell wall showing a decrease in green fluorescence by 38% and blue fluorescence by 40% when compared to the uncoated polystyrene. 3% NaOCl was used as positive control and the treatment reduced the metabolic activity and the cell membrane by 100%, and the cell wall by 45% when compared to biofilm on uncoated polystyrene (positive control) (Figure 5b). Furthermore, the curcuminoid **D** coating on polystyrene resulted in a threefold decrease in

CFUs of the 48-h biofilm compared to uncoated polystyrene (Figure 5c), while there was no effect on glass. The CFUs on coated polystyrene and glass became similar.

The metabolic activity of a 48-h old biofilm of *C. albicans* ATCC 10231 on polystyrene was exposed to 0 µg mL^{-1}, 31.2 µg mL^{-1}, 62.5 µg mL^{-1}, 156 µg mL^{-1} and 312 µg mL^{-1} curcuminoid **D** in growth medium for 24 h (Figure 6). The viability of the 48 h biofilm was reduced as the concentration increased. When exposed to 312 µg mL^{-1} (20 x MIC) for 24 h the biofilm viability decreased by 63%.

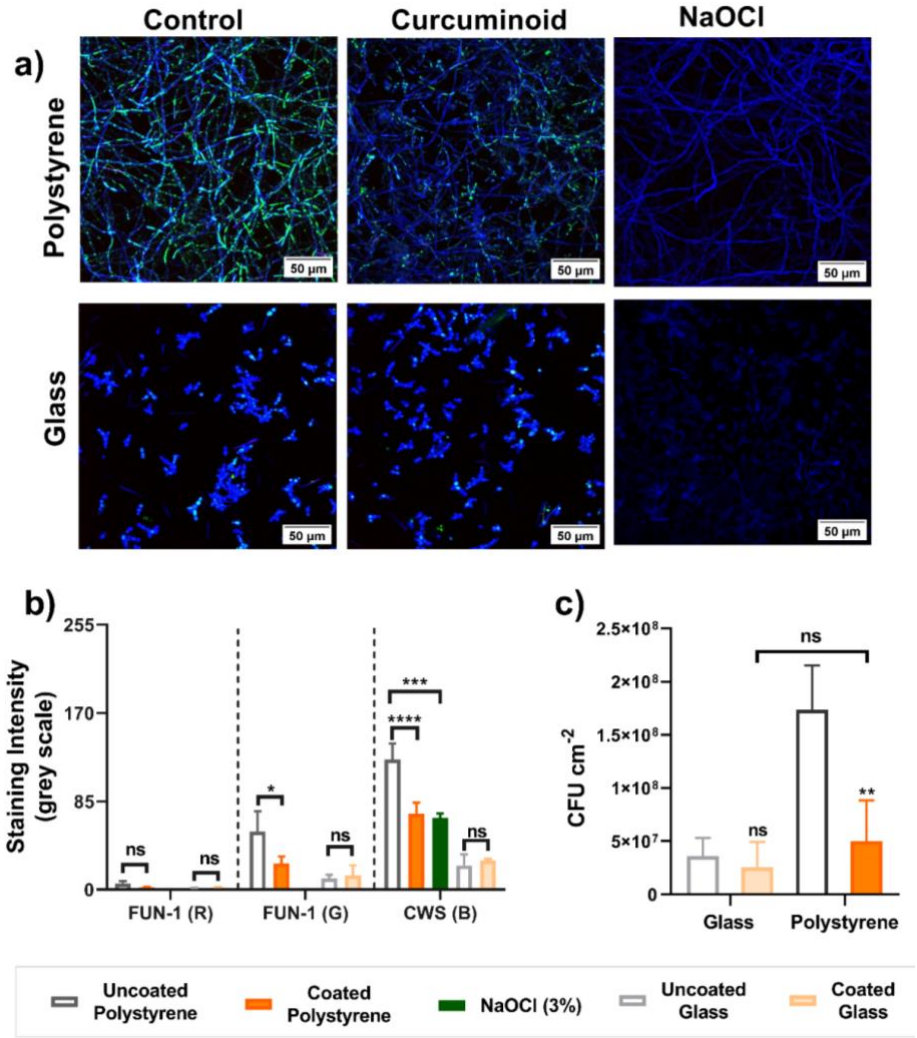

Figure 5. (**a**) Representative CLSM images of 48 h biofilms of *C. albicans* ATCC 10231 grown on uncoated and curcuminoid-coated polystyrene and glass. (**b**) The effect of the curcuminoid-coating on metabolically active intravacuolar structures (red-fluorescent, FUN-1 (R)), cell membrane (green-fluorescent, FUN-1 (G)), and cell wall (blue-fluorescent, CWS (B)). NaOCl

(3%) exposure for 30 s was used as a positive control. (**c**) Effect of curcuminoid **D** coating on 48 h biofilm formation of *C. albicans* ATCC 10231 expressed by colony forming units (CFU) per cm^2. Data represents means ± SD of three independent experiments.

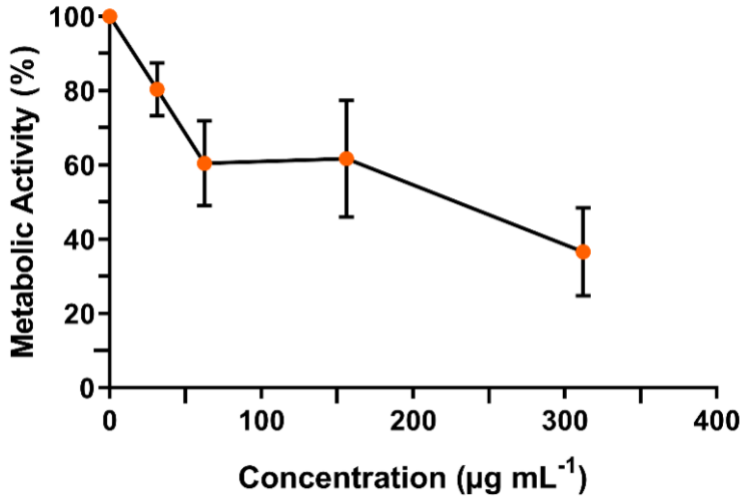

Figure 6. A 48 h biofilm of *C. albicans* ATCC 10231 exposed to different concentrations curcuminoid **D** evaluated by the metabolic activity using MTT reduction assay.

Total RNA isolation and real time RT-PCR

The results obtained from real-time PCR (Figure 7) suggested that the curcuminoid **D** coating on polystyrene downregulated genes associated with biofilm formation of *C. albicans*. In the analysis of gene expression under hyphal development conditions, the gene *HWP1* (hyphal wall protein 1) was significantly downregulated on coated surfaces, with an 15-fold reduction compared to uncoated surfaces. During the initial 2 h biofilm formation on curcuminoid-coated surfaces, the genes from ALS family, responsible for the adhesins, as *ALS3* (agglutinin-like sequence 3), *ALS5* (agglutinin-like sequence 5) and *HWP1* were significantly downregulated by 20-fold, 3-fold and 13-fold, respectively, when compared with uncoated surfaces. Notably, at the 48 h biofilm, *ALS1* expression was significantly upregulated on coated surfaces, showing a 5-fold increase compared to uncoated surfaces. These findings indicate that the coating significantly inhibits gene expression essential for initial fungal biofilm

development and adhesion, while potentially enhancing genes involved in later stages of biofilm maturation.

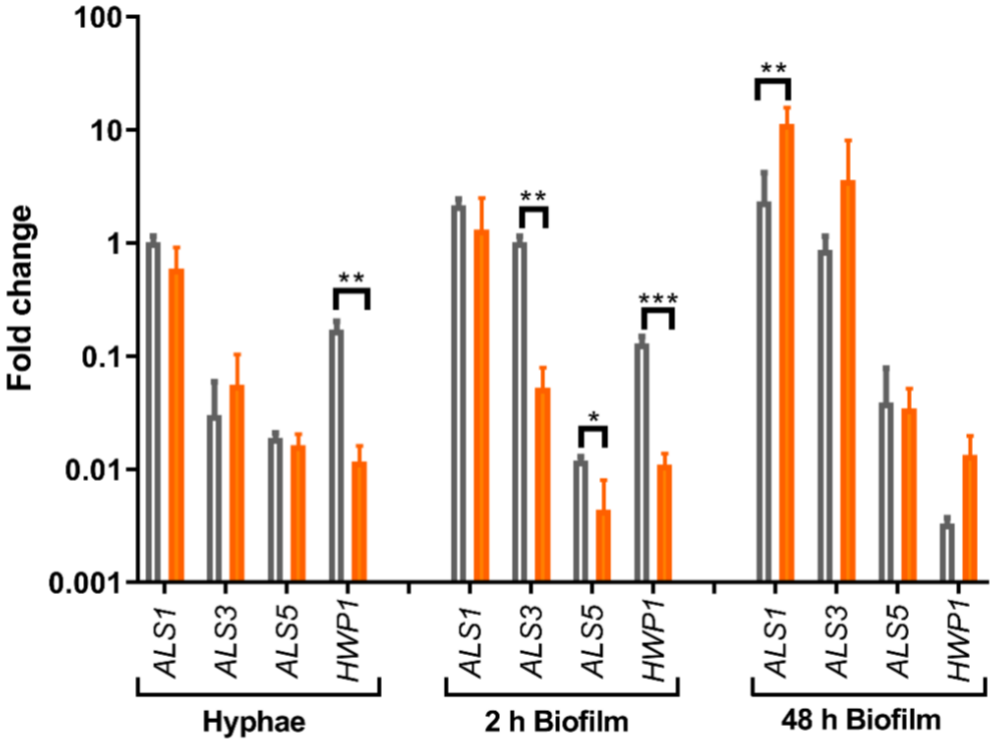

Figure 7. Gene expression of *C. albicans* ATCC 10231 biofilm during different stages of biofilm formation of *C. albicans* hyphal development, 2 h and 48 h biofilm on uncoated and curcuminoid-coated polystyrene. *ALS1*, *ALS3* and *ALS5* genes: agglutinin-like sequence; *HWP1* gene: hyphae cell wall protein. All data are represented relative to fold changes compared to *ACT1* housekeeping gene. The grey bar corresponds to the uncoated surfaces and the orange to the curcuminoid-coated surfaces. The standard bar error represents the mean of three replicates.

Discussion

In this study, we developed and evaluated the use of a monocarbonyl curcuminoid as a coating to inhibit biofilm formation of *C. albicans*. Seven monocarbonyl curcuminoids were evaluated for their anti-*Candida* activity (see Table 1). Among these compounds, curcuminoid **D** showed the most potent anti-*Candida* activity, exhibiting fungicidal effects against all tested *Candida*

species, with MFC values ranging from 15.6 to 125 µg mL^{-1}. The presence of a hydroxyl group at the 2' position significantly enhanced its anti-*Candida* activity, exceeding other structural modifications and curcumin (Table 2). Previous studies reported MIC values for curcumin ranging from 100 to 2000 µg mL^{-1} against planktonic *C. albicans* (Alalwan *et al.*, 2017; Shahzad *et al.*, 2014).

Adhesion force measurements demonstrated that curcuminoid **D** coatings on polystyrene surfaces significantly reduced *C. albicans* adhesion force compared to uncoated surfaces, whereas glass surfaces showed no significant difference in adhesion force (Figure 2). Since the AFM results on both glass and polystyrene-coated surfaces were equivalent, the hydrophobicity of the surface did not influence the properties of the coating. Both coated surfaces showed a significant reduction of *C. albicans* adhesion on glass (Figure 3).

A critical pathogenic mechanism in *C. albicans* biofilm formation is its ability to switch from yeast-form to filamentous-form cells. Curcuminoid **D** effectively inhibited this morphological transition on both glass and polystyrene surfaces as shown in Figure 4. These results were further supported by gene expression analysis for hyphal development conditions, which showed significant downregulation of the *HWP1* gene on coated surfaces (Figure 7). The *HWP1* gene regulates the adhesion stage and is uniquely expressed on the hyphal surface, being hyphal-specific adhesion (Nobile *et al.*, 2006). It is known that the *HWP1* gene is critical for adhesion and it is the first *C. albicans* cell surface protein required for biofilm formation *in vivo* (Nobile *et al.*, 2006).

The combined results demonstrated that the coating effectively impeded hyphal development, adhesion, and a reduction in biofilm formation (Atriwal *et al.*, 2021). Gene expression analysis further supported these findings, showing the downregulation of *ALS3* and *ALS5* genes, which are crucial for adhesion and biofilm development, during the initial 2 h of biofilm formation on coated surfaces. As part of the ALS family, the *ALS5* gene also encodes

adhesins, which possess amyloid properties and enhance aggregation. It was found that the expression of *ALS5* increases cell aggregation, implying that cell-cell contact promotes amyloid formation on the cell surface (Garcia *et al.*, 2011). Interestingly, at the 48 h biofilm stage, *ALS1* expression was upregulated, possibly as a compensatory response to the initial inhibitory effects of the coating (Figure 7). Probably the adhesion-force-induced gene expression extends into the biofilm through quorum sensing over a height limit above the substratum surface. Beyond this limit, autoinducer concentrations drop below the threshold required to invoke a response. These calling distances over microorganisms can communicate through quorum sensing have been reported in other studies with bacteria (Wang *et al.*, 2019).

Overall, our results demonstrate that curcuminoid **D** effectively impeded fungal adhesion, hyphal development, biofilm formation and additionally it reduces the metabolic activity of mature biofilms (Figure 6). Although curcumin was not tested as a coating in this study, studies have shown that curcumin is not chemically stable as it can degrade in less than 24 h under various conditions. In one study, curcumin degradation reached 60% in 1 h and over 90% in 4 h when exposed to light in phosphate buffer (pH = 7.2) (Appendino *et al.*, 2022). Incubating curcumin with proteins, such as in the presence of serum or cultured cells, increases the half-life time of curcumin, although this increase is limited to 1−2 h (Schneider *et al.*, 2015). Given the disadvantages of curcumin, curcuminoid **D** presents a promising alternative for coating applications, offering enhanced stability and efficacy. This study underscores the potential of monocarbonyl curcuminoids as antimicrobial coatings to prevent biofilm formation, contributing to the development of novel biofilm control strategies in clinical settings.

Conclusion

This study highlighted the potential of monocarbonyl curcuminoids as antimicrobial coatings. Curcuminoid **D** (2-hydroxy-dibenzylideneacetone) demonstrated potent anti-*Candida* activity, effectively inhibiting fungal adhesion, hyphal development, and biofilm formation on polystyrene surfaces. Gene expression analysis confirmed downregulation of the key adhesion and biofilm-related genes. Although its efficacy on glass was limited over 48 h, the coating still reduced adhesion and hyphal development in a shorter time period. These findings evidenced the role of monocarbonyl curcuminoids as multifaceted coatings for controlling device-associated infections and biofilm formation in clinical settings.

References

ABREU, A. C. *et al.* Current and emergent strategies for disinfection of hospital environments. **Journal of Antimicrobial Chemotherapy**, v. 68, n. 12, p. 2718–2732, 2013.

AFEWERKI, S. *et al.* Advances in antimicrobial and osteoinductive biomaterials. *Em*: **Racing for the Surface**. Cham: Springer International Publishing, 2020. p. 3–34.

ALALWAN, H. *et al.* The anti-adhesive effect of curcumin on *Candida albicans* biofilms on denture materials. **Frontiers in Microbiology**, v. 8, p. 669, 2017.

ALVES, D. *et al.* Design of an antifungal surface embedding liposomal amphotericin B through a mussel adhesive-Inspired coating strategy. **Frontiers in Chemistry**, v. 7, 2019.

APPENDINO, G. *et al.* Shedding light on curcumin stability. **Fitoterapia**, v. 156, p. 105084, 2022.

ATRIWAL, T. *et al.* Mechanistic Understanding of Candida albicans Biofilm Formation and Approaches for Its Inhibition. **Frontiers in Microbiology**, v. 12, 2021.

BUSSCHER, H. J.; MEI, H. C. VAN DER. Microbial adhesion in flow displacement systems. **Clinical Microbiology Reviews**, v. 19, n. 1, p. 127–141, 2006.

CAMPOCCIA, D.; MONTANARO, L.; ARCIOLA, C. R. A review of the biomaterials technologies for infection-resistant surfaces. **Biomaterials**, v. 34, n. 34, p. 8533–8554, 2013.

CARNIELLO, V. *et al.* Role of adhesion forces in mechanosensitive channel gating in Staphylococcus aureus adhering to surfaces. **npj Biofilms and Microbiomes**, v. 6, n. 1, p. 31, 2020.

CLSI. Reference method for broth dilution antifungal susceptibility testing of yeasts; approved standard—Third Edition. **CLSI document M27-A3**, v. 28, n. April, 2008.

DAI, F. *et al.* Insights into the importance for designing curcumin-inspired anticancer agents by a prooxidant strategy: The case of diarylpentanoids. **Free Radical Biology and Medicine**, v. 85, p. 127–137, 2015.

GARCIA, M. C. *et al.* A Role for amyloid in cell aggregation and biofilm formation. **PLoS ONE**, v. 6, n. 3, p. e17632, 2011.

GAYDHANE, M. K.; KANUGANTI, J. S.; SHARMA, C. S. Honey and curcumin loaded multilayered polyvinylalcohol/cellulose acetate electrospun nanofibrous mat for wound healing. **Journal of Materials Research**, v. 35, n. 6, p. 600–609, 2020.

LAMONT-FRIEDRICH, S. J. *et al. Candida auris* susceptibility on surfaces coated with the antifungal drug caspofungin. **Medical Mycology**, v. 60, n. 1, 2021.

MAGILL, S. S. *et al.* Multistate point-prevalence survey of health care–associated infections. **New England Journal of Medicine**, v. 370, n. 13, p. 1198–1208, 2014.

MANOHAR, C. M. *et al.* Design of a papain immobilized antimicrobial food package with curcumin as a crosslinker. **PLoS ONE**, v. 10, n. 4, p. 1–17, 2015.

MODAK, S. M. *et al.* **Coatings and methods for infection-resistant medical devices**. United States Patent Application US 2019/0133126 A1, 2019.

NADERI, J. *et al.* Combatting fungal biofilm formation by diffusive release of fluconazole from heptylamine plasma polymer coating. **Biointerphases**, v. 15, n. 6, 2020.

NAGARGOJE, A. A. *et al.* Quinoline based monocarbonyl curcumin analogs as potential antifungal and antioxidant agents: synthesis, bioevaluation and molecular docking study. **Chemistry and Biodiversity**, v. 17, n. 2, p. e1900624, 2020a.

NAGARGOJE, A. A. *et al.* Propargylated monocarbonyl curcumin analogues: synthesis, bioevaluation and molecular docking study. **Medicinal Chemistry Research**, v. 29, n. 10, p. 1902–1913, 2020b.

NELSON, K. M. *et al.* The essential medicinal chemistry of curcumin. **Journal of Medicinal Chemistry**, v. 60, n. 5, p. 1620–1637, 2017.

NOBILE, C. J. *et al.* Function of *Candida albicans* adhesin Hwp1 in biofilm formation. **Eukaryotic Cell**, v. 5, n. 10, p. 1604–1610, 2006.

PFALLER, M. A.; DIEKEMA, D. J. Epidemiology of invasive candidiasis: a persistent public health problem. **Clinical Microbiology Reviews**, v. 20, n. 1, p. 133–163, 2007.

POLAQUINI, C. *et al.* Design, synthesis and anti-*Candida* activity of diarylideneacetones inspired by curcumin. **SSRN**, 2024.

POLAQUINI, C. R. *et al.* Antibacterial activity of a new monocarbonyl analog of curcumin MAC 4 is associated with divisome disruption. **Bioorganic Chemistry**, v. 109, p. 104668, 2021.

SCHNEIDER, C. *et al.* Degradation of curcumin: from mechanism to biological implications. **Journal of Agricultural and Food Chemistry**, v. 63, n. 35, p. 7606–7614, 2015.

SHAHZAD, M. *et al.* Utilising polyphenols for the clinical management of *Candida albicans* biofilms. **International journal of antimicrobial agents**, v. 44, n. 3, p. 269–273, 2014.

SHEN, T. *et al.* A curcumin derivative that inhibits vinyl carbamate-induced lung carcinogenesis *via* activation of the Nrf2 protective response. **Antioxidants & Redox Signaling**, v. 23, n. 8, p. 651–664, 2015.

SHETTY, D. *et al.* Eliminating the heart from the curcumin molecule: monocarbonyl curcumin mimics (MACs). **Molecules**, v. 20, n. 1, p. 249–292, 2014.

SINGH, A. K.; GAUR, V.; MAURYA, A. K. The role of biofilm in originating, mediating, and proliferating infectious diseases. *Em*: **Biofilms in Human Diseases: Treatment and Control**. Cham: Springer International Publishing, 2019. p. 43–57.

SRIVASTAVA, A.; CHANDRA, N.; KUMAR, S. The role of biofilms in medical devices and implants. *Em*: **Biofilms in Human Diseases: Treatment and Control**. Cham: Springer International Publishing, 2019. p. 151–165.

SUNITHA S *et al.* Fabrication of surgical sutures coated with curcumin loaded gold nanoparticles. **Pharmaceutica Analytica Acta**, v. 08, n. 01, 2017.

VIRK, R. S. *et al.* Curcumin-containing orthopedic implant coatings deposited on poly-ether-ether-ketone/bioactive glass/hexagonal boron nitride layers by electrophoretic deposition. **Coatings**, v. 9, n. 9, p. 572, 2019.

WANG, C. *et al.* Emergent properties in streptococcus mutans biofilms are controlled through adhesion force sensing by initial colonizers. **mBio**, v. 10, n. 5, 2019.

WEBER, W. M. *et al.* Anti-oxidant activities of curcumin and related enones. **Bioorganic & Medicinal Chemistry**, v. 13, n. 11, p. 3811–3820, 2005.

ZHOU, J. *et al.* Antimicrobial evaluation and action mechanism of pyridinium-decorated 1,4-pentadien-3-one derivatives. **Bioorganic & Medicinal Chemistry Letters**, v. 28, n. 10, p. 1742–1746, 2018.

Supporting Information

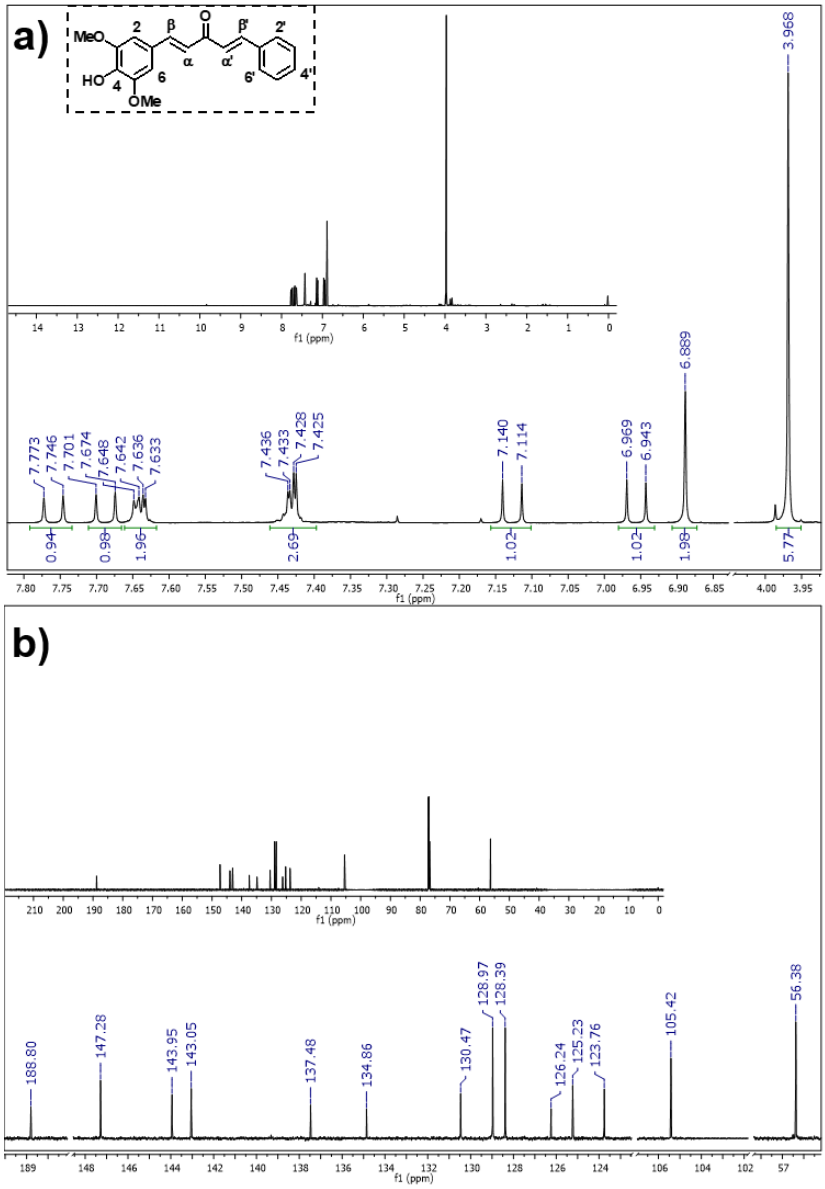

Figure S1. NMR spectra of Curcuminoid **A** (1*E*,4*E*)-1-(4-hydroxy-3,5-dimethoxyphenyl)-5-phenylpenta-1,4-dien-3-one dissolved in $CDCl_3$. a) ^{1}H NMR spectrum at 600 MHz. b) ^{13}C NMR spectrum at 150 MHz.

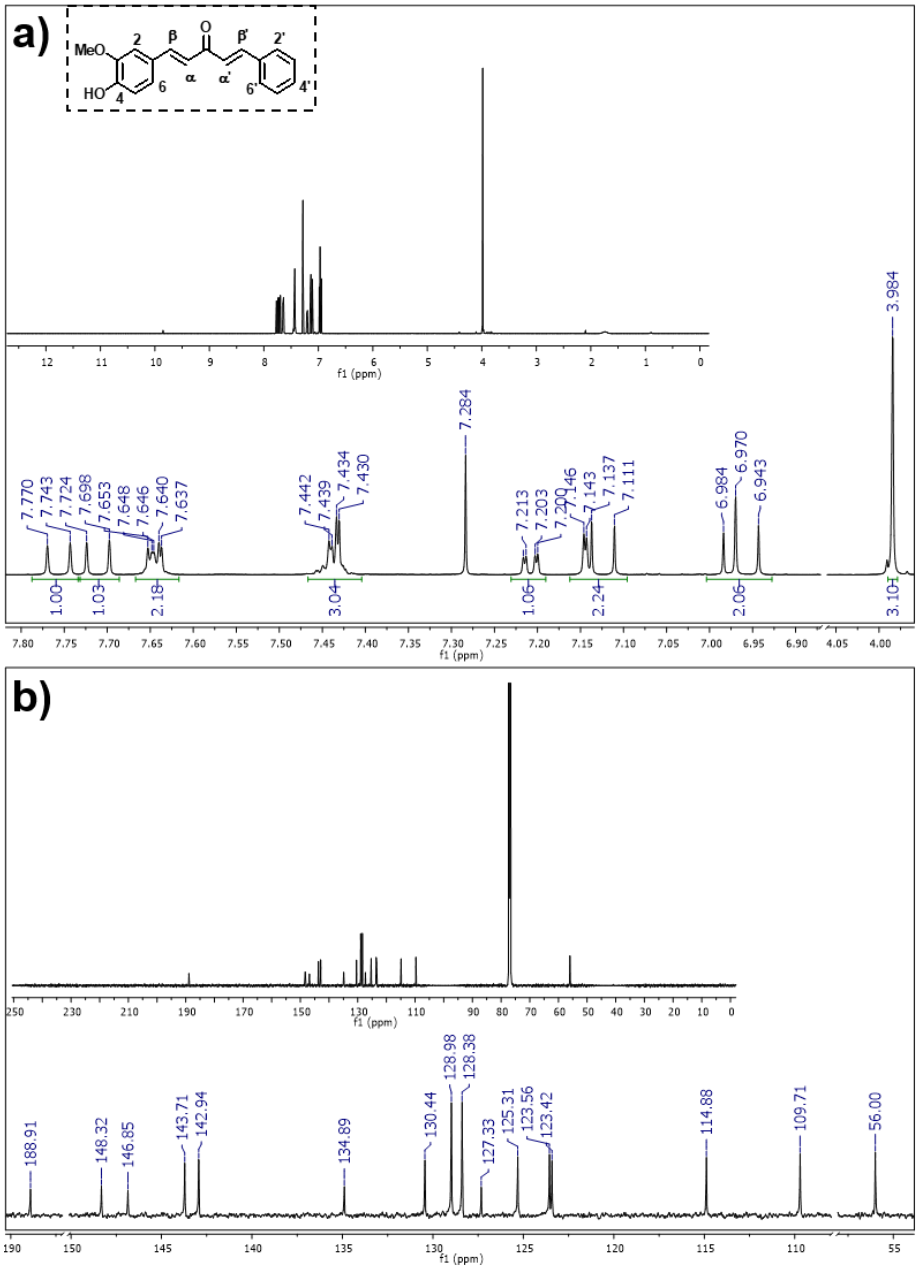

Figure S2. NMR spectra of Curcuminoid **B** (1*E*,4*E*)-1-(4-hydroxy-3-methoxyphenyl)-5-phenylpenta-1,4-dien-3-one (Polaquini *et al.*, 2021; Weber *et al.*, 2005) dissolved in $CDCl_3$. a) ^{1}H, NMR spectrum at 600 MHz. b) ^{13}C NMR spectrum at 150 MHz.

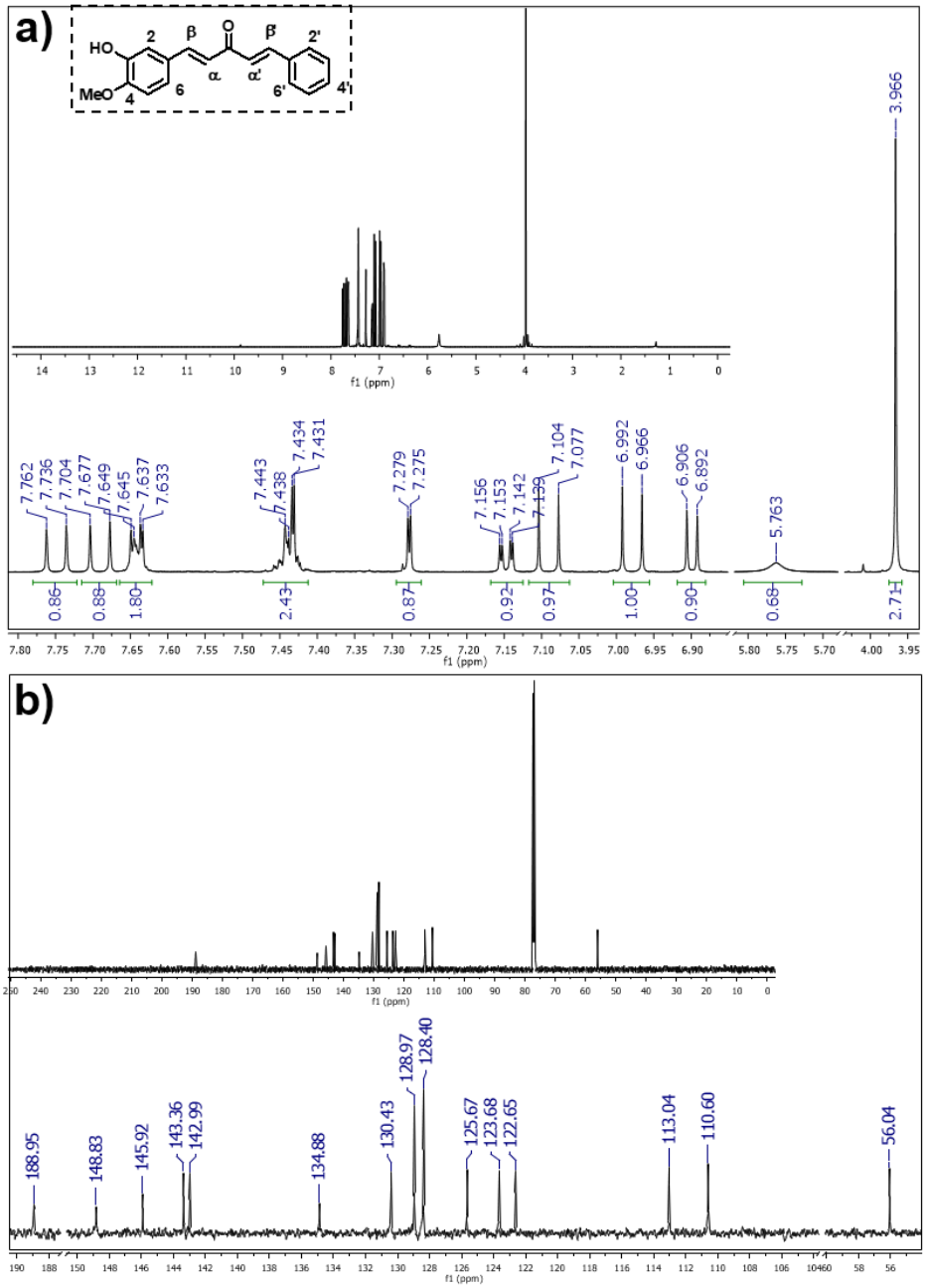

Figure S3. NMR spectra of Curcuminoid **C** (1*E*,4*E*)-1-(3-hydroxy-4-methoxyphenyl)-5-phenylpenta-1,4-dien-3-one(Polaquini *et al.*, 2024) dissolved in $CDCl_3$. a) ^{1}H NMR spectrum at 600 MHz. b) ^{13}C NMR spectrum at 150 MHz.

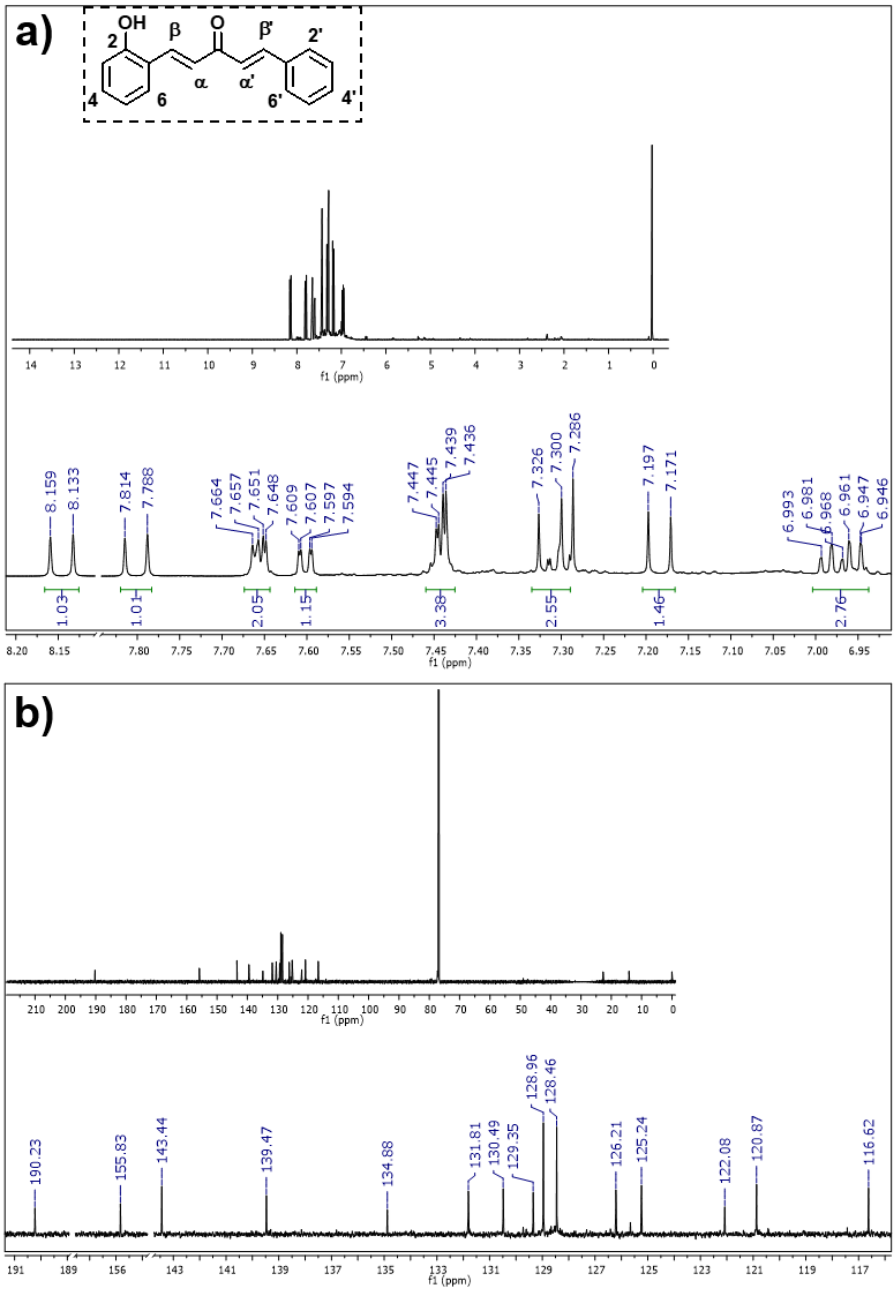

Figure S4. NMR spectra of Curcuminoid **D** (1*E*,4*E*)-1-(2-hydroxyphenyl)-5-phenylpenta-1,4-dien-3-one (Dai *et al.*, 2015; Polaquini *et al.*, 2024; Shen *et al.*, 2015) dissolved in $CDCl_3$. a) ^{1}H NMR spectrum at 600 MHz. b) ^{13}C NMR spectrum at 150 MHz.

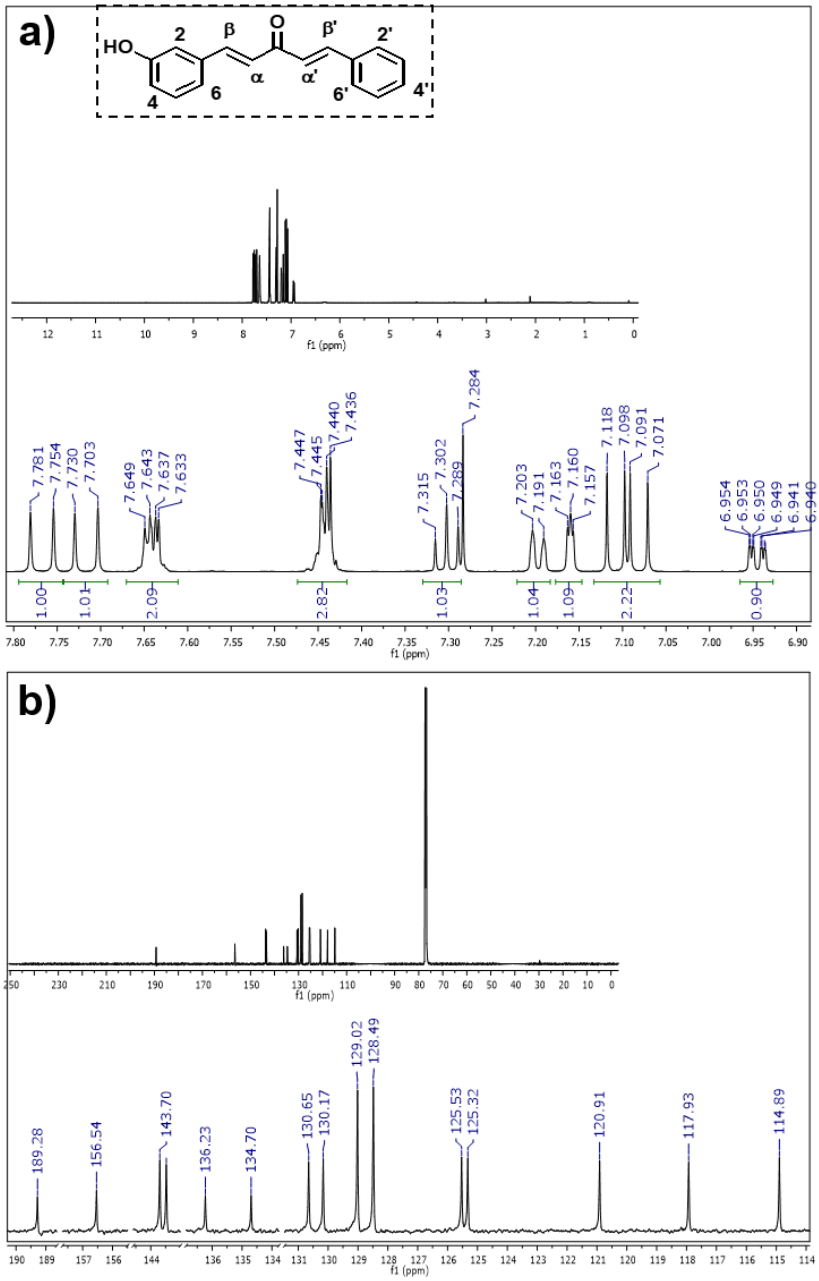

Figure S5. NMR spectra of Curcuminoid **E** (1*E*,4*E*)-1-(3-hydroxyphenyl)-5-phenylpenta-1,4-dien-3-one 2-5 disolved in $CDCl_3$. a) ^{1}H NMR spectrum at 600 MHz. b) ^{13}C NMR spectrum at 150 MHz.

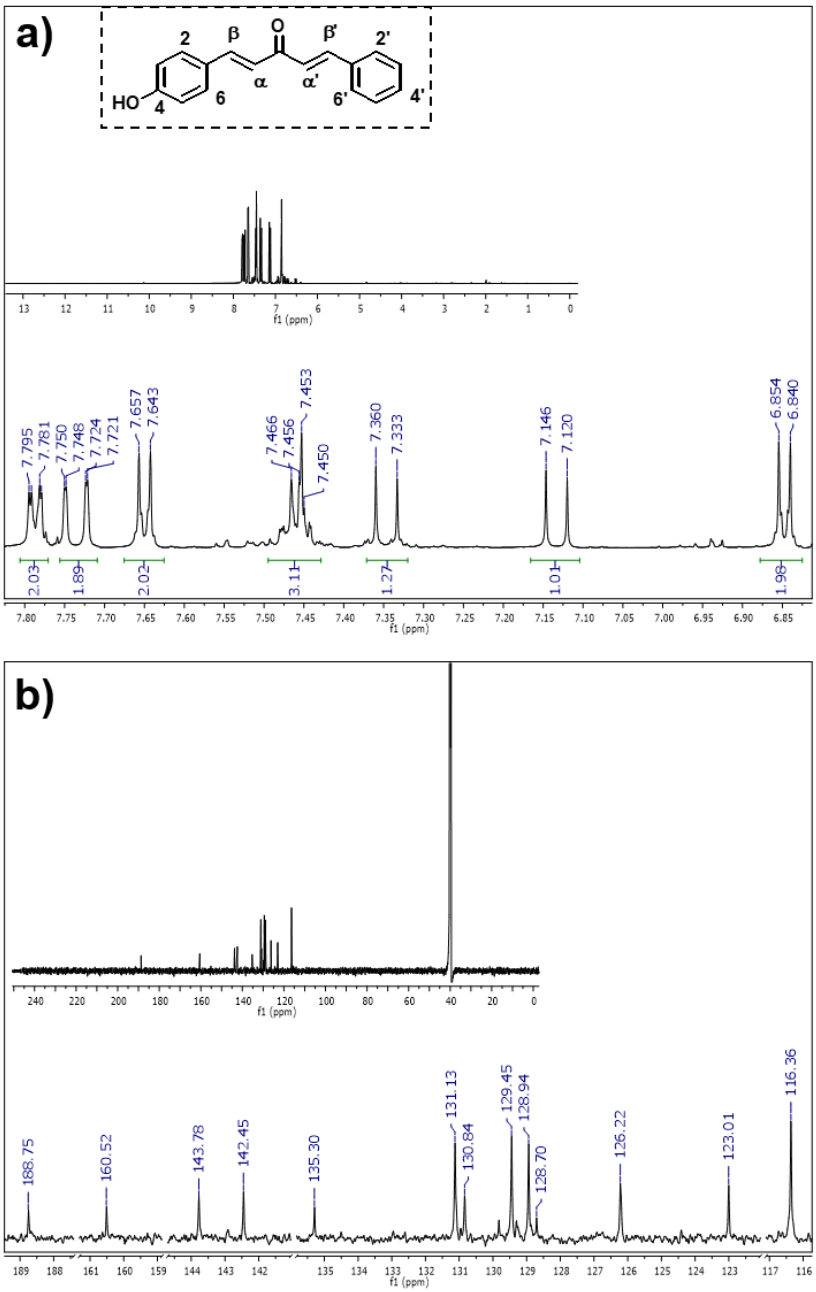

Figure S6. NMR spectra of Curcuminoid **F** (1*E*,4*E*)-1-(4-hydroxyphenyl)-5-phenylpenta-1,4-dien-3-one (Polaquini *et al.*, 2021; Zhou *et al.*, 2018) dissolved in DMSO-d_6. a) ^{1}H NMR at 600 MHz. b) ^{13}C NMR spectrum at 150 MHz.

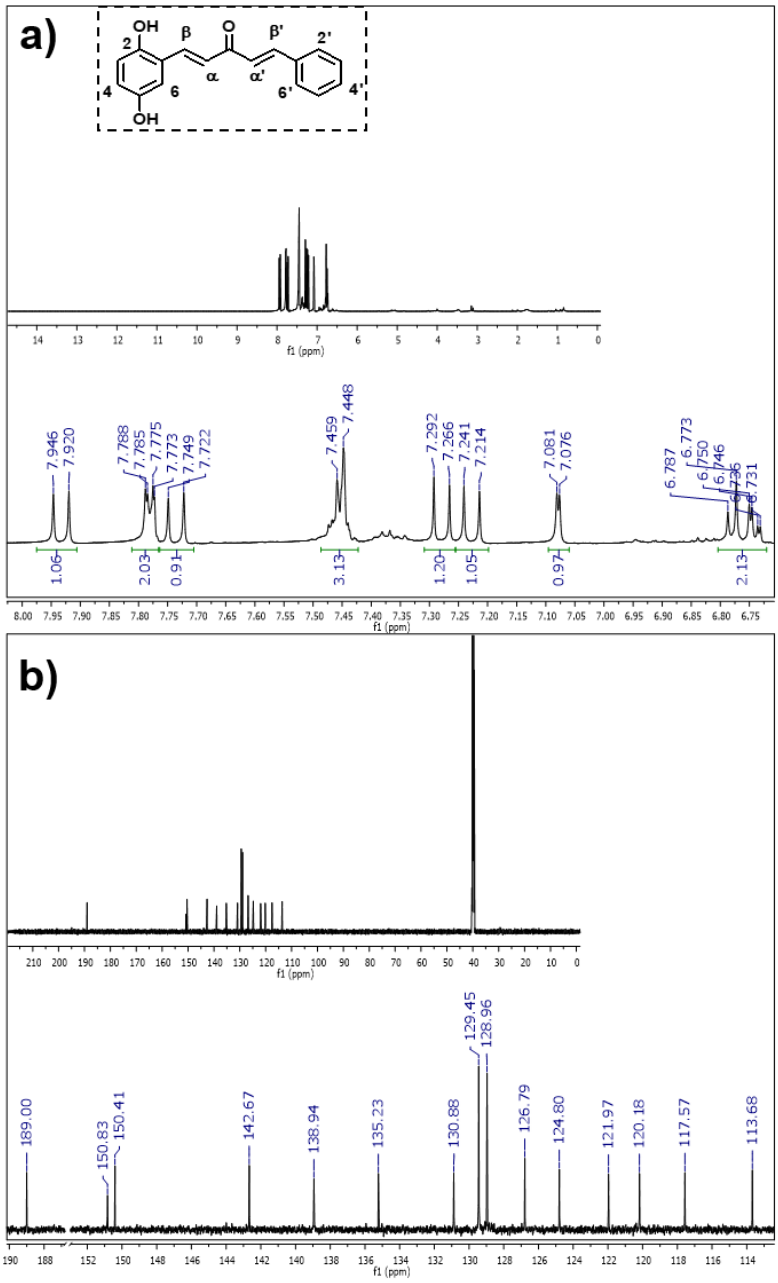

Figure S7. NMR spectra of Curcuminoid **G** (1*E*,4*E*)-1-(2,5-dihydroxyphenyl)-5-phenylpenta-1,4-dien-3-one (Polaquini *et al.*, 2024) dissolved in DMSO-d_6. a) ^{1}H NMR at 600 MHz. b) ^{13}C NMR spectrum at 150 MHz.

Table S1. Sequences of Primers for Genes

Code	Gene name	Primer	Primer sequence (5'-> 3')	References
ALS1	**Agglutinin-like sequence 1**	Forward	TTC TCA TGA ATC AGC ATC CAC AA	Wartenberg *et al.*2018
		Reverse	CAG AAT TTT CAC CCA TAC TTG GTT TC	
ALS3	**Agglutinin-like sequence 3**	Forward	AAT GGT CCT TAT GAA TCA CCA TCT ACT A	Wartenberg *et al.*2018
		Reverse	GAG TTT TCA TCC ATA CTT GAT TTC ACA T	
ALS5	**Agglutinin-like sequence 5**	Forward	CTG CCG GTT ATC GTC CAT TTA	Wartenberg *et al.*2018
		Reverse	ATT GAT ACT GGT TAT TAT CTG AGG GAG AAA	
HWP1	**Hyphal wall protein 1**	Forward	ATCAGCTCCTGCCACTGAAC	Green, Zhao e Hoyer, 2005
		Reverse	TGAGTGGAACTGATTCTAATGTAGTTG	
ACT1	**Actin 1**	Forward	TCAGACCAGCTGATTTAGGTTTG	Green, Zhao e Hoyer, 2005
		Reverse	GTGAACAATGGATGGACCAG	

References

DAI, F. *et al.* Insights into the importance for designing curcumin-inspired anticancer agents by a prooxidant strategy: The case of diarylpentanoids. **Free Radical Biology and Medicine**, v. 85, p. 127–137, 2015.

GREEN, C. B.; ZHAO, X.; HOYER, L. L. Use of green fluorescent protein and reverse transcription-PCR to monitor *Candida albicans* agglutinin-like sequence gene expression in a murine model of disseminated candidiasis. **Infection and Immunity**, v. 73, p. 1852–1855, 2005.

POLAQUINI, C. et al. Design, synthesis and anti-*Candida* activity of diarylideneacetones inspired by curcumin. **SSRN**, 2024.

POLAQUINI, C. R. *et al*. Antibacterial activity of a new monocarbonyl analog of curcumin MAC 4 is associated with divisome disruption. **Bioorganic Chemistry**, v. 109, p. 104668, 2021.

SHEN, T. *et al*. A curcumin derivative that inhibits vinyl carbamate-induced lung carcinogenesis via activation of the Nrf2 protective response. **Antioxidants & Redox Signaling**, v. 23, p. 651–664, 2015.

WARTENBERG, A. et al. Microevolution of *Candida albicans* in macrophages restores filamentation in a nonfilamentous mutant. **PLoS Genetics**, v. 10, e1004824, 2014.

WEBER, W. M. *et al.* Anti-oxidant activities of curcumin and related enones. **Bioorganic & Medicinal Chemistry**, v. 13, p. 3811–3820, 2005.

ZHOU, J. et al. Antimicrobial evaluation and action mechanism of pyridinium-decorated 1,4-pentadien-3-one derivatives. **Bioorganic & Medicinal Chemistry Letters**, v. 28, p. 1742–1746, 2018.

5. GENERAL DISCUSSION

In recent decades, fungal infections have increased considerably, with a mortality rate equivalent to tuberculosis and three times higher than malaria (Bongomin *et al.*, 2017; World Health Organization, 2019b, 2019a). In this scenario, *Candida albicans* stands out as the most frequent opportunistic fungus among nosocomial infections (Macias-Paz *et al*., 2023). The therapeutic antifungal potential of curcumin has been widely known and used since ancient times. However, the clinical application of curcumin is limited due to its poor solubility in water and bioavailability (Nelson *et al.*, 2017). This challenge has led to the synthesis and exploration of curcumin analogs, which aim to retain the biological efficacy of curcumin while overcoming its chemical and pharmacokinetic limitations (**Introduction, Chapter 1**) (Noureddin; El-Shishtawy; Al-Footy, 2019).

The major focus of this PhD thesis was to design curcumin analogs to improve curcumins' chemical stability, antifungal activity and to reveal aspects of curcuminoids as a coating on a surface for biomedical applications.

Chemical strategies

In order to enhance curcumins' chemical stability curcumin analogs were designed, known as curcuminoids. This can be achieved by modifying the substitutes on its aromatic rings (**Chapter 2)** or by simplifying the central side chain, such as substituting the β-diketone moiety with a monoketone group (**Chapter 3)**, as shown in Figure 1. In both strategies, the functional groups' substituent is increasing the stabilization, solubility, and bioactivity.

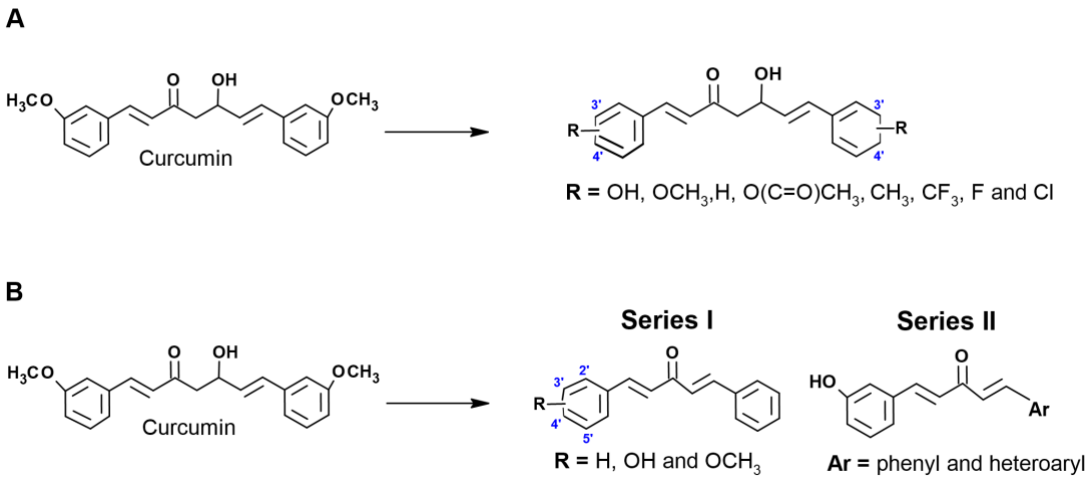

Figure 1. Chemical strategies to improve curcumin chemical stability (**A)** by modifying the substitutes on its aromatic rings or (**B**) by substituting the β-diketone moiety with a monoketone group. **R** can be at positions 2', 3', 4'and 5'(indicated in blue).

The monocarbonyl curcuminoids (**Chapter 3**) showed a higher antifungal activity than analogs with β-diketone moiety (DMC in **Chapter 2**). The curcuminoid DMC exhibited significant antifungal activity against filamentous fungi and *Candida* species. However, 6 out of 10 curcuminoids on which the β-diketone moiety was preserved, did not achieve MIC values below 62.5 μg mL^{-1} for more than two strains. In contrast, the curcuminoids with a monoketone group (Figure 1 B) showed much stronger antifungal activity and had lower MIC values for *Candida* species.

We also investigated monocarbonyl curcuminoids against filamentous fungi. 3-Hydroxy-dibenzylideneacetone and 4-hydroxy-dibenzylideneacetone demonstrated strong activities against clinically relevant dermatophyte species such as *Trichophyton rubrum*, *Trichophyton mentagrophytes*, *Microsporum canis* and clinical strains of *Epidermophyton floccosum*. These curcuminoids achieved MIC and MFC values between 1.9 to 3.9 μg mL^{-1}, showing fungicidal activity, while DMC (the most active curcuminoid of **Chapter 2**) presented fungistatic activity, with MIC ranging from 1.9 to 62.5 μg mL^{-1} against dermatophyte species,

confirming the promising outcomes of monocarbonyl curcuminoids and showing a better strategy for curcumin improvement than preserving the β-diketone moiety.

Additionally, our studies highlight the increase of antifungal activity of hydroxylated substituents compared to methoxylated, emphasizing the critical role of hydroxyl groups in enhancing antifungal activity. Hydroxylated curcuminoid derivatives exhibit higher overall biological activity than curcumin, such as antioxidant, antineoplastic, and antimicrobial effects due to the electron-donating nature of their hydroxyl group. This group plays a key role in both free radical scavenging and disrupting microbial cells (Amalraj *et al.*, 2017). In curcuminoids, the phenolic hydroxyl enhances antimicrobial effects by disrupting the cell membranes of bacterial species (Polaquini *et al.*, 2019). Similarly, in terpenoids (specialized metabolites from isoprenyl pathways), the phenolic hydroxyl is crucial for antifungal activity by disrupting the cell membrane integrity, affecting ion homeostasis, and leading to cell death (Konuk; Ergüden, 2020).

Another key observation from this study is the significant role played by the position of the hydroxyl groups in aromatic systems, particularly at the *ortho* (2'), *meta* (3'), and *para* (4') positions, which are relevant for antifungal activity of curcuminoids. The hydroxyl group at 3' position has been described as crucial for enhancing the antibacterial activities of a curcumin analog (Polaquini *et al.*, 2019). Moreover, the presence of hydroxyl groups at 3' and 4' positions in a monocarbonyl curcuminoid structure demonstrated potent activity against Gram-negative and Gram-positive bacterial species (Polaquini *et al.*, 2021). The hydroxyl group attached at 4' position of the aromatic ring contributed to the stability of curcumin, facilitating electron delocalization (Jamil *et al.*, 2023). Although the 3' and 4' positions are more commonly described as important positions for enhancing the antibacterial activities of curcuminoids, our study demonstrates that the hydroxyl group at 2' position also plays an important role in improving antifungal activity. Also in other compounds like chalcones the

hydroxyl group at 2' position is increasing antimicrobial activity (Ngaini; Fadzillah; Hussain, 2012). Furthermore, the hydroxyl group at 2' position of curcumin analogs was described responsible for enhancing the inducer potency of detoxification enzymes (Dinkova-Kostova; Talalay, 1999), as well as inhibiting angiogenesis and metastasis markers more effectively than curcumin itself (Mohankumar *et al.*, 2015). Therefore, exploring the potential of monocarbonyl curcuminoids with hydroxylated substitutions could yield more effective antifungal agents than curcumin and its analogs with β-diketone moiety.

Biomedical applications of monocarbonyl curcuminoids

The biomedical applications of monocarbonyl curcuminoids, focusing on their potential as antifungal and antibiofilm agents, were investigated by using the curcuminoids as a coating on different materials. 2-Hydroxy-dibenzylideneacetone (compound **D**) was the most effective in inhibiting not only the growth of reference strains but also of clinical *Candida* isolates. It inhibited the cell adhesion of *C. albicans* on coated glass by 66% before an air-liquid interface and by 86% after an air-liquid interface under flow conditions. In addition, it also demonstrated the prevention of *C. albicans* biofilm formation, inhibiting cell membrane and cell wall formation. The activity of compound **D** can be attributed to the hydroxyl group at the 2' position, similar to the effects observed with the hydroxyl group at the 3' position (**Article 3**). These conclusions re-iterates the critical role of hydroxyl groups at adequate positions in enhancing the therapeutic potential of monocarbonyl curcuminoids.

Compounds **E** (3-hydroxy-dibenzylideneacetone, hydroxyl group at 3' position) and **F** (4-hydroxy-dibenzylideneacetone, hydroxyl group at 4' position) were also selected to study the inhibiting effect of *Candida* adhesion on glass because they showed low MIC values. The anti-adhesion activity of compounds **E** and **F** exceeded 60% under flow conditions. However, despite this activity, there was no significant reduction in CFU, probably due to a decreased activity of the curcuminoid coated on a glass surface, leading to the decision not to pursue

further investigation with these curcuminoids. Nonetheless, considering that compound **D** also showed limited effectiveness in CFUs on coated glass but performed much better on polystyrene surfaces, it would have been worthwhile to further investigate the potential of compounds **E** and **F** on other materials. Therefore it is very important to select different materials for testing curcuminoids as surface coatings and investigate adhesion and biofilm inhibition, because charge, hydrophobicity, and roughness have an influence.

Future perspectives

This work underscores the relevance of curcumin as a privileged structure for developing antifungal compounds. While this study has achieved significant successes, it also identifies key areas for further investigation to optimize and broaden the application of our findings.

Specifically, we demonstrated that 3-hydroxy-dibenzylideneacetone remains stable for 24 h and 2-hydroxy-dibenzylideneacetone (compound **D**) exhibits activity for up to 48 h at 37 °C, surpassing curcumin, which degrades significantly in less than 24 h (Appendino *et al.*, 2022; Schneider *et al.*, 2015). Future research should focus on the chemical stability of curcuminoids under various environmental conditions, including different temperatures, pH levels, and time frames, to enhance their practical application in medical settings.

Furthermore, it is worth investigating the potential of 3-hydroxy-dibenzylideneacetone (compound **E**) and 4-hydroxy-dibenzylideneacetone (compound **F**) on other materials, with the expectation that they may exhibit high anti-*Candida* activity similar to that of compound **D**. Although compound **D** has shown promising results, its synthesis is relatively complex, involving four steps, which requires more time and reagents and result in a relatively low yield (21%). In contrast, compounds **E** and **F** can be synthesized in two steps, making them more cost-effective, faster, and simpler to produce, while providing yields of over 50%. Additionally, expanding the research to include a broader range of microorganisms, such as diverse bacteria,

and fungi, and investigating their potential in mixed-species biofilm assays, could significantly increase their potential for infection control.

Given that these compounds also demonstrated activity against dermatophyte species, which are the primary causative agents of dermatomycoses, it would be interesting to explore their use as coatings in textiles for the treatment of dermatomycoses, and wound healing, as an active agent in nail polish for onychomycoses treatment or as a cream formulation. To pursue these applications, it would be necessary to assess their chemical stability under these specific environmental conditions, and to evaluate their cytotoxicity to ensure safety for topical use.

To move these findings from the laboratory to the clinic we need to take into account costs, time, stability of the product, shelf-life, and safety. It will be essential to conduct extensive preclinical studies, including efficacy assessments in animal models, long-term stability testing under various conditions (temperature, humidity, light), and ensure regulatory compliance. Early-phase clinical trials will be needed to establish safety and efficacy, followed by advanced trials for confirmation. This comprehensive approach will ensure that the promising results of this thesis can be effectively translated into tangible medical benefits.

References

AMALRAJ, A. *et al.* Biological activities of curcuminoids, other biomolecules from turmeric and their derivatives – A review. **Journal of Traditional and Complementary Medicine**, v. 7, n. 2, p. 205–233, 2017.

APPENDINO, G. *et al.* Shedding light on curcumin stability. **Fitoterapia**, v. 156, p. 105084, 2022.

BONGOMIN, F. *et al.* Global and multi-national prevalence of fungal diseases — Estimate Precision. **Journal of Fungi**, v. 3, p. 57, 2017.

DINKOVA-KOSTOVA, A. T.; TALALAY, P. Relation of structure of curcumin analogs to their potencies as inducers of Phase 2 detoxification enzymes. **Carcinogenesis**, v. 20, n. 5, p. 911–914, 1999.

JAMIL, S. N. H. *et al.* Curcumin and its derivatives as potential antimalarial and anti-inflammatory agents: a review on structure–activity relationship and mechanism of action. **Pharmaceuticals**, v. 16, n. 4, p. 609, 2023.

KONUK, H. B.; ERGÜDEN, B. Phenolic –OH group is crucial for the antifungal activity of terpenoids via disruption of cell membrane integrity. **Folia Microbiologica**, v. 65, n. 4, p. 775–783, 2020.

MACIAS-PAZ, I. U. *et al. Candida albicans* the main opportunistic pathogenic fungus in humans. **Revista Argentina de Microbiología**, v. 55, n. 2, p. 189–198, abr. 2023.

MOHANKUMAR, K. *et al.* BDMC-A, an analog of curcumin, inhibits markers of invasion, angiogenesis, and metastasis in breast cancer cells via NF-κB pathway—A comparative study with curcumin. **Biomedicine & Pharmacotherapy**, v. 74, p. 178–186, 2015.

NELSON, K. M. *et al.* The essential medicinal chemistry of curcumin. **Journal of Medicinal Chemistry**, v. 60, n. 5, p. 1620–1637, 2017.

NGAINI, Z.; FADZILLAH, S. M. H.; HUSSAIN, H. Synthesis and antimicrobial studies of hydroxylated chalcone derivatives with variable chain length. **Natural Product Research**, v. 26, n. 10, p. 892–902, 2012.

NOUREDDIN, S. A.; EL-SHISHTAWY, R. M.; AL-FOOTY, K. O. Curcumin analogues and their hybrid molecules as multifunctional drugs. **European Journal of Medicinal Chemistry**, v. 182, p. 111631, 2019.

POLAQUINI, C. R. *et al.* Antibacterial activity of 3,3′-dihydroxycurcumin (DHC) is associated with membrane perturbation. **Bioorganic Chemistry**, v. 90, p. 103031, 2019.

POLAQUINI, C. R. *et al*. Antibacterial activity of a new monocarbonyl analog of curcumin MAC 4 is associated with divisome disruption. **Bioorganic Chemistry**, v. 109, p. 104668, 2021.

SCHNEIDER, C. *et al.* Degradation of Curcumin: From Mechanism to Biological Implications. **Journal of Agricultural and Food Chemistry**, v. 63, n. 35, p. 7606–7614, 2015.

WORLD HEALTH ORGANIZATION. **World Malaria Report 2019**. Genebra: World Health Organization, 2019a. 232 p. ISBN 978-92-4-156572-1.

WORLD HEALTH ORGANIZATION 2019. **Global tuberculosis report 2019**. Genebra: World Health Organization, 2019b. 284 p. ISBN 978-92-4-156571-4.